CONSTRUCTION OF DAMS

BY DUMPING STONES INTO FLOWING WATER

S. ISBASH.

Leningrad 1932

Translated by A. Dovjikov

War Department

United States Engineer Office, Engineering Division

Eastport, Maine

September 1935

SYNOPSIS

S. ISBASH

On the Construction of Weirs by Dropping Stones into Flowing Water.

Engineers have known for some time of the method of constructing weirs by dumping stones into flowing water, but it is only quite recently that the problem has been the subject of intensive research. Until the advent of a rational basis of design, isolated primitive dams afforded the only examples of this form of construction. A search of engineering literature disclosed a single instance, in America, in which the design had been predicated upon the results of laboratory model experiments.

The construction of dams by the method of dumping stones in open water is characterized by certain well-defined stages; initially the cross-section takes the form of an isosceles triangle; then after reaching a somewhat greater height the triangle loses the isosceles form and the downstream slope becomes elongated; subsequently the cross-section loses its original sharp angular outline and passes to the trapezoidal form with rounded curves and a comparatively long crest having a gradual slope in the downstream direction, the thickness of the overflowing nappe becoming steadily thinner. Finally a critical stage is reached at which it is necessary to increase the size of stones to resist displacement by the overflow; from this stage on until the crest of the dam rises above the water surface, the size of stone necessary to resist displacement at any elevation is a direct function of the overflow velocity.

The outline of the cross-section at any given stage of construction may therefore be considered as a graphic representation of a state of equilibrium between the weight of the component stones and the hydraulic forces tending to cause displacement and subsequent disintegration.

In the course of analyzing this complex type of structure, the following basic factors require investigation:

(1) The ability of the individual stone, located in the downstream slope of dam, to resist displacement by the combined hydraulic forces due to overflow and percolation through the body of the dam.

(2) The spillway discharge coefficient of the partly completed dam section for various stages of completion.

(3) The general character of percolation flow through the relatively coarse-grained material forming the body of the dam, and the ejector action of the overflowing nappe in augmenting such percolation flow.

Each of the above factors was studied analytically and experimentally, the laboratory work, with models of several different scale ratios, serving as a check on the mathematical treatment. Chapter V is an application of the basic principles of hydraulic similitued to the specific problem of constructing dams by dropping stones into flowing water. The recent work of the author entitled "Percolation Flow in Coarse Grained Materials" has been used as the basis for developing the law of similitude for the flow component due to percolation.

Chapter VI treats of the method of calculating the dam profile for any given site and corresponding available materials, the graphical charts furnishing an aid to computation. The numerical example given constitutes a case of reasonable agreement between theoretical calculation and laboratory model tests.

The concluding chapter deals with experiments relative to the construction of impervious blankets for sealing the upstream face of dam subsequent to the completion of the supporting rockfill section, the basic law as derived from the laboratory work being experessed:

$$H_{cp} = \nabla x^2$$

in which H_{cp} is the critical head at which the blanket starts to become permeable, ∇ is the permeability coefficient and x is the blanket thickness. It therefore appears that the rational method of designing a sealing blanket is to vary the thickness in proportion to the square root of the hydr ostatic head.

CONTENTS

CHAPTER II

SUBMERGED ROCKFILL DAMS AS OVERFLOW STRUCTURES

CHAPTER III

ROUGHNESS COEFFICIENT IN ZONE OF FREE OVERFLOW

CHAPTER IV

PERCOLATION FLOW THROUGH SUBMERGED ROCKFILL DAMS

CHAPTER V

THE LAWS OF HYDRAULIC SIMILITUDE AS APPLIED TO ROCKFILL DAMS

CHAPTER VI

CALCULATIONS FOR ROCKFILL DAM DESIGN

Translator's Note

For the convenience of the reader, the translator has assembled the following explanatory table, (Refer to Figures 46 and 47) giving the symbols and notation used throughout the text:

A - a coefficient to be applied to Froude scale model transference ratios to compensate for Reynolds' number effects.

a - the height of stone in feet.

b - the width of stone in feet.

C_o - a generalized coefficient of the Chezy type, modified and adapted to apply to percolation flow.

c - the length of stone in feet.

d - the size of stone reduced to the diameter of an equivalent sphere in feet.

f - the coefficient of friction for stone on stone under water.

q'_p - the assumed percolation discharge in cubic feet per second passing through the body of the dam per foot length of crest.

q_t - the combined percolation and overflow discharge in cubic feet per second per foot length of dam crest.

R - the hydraulic radius in feet.

s - $\frac{h_s}{h_t}$ - the coefficient of submergence for the submerged condition.

T - the tractive component of the submerged weight of an individual stone located on the downstream slope of dam.

V - the velocity of flow acting on the individual stones of the dam in feet per second.

V_a - the velocity of approach in feet per second.

$V_q = \frac{q_t}{h_t}$ - the discharge velocity of the stream below the dam in feet per second.

V_p - the velocity of percolation flow in feet per second

$$x\frac{\text{area of voids}}{\text{area of dam}}$$

V_v - the actual local velocity of percolation flow measured in the voids of the rockfill, in feet per second.

W_s - the total weight of an individual stone in tons of 2000 lbs.

$Y = \sqrt{\frac{f}{k}}$ - a coefficient expressing the combined effect of friction and form factor of the individual stone. (Y_1, Y_2,....Y_3 indicate Y at construction stages 1, 2, ...3.)

Z_o - the difference in elevation between the head and tailwater for the free overflow condition in feet.

Z_s - the difference in elevation between the head and tailwater for the submerged condition in feet.

α - the angle between the horizontal and the sloping crest of dam for the free overflow condition.

G - the shear modulus of elasticity of the fluid.

H - the maximum height of dam in feet.

h_s - the difference in elevation in feet between the tailwater surface and the downstream edge of dam crest.

h_1 - the height of the downstream edge of crest above the channel bottom in feet.

h_o - the mean depth of overflowing sheet for the free overflow condition in feet.

h_t - the depth of tailwater above the channel bottom in feet.

I - the average hydraulic gradient for percolation flow.

i_o - the slope of crest for the free overflow condition or $\tan \alpha$.

k - a coefficient expressing the form factor of the individual stone with reference to streamlining.

L_o - the base width of the dam in feet.

l_p - the length of percolation path for the free overflow condition in feet.

l'_p - the length of percolation path for the submerged flow condition in feet.

n - the coefficient of roughness in stream flow calculations, having different characteristic ranges for the Manning, Forchheimer and Airy formulas.

p - the natural porosity or void ratio of the rockfill.

$q = q_t - q_p$ = the net overflow discharge in cubic feet per second per foot length of dam crest.

q_p - the actual percolation discharge in cubic feet per second passing through the body of the dam per foot length of crest.

β and α - parameters in the Airy formula as modified by Velicanov:

$$v^2/g = \alpha d + \beta$$

Δ_s - the unit weight of stone in pounds per cubic foot.

Δ_w - the unit weight of water in pounds per cubic foot.

γ - the coefficient of roughness in Bazin's formula

$\epsilon = 1 + \frac{1}{n^2 + 2n}$ - a coefficient involving the coefficient of roughness in the Airy formula

λ - the model scale ratio.

μ - the coefficient of viscosity.

ν - the coefficient of kinematic viscosity or $\mu/$ the specific density.

$\xi = \sqrt{\frac{1}{k}}$ = a frictional coefficient in form convenient for stability calculations.

Ω - the cross-sectional area of the submerged portion of dam in square feet.

$\psi = \sqrt{2g\left(\frac{\Delta s - \Delta w}{\Delta w}\right)}$ - a coefficient correlating the specific weights of stone and water in feet^2 seconds.

ρ = a fractional part of "a", representing the lever arm of the impulse force due to the overflow about the individual stones of the rockfill.

τ = the ratio of the height of obstruction to the height of the individual stone with reference to the interlocking action of the component stones of the fill.

INTRODUCTION

Section 1. The History of the Method.

Available literature furnishes no indication that this method has ever been selected for a permanent major structure, although it has been employed for building temporary cofferdams, as in the closure of the Island Narrows of the River Svir, Figure 1. In all probability no calculations at all were made to determine the proper outline of the cross-section, which is as a general practice based only upon personal judgment reinforced by experience on similar structures. Primitive submerged rock fill weirs are somewhat closely related to rock fill impounding dams built by dumping, but such structures seldom find a place in engineering literature.

The rockfill dams constructed in India upon pervious sand foundations, Figure 2, are an exception to the above rule. These dams are however, constructed in the dry, behind cofferdams, and the downstream faces are frequently paved by hand. With respect to high dams, only occasional scant reference is made to construction by stone dumping; even in the latest Russian Text-book by Anisimov ("Impounding Dams," 1928, p.65) the statement regarding the temporary coffers for the Assuan Dam is limited to the following: "temporary dam on the Nile made by stone-dumping; 165 feet high with slope of downstream face of 1 on 1.5; permitted the discharge of large quantities of water over the crest." With reference to the Escondido and Morena dams it is merely stated that "The Escondido dam with a downstream slope of 1 on 1 was undamaged by the discharge of water over the top. The Morena dam was subjected to an overflow of $1\frac{1}{2}$ feet without damage." Moreover, in the opinion of the author such dams constructed in the dry and later subjected to accidental overflow, should not be taken as bases for the design of sections for construction by stone dumping in the wet; as a matter of fact the latter type of section bears a closer relation to the proportions of standard earth fill structures.

The first noteworthy model experimentation applicable to rockfill dams subjected to overflow was undertaken by Professor A. Smrcek in the hydraulic laboratory at the University of Brun, Chechoslavakia, in reference to the problem of discharging the flow of the River Modeva over a proposed rock fill dam, 230 feet high, to be situated in a narrow rocky gorge near Chechovitch, above the City of Prague. The model of this dam is shown in Figure 3.

The original design did not however contemplate the use of the structure as on overflow spillway. The reason for the investigation was due to the popular fear that if the discharge tunnels were to become accidentally clogged during an unusual flood, the headwater would rise above the crest of the dam, causing saturation of the core and ultimate failure of the dam. Such a catastrophe would of course destroy the City of Prague, lying $12\frac{1}{2}$ miles downstream. Professor Smrcek studied the situation by means of 1 to

100 scale models and reported that failure of the dam would be inevitable.

The first instance in which it was deliberately proposed in advance to use the stone dumping method for dam construction was in the design of the Kama-Pechora waterway. In March 1930, at the request of the engineering organization charged with the design of the above canal, pertinent experiments were initiated at Energecentre, at the Laboratory of the Leningrad Hydrotechnical Institute, under the direction of N. N. Pavlovsky, to determine the basic features of the Kolva dam. The studies, conducted by the author and Engineer G. G. Shadrin, were completed in May 1930 and a laboratory report submitted stating that from a hydraulic standpoint the construction of a submerged rockfill dam by dumping was entirely feasible. The detailed laboratory investigations for the Kolva River Dam supplied much valuable data for design, as outlined in my second report to the Kama-Pechora Waterway Authority.

Following the suggestion of N. N. Pavlovsky, the final laboratory experiments relative to the construction of dams by dumping stones in flowing water were included in the work of my subdivision in the former hydrotechnical branch of the Leningrad section of the State Construction Institute for October-December 1930 under the title "Hydraulic Construction." These experiments (made with the assistance of Engineers P. M. Bobin and I. T. Satylnikoy) as well as the preparation of my report were concluded December 31, 1930. A month later specifications were received for the construction of a new American dam - Hoover Dam, 650 feet high, (Engineering News-record, October 25, 1930). In 1932, American engineers proposed to construct cofferdams for this project by the method of dumping stones in flowing water. The cofferdams themselves are very large structures 65 feet high, serving to divert the flow of the Colorado River into four previously constructed diversion tunnels, and must be constructed across Black Canyon, where the velocity reaches 20 feet per second. The American Government assumes all responsibility for any damages that may result from overtopping subsequent to the construction of the cofferdams.

As a final example I discovered in the "Canadian Engineer" that the method of dumping had already been used on a large scale in the construction of the submerged weir across the South Sault channel of the St. Lawrence River, under very difficult conditions due to a stream velocity of fifteen feet per second.

The list of examples outlined above, although incomplete, indicates a universal and growing interest among hydraulic engineers in the problems of rock-fill dam construction by dumping stones in flowing water. In the following section the attempt will be made to outline certain specific cases in which construction by the method of dumping is the only method available.

SECTION 2. Cases in which it may be necessary to employ the method of dumping stones in flowing water.

At the present time there are three basic cases as follows:

(a) First Group. These are for the most part temporary structures built to serve only during the period of construction of the dam. Frequently they are of small magnitude as in the cofferdam for closing the Svir Island Narrows mentioned in Section 1; but occasionally they reach large proportions as in the cofferdam for the Hoover Dam. However their basic characteristic in any case is that they are temporary.

(b) Second Group. The second group covers the case in which a by-pass is provided to accommodate the discharge during construction, and the rock-fill is a component part of the finished permanent structure. At the present time I do not know of any such structures; but plans for several to be erected in the near future have come to my attention.

(c) Third Group. The third group includes permanent structures with no provision for by-passing the construction discharge and built by dumping stones directly into the flowing stream without the help of an auxiliary cofferdam. With the exception of minor, unimportant structures there are no existing examples of this class and the theory of design is stillin the preliminary discussion stage.

Without any further discussion of the first group; consideration will be given to structures of the second class in which a by-pass is provided to accommodate the discharge during construction.

The distinguishing feature of this group of structures is that only the lower section of the dam is made by dumping material inflowing water. As soon as the head-water is raised to any appreciable level by the submerged material, the by-pass tunnels come into action and carry the major portion of the discharge. Another basic feature is that the final section of the dam in this case is not designed to resist overflow. The function and relative importance of stone dumping in the structure vary widely as shown by the three following examples:

1st example. The Kolva River project on the Kama-Pechora waterway consists of a lock, power station, by-pass tunnel and a dam 115 feet high. The dam shown in cross-section by Figure 4, serves to impound a very large reservoir.

The foundation material consists of an upper layer of relatively impermeable blue sandy clay about 13 feet thick, beneath which is a stratum of high permeability, containing ground water under pressure. The level of the river bottom at the dam site is at Elevation 124 and the width of channel is about 370 feet. The normal reservoir level is at Elevation 750. The normal discharge of the river during the construction period is 21,000 c.f.s. and the corresponding tailwater is at Elevation 656. It was proposed to construct only portion "A" of the dam by dumping in flowing water, the primary purpose being to create a cofferdam which could later be incorporated as an integral part of the finished structure.

The invert of the by-pass tunnel is located at Elevation 656 and consequently the by-pass action starts when the water in the upstream reservoir reaches that elevation. As the height of portion "A" increases, the tunnel discharge steadily increases. When the upstream water level reaches Elevation 670 the entire discharge goes through the tunnel. With the exception of the lower layer which serves as part of the sealing blanket system, stones weighing between 175 and 225 pounds are necessary for the body of the dam. Consequently the physical dimensions of the cross-section are determined by the stability of such stones under the action of the overflowing water.

Upon completion of portion "A", the river discharge is accommodated by the by-pass tunnel and there is no further necessity for discharging over the partially completed dam section. From this stage on, there are two alternative methods of construction: first, the stone dumping operation may be continued until the requisite cross-section is obtained after which a sealing blanket, consisting of alternate layers of sand and stone, may be deposited; and second, an additional rock-fill section "B", of the same height as "A", may be constructed upstream from "A" to serve as an upstream section of the cofferdam, behind which the necessary bottom sealing blanket may be deposited and the entire remainder of dam erected in the dry. The hydraulic laboratory experiments for the Kolva Dam were conducted at the Leningrad Hydrotechnical Insititue and will be described subsequently.

2nd example. The foundation material for the Svir Dam #2. (Figure 5) consists of a layer of glacial till 20 feet thick, overlying an impervious clay stratum. The bottom of the dam will be located at Elevation 50 and the top at Elevation 118. The average width of river is about 800 feet and the calculated discharge during construction is about 42,000 c.f.s. with the corresponding water surface at Elevation 60. A by-pass channel is provided, 330 feet wide with bottom at Elevation 60. When construction of the dam reaches Elevation 70 the entire discharge is accommodated by the auxiliary channel. The purpose of the stone dumping is to create still water in which to sink caissons for a cut-off wall. The size of stones and their stability against displacement by the flow must be such that the length of dumped cross-section will lie within the profile of the entire dam as designed. Construction conditions are very severe, the stream velocities in the rapids section being between 6 and 10 feet per second and the depthe of flow about 10 feet. I was responsible for the design, which was based upon the results of laboratory model experiments. At the critical height of dam, 1 yard stones weighing two tons each, were required for stability against displacement by the overflow. No difficulty was encountered in designing construction plant to handle such large sizes of stone.

3rd example. The hydroelectric development at Pine Lake on the River Niva, see figure 6, includes a dam having a crest length of 2600 feet under a head of 50 feet, a side channel spillway and an intake canal. The foundation of the dam is given as pebble glacial till 5 feet thick underlying glacial detritus. The maximum discharge during construction is 16,500 c.f.s., the minimum discharge 1400 c.f.s., the minimum river bottom Elevation 375 feet, and the maximum operating reservoir level Elevation 425 feet. The invert

of the side-channel spillway is at Elevation 400 and the side-channel discharge is 16,500 c.f.s. when the reservoir reaches Elevation 413. The dam is designed as a rock-fill supporting section with an earth sealing blanket. With the side-channel invert at the above elevation, it would be necessary to construct sections 40 feet high in order to dewater the site by cofferdaming. Such heights are considered prohibitive. To permit construction at the original site and adhere to the original plan of development as far as possible, any of the following schemes might be employed:*

The general design of dam, see Figure 6, includes a concrete cut-off wall penetrating into the pebble glacial stratum, a bottom sealing blanket carefully constructed in the dry, and cofferdams which are to be incorporated subsequently as toes for the main body of the permanent cross-section. The work is to be started by constructing the cut-off walls and bottom sealing blankets on the side slopes of the river channel, above the normal water surface level at Elevation 370, stone up to 100 pounds weight being available for this section of the work.

After constructing the cofferdams up to Elevation A-A (Figure 6) the river discharge is handled through notches extending across the cofferdam area, and in the meantime the rock-fill forming the body of the dam is deposited up to Elevation A-A in the dry between the notches. As may be shown by a simple computation, the required height of cofferdam will not be greater than 21 feet. The notches are then filled and the remainder of the dam completed by dumping material into flowing water, the sealing blanket being deposited as the upstream face as the construction progresses.

In the three examples given, the method of stone dumping in flowing water plays an increasingly important part.

As outlined on page 5, the characteristic feature of the third type of rock-fill dam is that they are designed to accommodate an overflowing discharge at all stages of the construction without assistance from a by-pass channel or tunnel. Except for a few small dams across mountain streams for the headraces of local mills or for small irrigation projects, I have never seen any examples of this type of construction. I have however indicated in figure 7 four schemes, which, according to my opinion, are feasible.

The first sketch represents a rock-fill barrier of the shape usually obtained in model experiments. Two sealing blankets are provided to prevent excessive percolation with the attendant dangerous washing out of "fines" from the body of the dam. The bottom sealing blanket is deposited on the natural stream bed before rock dumping starts, while the blanket on the upstream slope is placed subsequent to construction of the supporting rock fill. In locations having a natural foundation of impervious material the bottom sealing blanket may of course be omitted.

* Presented in my report to the Leningrad Hydraulic Construction Division.

The scheme shown by the second sketch differs from the first in that tripods of the form commonly used in river regulation work are used to anchor and stabilize the component stones of the downstream face against displacement by the overflowing dischcarge. These tripods or skeletal tetrahedrons are so designed as to take upright stable positions when dropped into the overflowing stream. I know from personal observation on the construction of regulating dikes during spring flood conditions on the Tala Char River in Asserbajan, Southern Caucasus, that such devices may be depended upon to maintain the desired upright position.

The third sketch illustrates the use of anchor rods which are deposited in the rock-fill during the dumping operation, the rods being attached to flexible cables which in turn are ultimately connected to articulated precast slabs on the downstream slope of the completed section. The use of such anchors was, I believe, first suggested by the hydraulic laboratory of the Don Polytechnic Institute.

The fourth sketch illustrates the use of very heavy individual stones to insure stabilization of the downstream slope. Such stones should preferably be deposited by overhead cableway as is often done in typical heavy harbor constructed projects.

SECTION 3. THE Phenomena of Stone Dumping in Flowing Water.

According to laboratory model experiments there is a definite sequence of events accompanying the deposition of stones in flowing water, regardless of whether a by-pass tunnel is provided to accommodate the discharg during construction. Initially the profile of the dumped material takes the form of an isosceles triangle with side slopes at an inclination of 1 on 1 as shown by figures 8a and 9a and photograph Figure 10.

The isosceles form of profile, accompanied by relatively smooth water surface conditions continues up to a certain height, above which the profiles lose the true isosceles form and the downstream slope becomes elongated in accordance with figures 8b and 9b. There is also a more pronounced drop in the water surface over the dam at this transition stage and the downstream water surface becomes slightly undulatory in appearance.

As the dumping operation is still further continued, it becomes increasingly difficult to make progress in the vertical direction as the dumped material tends to flow downstream, giving the downstream face a flatter slope as compared with the original inclination of between 1 on 1 and 1 on $1\frac{1}{2}$. The difference in elevation between head and tail water also becomes larger and tail water surface shows marked undulations (Photograph, Figure 11).

The profile of the submerged section which up to this time could be considered as triangular becomes definitely trapezoidal in outline as shown by Figures 8c and 9c. It is at this stage that the ability of the individual component stones to resist displacement by the overflow becomes a definite factor. The effect of the

overflow velocity is noticed first on the trajectory of the dumped material. The stones do not fall vertically in the water as was observed during the construction of the triangular stage, but under the increased velocity are transported noticeably in a lateral direction during their descent through the water. After reaching the downstream face many of the stones do not remain in place, but being subject evidently to the impulse of the overflow, roll along the downstream slope until reaching a stable position at a lower elevation. This characteristic instability of individual stones occurs throughout construction of the remainder of the section.

As a result of the above mentioned phenomena the length of the submerged section increases rapidly, but the accompanying increase in height is retarded. The top surface of the trapezoid carries a slope of from 1 on 5 to 1 on 8, referred to the upper surface of the tail water, as is shown by figures 8c, 8d, 9c, 9d, and photographs figures 12 and 13.

In the following, consideration will be given to two separate cases. First, where a by-pass is provided for accommodating a discharge during construction and second, the case in which no by-pass is provided and the entire discharge passes over the rock-fill section for all stages of construction.

In cases where a by-pass is provided the upper portion of the slanting downstream face becomes steeper, the vertical height is obtained more quickly and the downstream face exhibits two definite points of contra-flexure. The thickness of the overflowing nappe gradually becomes reduced (Figure 13) and eventually the upper part of the section rises above the water surface (Figures 8f and photograph, Figure 14). There is a noticeable percolation discharge through the entire body of the submerged dam. The final shape obtained under the above conditions is shown by Figure 8f and photograph, Figure 15. The profiles obtained at various successive stages during the experimental work are shown in Figure 16.

The case in which no facilities are provided for by-passing the construction discharge may be further subdivided into two sections. Under the first subdivision the size and permeability of the stones are such that it is possible to continue construction by dumping until the profile of the section emerges above the water surface. Under the second subdivision the proportion between the velocity of overflow and the size of component stones is such that it is impossible to carry the construction above water surface without resorting to auxiliary means. The trapezoidal submerged section increases in height much more slowly and the base width spreads out more rapidly. An example of this elongated submerged profile is shown by Figures 9e and 9f.

Figure 17 gives a summary of successive profiles for various stages of construction for this subdivision.

SECTION 4. Fundamental Problems.

At all times during the continuous process of dumping stone to form a submerged overflow dam thereis equilibrium between the impulse of the overflow and the weight of the component stones, affording a rare graphical illustration of the utilization of natural dynamic forces in dam construction.

Let us take as a starting point for investigation the completed final profile (Figure 18) obtained from our laboratory experiments. It is apparent from the shape of the upper portion of the section that the stones forming the surface MLN are in equilibrium under the action of hydraulic impulse forces and gravity. In the attempt to analyse the action of these forces four topics are immediately suggested:

(1) The stability of individual stones on the downstream face under the impulse of the overflowing discharge.

(2) The discharge coefficient of the submerged section for various shapes of crest LN and various stages of construction.

(3) The coefficient of roughness of the surface LM and its effect on energy losses for the condition of free overflow.

(4) The effect of percolation flow through the body of the dam. The portion of the total discharge due to percolation will depend upon the porosity of the rockfill. As the percolation flow emerges at the downstream face ML its impulse will tend to decrease the stability of individual stones against displacement.

All four of these factors are of course more or less interdependent.

The arbitrary classification outlined above is nothing more than a convenient schedule for analyzing the hydraulic side of the problem.* Since laboratory experiments must be employed as a means of investigating the various pertinent factors, consideration must be given to the laws of hydraulic similitude as applied to the specific case of the construction of dams by dumping stone in flowing water.

The ultimate object of all experimental data and theoretical investigation is to furnish a rational basis for detailed design. Chapter VI is devoted to the development of procedure for making and expediting specific detailed calculations to obtain the required profile for any given site with the materials available locally. Chapters I to V contain an extended treatment of the five principal topics listed above.

* Our investigation is primarily hydraulic in character and does not attempt to deal with structural considerations, which, as is well known, are difficult to simulate in small scale models.

CHAPTER I

THE STABILITY OF INDIVIDUAL STONES

SECTION 5. General Considerations.

If, in Figure 20, the areas of submerged cross-section of dam, Ω, in square feet, be taken as abscisses, and the heights of these submerged sections, H, be taken as ordinates, the resultant locus will be a curve of the form ABCD.

As long as the submerged cross-section retains the triangular form (Figures 8a and 9a) the graph will lie along the straight line AB, the point B representing the stage at which the transporting power of the overflow is barely able to dislodge the first few stones from the apex of the section. The line BC corresponds to a zone of "neutral" equilibrium in which successive dumped increments of stone serve only to increase the length of cross-section without any attendant gain in height. At point C the stones recover some capacity for resisting displacement and the cross-section gains height in accordance with portion CD of Figure 20.

The above curve shows some similarity to the familiar stress-strain test diagram for steel, the region BC corresponding roughly to the yield point of the steel, that is the point at which elongation of the material continues, unaccompanied by any increase in the stretching stress. These stress-strain curves which have many common characteristics for a wide range of structural materials also apply in the case of rock-fill dams. Detailed consideration will now be given to certain characteristic stages of dam construction.

SECTION 6. The First Stage of Construction.

During the process of construction by the stone dumping method, a certain limiting height is reached at which the cross-sections begin to lose the isosceles form, depending upon the original natural velocity of the stream, the effect of the partially completed structure in raising this velocity, and the physical dimensions of the individual component stones. Let us consider for a moment the stability of an individual stone located near the apex A (Figure 19) of the cross-section under the condition of "neutral" equilibrium corresponding to point B of the curve, Figure 20. Such a stone having the basic dimensions a, b, and c is shown to a somewhat larger scale in Figure 21. Using the method of attack developed by Wilfred Airy we may now write equations for the basic forces, neglecting percolation flow for the time being:

For Sliding:

$$kab\Delta_w \frac{V_1^2}{2g} = fabc\ (\Delta_s - \Delta_w)$$

(1) $V_1 = \sqrt{\frac{f}{k}} \cdot \sqrt{2g\ \frac{(\Delta_s - \Delta_w)}{\Delta_w}} \cdot \sqrt{c}$

or using the adopted notation

(2) $V_1 = Y\ \psi \sqrt{c}$

For overturning about the edge 0-0:

$$kab \Delta_w \frac{Y_1'^2}{2g} \cdot \frac{a}{2} = abc\ (\Delta_s - \Delta_w)\ \frac{c}{2}$$

(3) $V_1' = \sqrt{\frac{1}{k}} \cdot \sqrt{2g\ \frac{(\Delta_s - \Delta_w)}{\Delta_w}} \cdot \frac{c}{\sqrt{a}}$

or using the adopted notation:

(4) $V_1' = \xi \psi \frac{c}{\sqrt{a}}$

For the convenience of the reader the physical constants in the above derivation will be grouped and defined as follows:

k = A coefficient expressing the form factor of the individual stone with reference to streamlining.

Δ_s = the unit weight of stone in pounds per cubic foot.

Δ_w = the unit weight of water in pounds per cubic foot.

$\psi = \sqrt{2g\ \frac{(\Delta_s - \Delta_w)}{\Delta_w}}$ = a coefficient correlating the unit weights of stone and water in feet $\frac{1}{2}$ seconds.

$Y = \sqrt{\frac{f}{k}}$ = a coefficient expressing the combined effect of friction and form factor of the individual stone. (Y_1, Y_2 ..... Y_n indicate Y at construction stages 1, 2, ... n.)

$\xi = \sqrt{\frac{1}{k}}$ = a frictional coefficient in form convenient for stability calculations.

Equating (2) and (c):

(5) $V_1 = V_1' \sqrt{f} \sqrt{\frac{a}{c}}$

It is evident from Equation 2, $V_1 = Y \psi \sqrt{c}$, that the velocity at which sliding of the individual stones is incipient, for any given unit weight and characteristic shape of stone and any given fluid, varies directly as the square root of the length of stone.

It is evident from Equation 4, $V_1' = \xi \psi \frac{c}{a}$, that the velocity at which overturning of the individual stones is incipient, for any given unit weight and characteristic shape of stone and any given fluid, varies, directly as the length of the stone c,

and inversely as the square root of its height a. In other words the stability of the stone varies directly with the expression $\frac{c}{\sqrt{a}}$.

From equation 5, it appears that since f, the friction coefficient, is always less than unity and since as a general rule in rock-fill a is less than c, V_1 will always be less than V_1'. In other words the stone at the apex A, of the isosceles triangle, Figure 20, will slide rather than overturn.

It may therefore be concluded that for the first stage of construction, the isosceles triangle stage, it is desirable to use thin, flat elongated stones*.

In calculating the limiting height of the isosceles form ABC, characterizing the first stage of construction, the coefficient of stability with reference to sliding, that is $Y_1 = \sqrt{\frac{f}{k}}$ will govern.

SECTION 7. The Second Stage of Construction.

When, for any given type and size of stone, the magnitude of Y is not sufficient to maintain stability and preserve the initial isosceles profile, the stone dropped subsequently will roll along the downstream face, increasing its length and decreasing its slope. The stones are seeking a position of stable equilibrium and for a comparatively short period the cross-sectional area of the dam increases with no attendant gain in height, in other words the constituent material of the dam may be considered as flowing as shown by segment BC of the curve, Figure 19. This stage is known as the second or intermediate stage of construction.

SECTION 8. The Third Stage of Construction.

The third stage of construction begins when, in the course of the dumping operation, a definite flat surface starts to develop at Point A. Figure 21A. Referring to Figure 21c, the equation for stability against overturning for a stone of basic dimension "a" is developed as follows, the subscripts "3" denoting the third stage of construction:

Moment of Impulse Force $k_3 \Delta_w \frac{V_3^2}{2g} a^2 \int a$ + Moment of tangential component submerged stone weight. $(\Delta_s - \Delta_w) a^3 \sin\alpha (\frac{a}{2} - \tau a)$

Moment of Normal Component of submerged stone weight.

$$= (\Delta_s - \Delta_w) a^3 \cos\alpha \frac{a}{2}$$

* The dimension b must however be large enough to prevent overturning in the direction of b.

Collecting like terms and transposing:

$$V_3^2 = \frac{1}{2\rho k_3} 2g\left(\frac{\Delta s - \Delta w}{\Delta w}\right) a \left[\cos\varphi - \sin\varphi(1-2\tau)\right]$$

$$V_3 = \sqrt{\frac{1}{2\rho k_3}} \cdot \sqrt{2g \frac{(\Delta s - \Delta w)}{\Delta w}} \cdot \sqrt{a} \left[\sqrt{\cos\varphi - \sin\varphi(1-2\tau)}\right]$$

Let us consider an individual stone located at poing B on the down stream slope, Figure 21B, at the moment when overturning is incipient, the basic dimension of stone being "a". As in the discussion of the first stage, the effect of percolation flow through the body of the dam and the "drag" due to the overflow are neglected for the time being, although the resultant error is not in the side of safety. Just as stability in the first stage of construction is governed by the coefficient of friction with respect to sliding, which in turn depends upon the granular structure of the material composing the stones, so in the third case stability against overturning is dependant upon the ability of the component stones to nest together and resist displacement by interlocking. Stones dumped on the sloping face move along until reaching a suitable nest and a neighboring obstruction. Once established in such a protected position, the stone remains there.

Returning again to figure 21c, the magnitude of τ, the ratio of the height of obstruction to basic dimension "a" determines the moment of T, the tractive component of the submerged weight of stone. When τ is less than $\frac{1}{2}$, the component T contributes to overturning; when τ equals $\frac{1}{2}$ the component T will have zero moment; and when τ is greater than $\frac{1}{2}$ the component T will contribute to stability of the stone.

The usual method of depositing stones is such that τ is greater than $\frac{1}{2}$. We will however, for the sake of safety, assume an average value of τ to equal to $\frac{1}{2}$ and obtain from Equation 6:

$$(7) \quad V_3 = Y_3 \psi \sqrt{a} \cdot \sqrt{\cos\varphi}$$

in which $Y_3 = \sqrt{\frac{1}{2\rho k_3}}$, the coefficient governing the stability of the individual stone during the third stage of construction.

Referring to the above coefficient, $Y_3 = \sqrt{\frac{1}{2\rho k_3}} \cdot k_3$ is less than k_1, the corresponding form factor for the first stage of construction, because the overflow is more turbulent around the individual stones during the third stage, and also because the interlocking and nesting characteristic of the third stage expose less area of individual stone to the impulse of the overflow. The same comment applies to ρ, which is a constant expressing the relation between the basic stone size "a" and the lever arm of the impulse force, see Figure 21c.

For any given size of stone, the coefficient of resistance for the third stage of construction will therefore depend upon the capacity of the component stones to interlock as measured by the coefficient $\sqrt{\frac{1}{2\rho k_3}}$, and theoretically, at least, even small stones may resist displacement against a high overflow velocity provided they possess the requisite capacity to interlock and form mutual shelter.

It is also evident that the magnitude of the above stability coefficient depends upon the structure of the rock-fill and not upon the absolute size of stones. It may therefore be stated as a corollary, that the mutual interlocking and sheltering action of stones of a given physical size is always decreased by mixing them with stones of smaller size.

Having a given type of stone available for construction, the question arises: How will the degree of slope affect the ability of the particular stone to resist displacement by the overflow? From Equation 7 it is evident that the resistance is proportional to the square root of the cosine of the angle of inclination of the downstream slope.

SECTION 9. The Fourth Stage of Construction.

The so-called fourth stage of construction can occur only when a reduction of the rate of the overflowing discharge is effected by some means such as the operation of a discharge tunnel or by-pass, or an increase in the percentage of flow chargeable to percolation. The form of construction reverts to the second stage and, after emerging above the water surface, takes the initial or isosceles form. The corresponding conditions for equilibrium are substantially the same as given previously for the first and second stages.

SECTION 10. Experiments to Determine Stone Stability Coefficients.

Experiments were conducted on two basic types of stones, (a) spheroidal and (b) cubical.

(a) Rounded Stones - Rounded stones having an average diameter of equivalent sphere equal to 0.55 inches, an average volume of 0.17 cubic inches, a void percentage of 37 per cent, a specific gravity of 2.64 and a value of the constant $\psi =$

$$\sqrt{2g\ \frac{(\Delta_s - \Delta_w)}{\Delta_w}} = 6.44 \text{ feet}^{\frac{1}{2}} \text{ seconds.}$$

The mechanical or sieve analysis of the stone is as follows:

Diameter in inches	Per cent of total volume	Product Col 1 x Col 2
0.67	11.75	7.88
0.63	11.75	7.41
0.57	23.51	13.40
0.50	47.02	23.50
0.40	5.97	2.39
	100.00	54.58

Average diameter of stone = $\frac{54.58}{100.00}$ = 0.55 inches.

The experiments were conducted upon a definite structure for the three typical stages of construction, the isosceles triangle stage, the intermediate stage and the trapezoidal stage. Measurement of total discharge was made by a Thomson V-notch weir; hook gages were employed to determine the water surface elevation for the overflowing discharge; the profile of the cross section was observed by means of a system of rectangular coordinates painted upon the glass side of the flume; velocities in the vicinity of the top were observed by universal Pitot-Rehbock tube; and the percolation flow through the body of the dam was observed by noting the time required for the passage of dyes along several flow lines.

Using the basic formulas, $V_1 = Y_1 \psi \sqrt{a}$ and $V_3 = Y_3 \psi \sqrt{a \cos \varphi}$, the coefficients Y were determined for various stages of construction and various methods of stone dumping.

(b) Cubical Stones. For the tests on stones of cubical form, model cubes were constructed of 1 to 3 concrete, having a side length a = 0.95 inches, a void percentage of 47.5%, a specific gravity of 2.21 and a value of

$$\psi = \sqrt{2g \frac{(\Delta_s - \Delta_w)}{\Delta_w}} = 5.53 \text{ feet } \tfrac{1}{2} \text{ seconds.}$$

The program of observations was similar to the procedure for spheroidal stones, except that additional tests for percolation velocity were made using apparatus of the Darcy type, which gave the percolation velocity as a function of the hydraulic gradient. It should be carefully noted that in conducting the above experiments the relative values of overflow and percolation discharge were determined for the cross-section normal to the longitudinal axis of the dam. The velocity distribution in oblique sections would naturally be something quite different.

SECTION 11. Determination of Coefficient "Y" for Rounded Stones.

For rounded stones separate determinations were made to obtain the value of Y_1 corresponding to the initial or triangular stage of construction and Y_3, corresponding to the third or polygonal stage. The data for Y_1 are given in the following:

TABLE I

Stones of Rounded Shape.

Results of experiments for determination of coefficient Y_1.

Note: Y_1 is a dimensionless number.

Date of experiments. 1930	Calculated velocity of overflow - assuming that 10% of total discharge is due to percolation. Feet per second	Y_1 - triangular shape definitely retained.	Y_1 - triangular shape distorted	Remarks
Sept. 28	1.47	0.675		
Sept. 28	2.30		1.06	Profile no longer triangular.
Sept. 29	1.07	0.79		Sharp triangular profile.
Sept. 21	1.43	0.66		Sharp triangular profile
Sept. 21	1.93		(0.89)	Triangle with rounded apex, 2nd or intermediate stage.
Apr. 6 Apr..10	1.85	(0.86)		Intermediate stage.

In the above tabulation the values of the coefficient corresponding to the second or intermediate stage have been circled. The other values represent either the sharply defined triangular profile or the stage where distortion was

quite advanced and the polygonal form incipient. The coefficient typical of the first stage of construction may therefore be taken from the tabular values as:

$$Y_1 = \sqrt{\frac{f}{k}} = \text{from } 0.86 \text{ to } 0.90$$

corresponding to values of $\frac{f}{k}$ from 0.74 to 0.81. This value of $\frac{f}{k}$ agrees closely with the value of 0.80 obtained experimentally by Dubois in studying the movement of transportable material using a wooden flume 130 feet long. The results of Dubois' experiments were published in 1786, "Traite d'Hydraulique."

As can readily be seen from Table 2, there is considerable variation in the values of Y_3, which is to be expected in view of the roughness of surfaces. It should also be noted that the values in Column 13 are admittedly low, because of the low quantity of overflowing discharge, which was obtained in this case by subtracting the percolation discharge across a normal section from the total discharge. The data in Columns 14 to 17 inclusive are obtained by Pitot tube measurements. The accuracy of such measurements is however decreased by the turbulent character of the overflow and the presence of air bubles in the stream. After analysing the data in Table 2, we may accept as a fair value for the third stage of construction:

$$Y_3 = \text{between } 1.10 \text{ and } 1.20$$

TABLE 2

STONES OF ROUNDED SHAPE

RESULTS OF EXPERIMENTS FOR DETERMINATION OF COEFFICIENT Y_3

Date of experiments 1930	Per cent of total discharge going over crest.	Cross-section of discharge over crest. s.f.	Total Discharge c.f.s.	Average velocity neglecting percolation f.p.s.	Average velocity allowing for percolation f.p.s.	Velocities measured on the downstream face by means of pitot tubes - V^{III}_{V}			
						Upper part of the flow		Lower part of the flow	
						Aver. V^{III}_{V} f.p.s.	Max. V^{III}_{V} f.p.s.	Aver. V^{III}_{V} f.p.s.	Max. V^{III}_{V} f.p.s.
1	2	3	4	5	6	7	8	9	10
Sept. 28	83.5	0.206	0.605	2.95	2.46	2.59	2.64		
Oct. 1	76.5	0.218	0.605	2.79	2.13	2.16	2.49		
	73	0.174	0.517	2.98	2.18	2.23	2.66	2.95	3.38
	70	0.148	0.517	3.51	2.46	2.04	2.52	2.72	2.82
Sept. 21	90	0.216	0.605	2.82	2.54				
	90	0.242	0.605	2.51	2.26				
	85	0.189	0.605	3.22	2.74				
	85	0.189	0.605	3.22	2.74				
	84	0.189	0.605	3.22	2.70				
	83.5	0.189	0.605	3.22	2.69				
	73	0.216	0.517	2.42	1.76				
	70	0.162	0.517	3.22	2.25				
	73	0.189	0.517	2.75	2.02				
Sept. 23	70	0.162	0.517	3.22	2.25				
Apr. 6	85	0.174	0.517	2.98	2.52				
Apr. 10	70	0.189	0.517	2.75	1.93				
Apr. 15	76.5	0.174	0.517	2.97	2.28				
	70	0.174	0.517	2.97	2.08				

Note: Y_3 is a dimensionless number.

TABLE 2 (Continued)

$Y_3 = V^{III} / \psi\sqrt{\epsilon}\sqrt{\cos\alpha}$ Calculated according to:

	$\cos\alpha$ α = angle downstream slope	V^{I}	V^{II}	V^{III} Average velocity Upper part of flow	V^{III} Maximum velocity Upper part of flow	V^{III} Average velocity Lower part of flow	V^{III} Maximum velocity Lower part of flow
	11	12	13	14	15	16	17
Sept. 28	0.988	1.37	1.14	1.22	1.24		
Oct. 1	0.993	1.29	0.99	1.01	1.16		
	0.990	1.38	1.01	1.03	1.23	1.37	1.56
	0.983	1.64	1.15	0.95	1.18	1.27	1.32
Sept. 21	0.968	1.33	1.20				
	0.985	1.18	1.06				
	0.984	1.61	1.28				
	0.988	1.49	1.27				
	0.990	1.48	1.26				
	0.990	1.47	1.25				
	0.990	1.13	0.82				
	0.994	1.49	1.04				
	0.992	1.28	0.94				
Sept. 23	0.992	1.49	1.04				
April 6	0.989	1.39	1.18				
April 10	0.995	1.27	0.90				
April 15	0.990	1.38	1.06				
	0.994	1.37	0.96				

The results of the laboratory experiments show a substantial increase in coefficient Y_3 as compared with Y_1, confirming the theory that the resistance in the third stage of construction is due to interlocking whereas the resistance of the first stage derives principally from the simple friction of stone on stone.

In conclusion the coefficients of stability of the individual stones may be summarized for each of the three characteristic stages of construction as follows:

$$Y_1 = 0.86 \text{ to } 0.90$$
$$Y_2 = 0.90 \text{ to } 1.10$$
$$Y_3 = 1.10 \text{ to } 1.20$$

SECTION 12. Determination of Coefficient "Y" for stones of Cubic Form.

The purpose of experimenting with small concrete cubes was to make a detailed study of the effect of shape of stone upon the percolation discharge. Referring to Table 3, Experiment 2, November 14, Columns 9 and 10, we note that the value of coefficient $Y_1 = 0.838$ to 0.842 for concrete cubes is very close to the value of $Y_1 = 0.80$ to 0.90 determined for spheroidal stones. By studying the values of Y_3 determined experimentally and listed in Table 3, it is to be noted that the velocities used in computing columns 9 and 10 have been corrected for merely calculated and not observed values of the percolation flow and must therefore be considered too low. The values of column 11 are certainly too high. Thus the actual values lie somewhere between the limits of these columns and it may be concluded that the coefficients Y_3 for cubic stones may be increased as compared with the same coefficients for rounded stones. It is believed, however, that this increase would not be very great and also that the apparent advantage of interlocking to be expected in cubical stones would be discounted by the increased frontal pressure exerted on this shape of stone. Due to these counter-acting forces there appears to be no reason to suggest an increase in the values of coefficients of stability in Section 11.

SECTION 13. The Scope of Experiments and Materials Used.

Two groups of spheroidal stones, both with a specific weight of 2.64 and percentage of voids of 37 to 40, were used. The first group is designated as "small stones" in which d = 0.55" (with the model scale of 25 this corresponds to a prototype weight of 175#) and the second is designated as "large stones" in which D = 0.94" (which corresponds to a prototype weight of 1050#).

The tail water (elevation 200) was held constant at a depth of 9.45" (which corresponds to a prototype depth of 19.7 feet). The discharge was equivalent to 21,200 c.f.s. in a stream of 368 foot average width. A tunnel by-pass was provided which went into action when the head water rose above elevation 200. At a depth in the upper pool of 32.8 feet (elevation 213.1)

TABLE 3

CONCRETE CUBES

RESULTS OF EXPERIMENTS FOR DETERMINATION OF COEFFICIENT Y

Date of Experiment	Number of Experiment	Calculated overflow velocity allowing for percolation flow through body of dam.			
		When percolation discharge is computed from dye observations		When percolation discharge is computed from void percentage	
		% Discharge due to percolation per cent	Overflow Velocity V^{I} f.p.s.	% Discharge due to percolation per cent	Overflow Velocity V^{II} f.p.s.
1	2	3	4	5	6
Nov. 14	1	26.0	1.63	29.7	1.54
Nov. 14	2	33.7	2.08	33.5	2.09
Nov. 7	5	38.8	1.68	37.7	1.71
Nov. 7	6	42.9	2.09	40.5	2.18
Nov. 18	7	54.3	1.55	42.7	1.90
Nov. 18	8	63.6	1.60	47.0	2.33
Nov. 19	9	63.6	1.47	45.2	2.19
Nov. 22	10	65.5	1.52	53.5	2.05
Nov. 22	11	67.4	1.43	55.9	1.68
Nov. 23	13	75.6	1.34	58.7	2.27

TABLE 3 (Continued)

Velocity of overflow on slope measured by pitot tube f.p.s.	Computed overflow velocity when percolation is neglected f.p.s.	Y corresponding to V^{I}	Y corresponding to V^{II}	Y corresponding to V^{III}	Type of Profile	$\sqrt{\cos\phi}$	Y_n corresponding to V_n	Remarks
7	8	9	10	11	12	13	14	
1.69	2.20	0.647	0.623	0.883	Triangle	1	0.679	Sharply defined triangle. Stones start to slide.
2.33	3.14	0.838	0.842	1.264	Triangle	1		
2.88	2.75	0.694	0.704	1.116	Trape-	0.976		
	3.66	0.857	0.891	1.500	zoidal	0.982		
2.01	3.38	0.632	0.779	1.385	Profile	0.982	0.823	
	4.40	0.662	0.960	1.812	"	0.975		
	3.99	0.604	0.901	1.639	"	0.979		
	4.39	0.624	0.843	1.809	"	0.979		
	4.39	0.585	0.687	1.792	"	0.987		
	5.50	0.547	0.926	2.240	"	0.985		

the by-pass will take all the discharge. The bottom of the test flume was covered with a layer of sand 2" thick.

The problem was to raise the level of the upper pool 11.5 feet using a minimum volume of fill with a minimum percentage of large stones constituting this fill.

The experiments were performed in an open glass flume about 1' -8" wide at the Leningrad Hydrotechnical Institute. A model scale of 1/25 was used.

The data obtained on transverse profiles and "Main Characteristics" are plotted in Figures 22 to 25. The curves show the relation of the following quantities to cross-section of the submerged dam:

(a) Height of rock fill = h
(b) depth of the upper pool above the tailwater.
(c) Effectiveness of stone dumping = ratio of increase of upper pool depth to increase of cross-section of dam.
(d) Total discharge passing the dam (overflow and percolation flow).

These experiments were carried on in four fundamental cycles as outlined in the following four sections.

SECTION 14. Using small Stones in Body of Dam and large Cover Stones on Downstream Face. (Experiment of Sept. 12)

The possibility of construction of a barrier of small stones protected against scour by large cover stones on the downstream face was investigated. Stones were dropped from the water surface at a fixed point designated as Station I (see Figure 22). Dumping was carried on through the various stages described in Section 3 until Stage #3 had been reached with a total deposition of 1.65 cubic feet of small stones. At this stage about 0.56 cubic feet of small stones. At this stage about 0.56 cubic feet of sand were deposited to increase the water tightness and raise the upper pool but failed to accomplish this purpose; the upper pool rose only 0.08 inches. A second barrier was then built up, down stream from the first, by dropping about 0.56 cubic feet of small stones at Station #25. The elevation of the upper pool did not change. Returning to Station I, small stones were again dropped. These however rolled over the existing upstream barrier filling up the hollow between the upper and lower barriers. Subsequent alternate deposition of large stones at II and small stones at I revealed that the completed third stage profile will be the same as one built up by deposition at Station I only. Comparison of the model profile built up by the former method and that of deposition at Station I only (see experiments of April 15, 1930, first series) shows a prototype base width increase of about 7 feet by the former method. Figure 22 shows the successive profiles obtained with alternate dumping at Stations #I and #II. The general character

of the curve $h = f(\Omega)$ is explained in Section 5. The curve $h_{ul} = f(\Omega)$ shows an approximate straight line relation. The curve of effectiveness shows a tendency to gradual increase except for one peak due to the deposition of sand.

SECTION 15. Construction by alternate dumping of small and large stones (Experiment 2, Sept. 21, 1930).

This experiment was based upon the fundamental principle that although large stones have the greater resistance to displacement, small stones offer greater resistance to percolation. The purpose of the tests was to determine whether any economy in material would be affected above the critical elevation at which large stones are required, by an admixture of small material to reduce percolation. The point of dumping and the successive profiles are shown by Figure 23. The so-called "curve of effectiveness of dumping" on which is marked the different sizes of stone employed, is the criterion for indicating where a change in stone size from larger to smaller or vice-versa is necessary. Even where the curve showing the change in elevation of upper pool level shows a uniform upward slope, the character of the curve of effectiveness may be materially different, even showing a negative slope in some cases.

SECTION 16. Construction using only small stones at the beginning and only large stones above the critical height. (Experiment 3, September 23-24, 1930)

Dumping was started at Station I (Figure 24), using small stones. After passing successively through the triangular, intermediate and trapezoidal phases, the rate of increase in height of the submerged dam was greatly retarded starting at about profile #2, profile #3 exhibiting a marked tendency to elongate in the down-stream direction. The effectiveness of dumping at this point was very small (Figure 24). Upon introducing large stones there was an immediate and sustained rise in the effectiveness curve.

SECTION 17. Construction Using (a) Large Stones Only (b) Small Stones Only.

For the purpose of comparison and to determine the relative economy, an experiment was also conducted using large stones only. The results are given in Figure 25, showing the principal features of the construction and the sequence of profiles of the submerged dam. The curves showing the results of the experiment using small stones only are not available.

SECTION 18. Comparison of Results Obtained by Different Methods.

Adhering strictly to the hydraulic features of construction and not touching at all upon questions of the strength of materials and effect of settlement in submerged dams, a comparison will be made of the following: (a) final volume of submerged dam; (b) percentage of large stone; (c) effectiveness of dumping. The summary of results is given in Table 4 and the curves of Figure 26. In the same figure are also shown comparative profiles of the submerged dams for different methods of construction.

SECTION 19. Conclusions regarding the rational method of Construction.

The above experiments support the following fundamental statements:

From the hydraulic standpoint, the most rational method of construction is to use only small stones at the beginning and subsequently to change to larger sizes. This method gives greatest economy in total volume of submerged dam, gives the minimum percentage of large size stones, gives a steadily increasing effectiveness of dumping, gives maximum insurance against "piping" due to percolation flow between the dam and the foundation, since the finer material reduces the percolation velocity to a minimum, and also results in the minimum total percolation flow through the body of the dam as explained in Chapter IV.

With reference to the plan of using only large stones, it can readily be seen that the attendant expense is not justified for the initial triangular stages because the equilibrium of stones situated near the apex is determined by the coefficient of stability against sliding, Y_1, rather than the coefficient of overturning Y_3. Furthermore the large stones in the lower interior section of the triangle are outside the zone of flow action and are never subjected to the higher velocities of overflow.

The method of using alternate portions of small and large stones decreases the resistance of the latter to overturning. Consequently, the large stones simply roll along over the smaller pieces and, not being able to find a hold capable of developing the requisite interlocking resistance, simply roll along the top of the dam and gradually acquiring high kinetic energy, sometimes damage and destroy previously constructed sections of the dam. The corresponding curve of effectiveness of dumping is subject to erratic changes and exhibits a series of negative slopes. At times an increment of stone actually results in a decrease in the height of dam for the reason given above. The final volume of a submerged dam constructed of alternate portions of small and large stones is greater than the volume of a similar dam section constructed entirely of small stones.

It is also essential to maintain uniformity of material in a direction along the axis of dam, because even in small scale laboratory experiments, chance irregularity in dumping creates local failures owing to the high velocity of overflow, and the repair of such failures is often a difficult task requiring a considerable volume of stone.

At times it might appear desirable to raise sections of the dam crest locally; for example, in case it was desired to increase the portion of the river discharge carried by a by-pass. Experience shows such a procedure to be decidedly precarious, as the overflowing discharge from the high level crests acquires considerable velocity and tends to erode the material on the lower levels completed downstream.

The three principles just enumerated constitute the fundamental hydraulic features of constructing submerged rodkfill dams by dumping stones in flowing water. Additional suggestions will now be offered in connection with the problems of general stability and provision to limit settlement of the completed structure under its own weight.

It may be stated on a general principle that settlement of the dam subsequent to completion will be reduced in proportion to the degree of consolidation or compacting acquired during the movement of the individual stones immediately after dumping; that is, the larger the paths traversed by a stone before getting firmly interlocked into final position, greater will be the resistance of the dam to the action of vertical loads. Thus the initial triangular stages of the construction will have the greatest void percentage, since the individual stones have not been subjected to the heavy rolling action that is present in subsequent stages. From the standpoint of reduced settlement subsequent to completion of the dam, it is therefore desirable to keep the area of the initial triangular stage as small as possible. This may be accomplished by selecting the proper size of stone.

From the standpoint of developing the maximum degree of interlocking of component stones, so as to give the optimum resistance of the individual pieces to overturning, it has been demonstrated that uniformity in size of rock is essential. However even from the hydraulic point of view a stratum consisting only of such large material would result in a very high percolation flow which might affect the advantages, due to improved interlocking power. As a matter of practical construction it is desirable to use a certain admixture of small material not only to restrict percolation but also to reduce settlement of the finished dam.

It is also necessary to remember that the stones forming the downstream face of dam are pressed into position to some extent by the action of the overflow discharge, so that the material is capable of maintaining a slope of the order of 1 on 1 during construction; but that subsequent to completion with the upper reservoir full and no overflow taking place, a flatter slope of the order of 1 to $1\frac{1}{4}$ or $1\frac{1}{2}$ may be necessary to insure structural stability.

Problems relating to the ecomomics of stone sorting in detail or the selection of contractor's plant are of course outside the scope of this volume and are in general dependent upon the local conditions of each individual job.

No claim is made to leaving completely covered the entire subject; but it is hoped that the basic principles developed will serve as a useful adjunct to the initiative of the individual engineer.

TABLE 4

Summary of results of the experiments for determination of the rational method for construction of dams by dumping stones into flowing water

No. of Exper.	Method of Construction	Volume of model liters	% of large stones	% relation of volume to experiment #4 as a basis	Effectiveness of dumping em/de^2_m	Remarks
1	Construction using large stones	175	28.6	128	0.34	
2	Alternate portions of large and small stones	189	35.4	138	0.68	For the upper pool, elevation 203.1 only was reached, instead of 203.5 as in other experiments.
3	First small stones only and later large stones only	172	28.5	122	2.88	
4	Large stones only	137	100	100	0.76	
5	Small stones only	195	0	131		

CHAPTER II

SUBMERGED ROCKFILL DAMS AS OVERFLOW STRUCTURES

SECTION 20. Discharge Coefficient During First Stage of Construction.

During the first stage of construction the rockfill assumes the form of a submerged weir of triangular shape closely approximating a type shown in N. N. Pavlovsky's "Hydraulic Hand book" for which, with similar conditions as to face slope and ratio of height of rockfill to head, the coefficient

$$C = 3.53$$

The American engineering practice of introducing a coefficient of submergence ∂_s, was checked experimentally on the triangular shaped rockfill, and has been stated by Pavlovsky, the corresponding computed results were found to give only rough approximations to actual conditions. Therefore, ∂_s cannot be considered applicable to conditions of deeply flooded crests such as obtain at this stage. It is therefore concluded from the data of Table 5 and of Pavlovsky's "Hydraulic Handbook" that for the first stage of construction we may take the coefficient

$$C_1 = 3.60$$

SECTION 21. Discharge Coefficient During Second Stage of Construction.

In the second stage a condition of submergence similar to the first stage exists, but the shape assumed by the fill has changed to one of trapezoidal cross-section with a curvilinear crest. Referring again to Pavlovsky, a similar type of structure approximating this shape (but for free overflow conditions) will be found for which the coefficient

$$C_2 = 3.70$$

Experimental check was made on the use of ∂_s in the discharge equation and was again found to give erroneous results.

It will be noted that the value of C_2 found at the second stage is equivalent to the discharge coefficient obtained for ideal profiles of ogee form. The explanation of this lies in the fact that the flowing water, by removing obstructing stones, tends to improve the conditions of flow.* However, there is no assurance that the above value of C will always be obtained. Consideration of the data of Table 6 in conjunction with Pavlovsky's data (for free overflow) gives an average working value of

$$C_2 = 3.68$$

* In some experiments it will therefore be found necessary to choose materials which lend themselves to the molding action of running water.

TABLE 5

Results of Experiment for Determination of the Coefficient of Discharge over the Submerged Dam at the First Stage

Date and Experiment #	H cm.	$H_o = H + \frac{V^2}{2g}$	Q liters/sec	$\frac{h_s}{H}$	σ_s	α	$m = \frac{Q}{\sigma_n B \sqrt{2g} H_o^{3/2}}$
Sept. 28 1930 #1	10	10.15	19.33	0.914	0.575	$36^{\circ}50$ 0.75	For the condition of no submergence that is if σ_n were = 1.00 m=0.46

Translator's Note: C in the English formula $Q = CLH^{\frac{3}{2}}$ equal to $m\sqrt{2g}$ above.

TABLE 6

Results of Experiment for Determination of the Coefficient of Discharge Over the Submerged Dam at the Second Stage.

Date and Experiment #	H cm.	$H_o = H + \frac{V^2}{2g}$	Q Liters/sec	$\frac{h_s}{H}$	σ_s	$m = \frac{Q}{\sigma_n B \sqrt{2g} H_o^{3/2}}$
Sept. 28 1930 #2	7.07	7.21	18.39	0.706	0.855	For the condition of no submergence, that is if σ_n were = 1.00 m = 0.48

SECTION 22. Discharge Coefficient for Third Stage of Construction.

Hydraulic conditions for the third stage of construction are the same as for a free-overflow broad-crested weir. This stage will be reached when the width of crest is sufficient to cause a close approach to shooting flow, as illustrated by Figure 12.

Once having obtained the minimum width of crest necessary to establish incipient shooting flow, the flow becomes stable, and remains a function of critical depth at the upstream edge of the crest. Further increase of crest width, changing the slope of the downstream face of the dam, (which is in the order of 5^{o} - 6^{o} relative to the horizontal) or changing the slope of the upstream water surface, has no influence on the discharge. These observations are verified by experimental data.* Also compare the coefficient of discharge from experiment #4 of April 13, 1930 with those of #5 and #6 of the same date: the coefficients C, differ little (2.97, 3.02 and 3.01) notwithstanding the difference in tailwater elevation.

Considerable influence was found to be exerted on the discharge by the form of crest and conditions of approach. In experiments #1 to #3, April 13, 1930 an accumulation of stones was built up along the crest. This produced a lowering of the coefficient C to an average of 2.64. In contrast, experiments #4 to #6, April 13, 1930, performed on a fill of comparatively flat horizontal crest show an average of C of 3.01. It is difficult to assume, however, that such horizontal flat-crested profiles could be obtained in actual practice (in the laboratory it was obtained by hand placing stones in the dry) and therefore, for safety, the coefficient for this stage such be assumed not to exceed C_3 = 2.80 (according to Pavlovsky, this corresponds to a sill with rounded approaches). Thus the coefficient for the third stage of construction should be

$$C_3 = 2.64 \text{ to } 2.80.$$

SECTION 23. Discharge Coefficient for Fourth Stage of Construction.

The fourth, and final, stage is characterized by the appearance on the submerged dam of a crest of rounded form with steep down-stream face. This crest is a repetition of the second stage and at the same time is transitional to the last stage of the dam construction - the moment when the submerged dam appears above the water surface. As should be expected, the coefficient of discharge over the dam for this stage must be close to the coefficients for the crest of curvilinear profile under free overflow. In fact, as Table 8 shows, the coefficient C increases to a value of 3.12 and may go as high as 3.90

* In Table 7 it will be seen that the depth h_1 at the end of the overflow section does not exceed the critical depth.

TABLE 7

Experimental Results - Determination of Coefficient C for Third Stage.
(Broad-crested weir - free overflow)
Date of Experiment: April 15, 1930

#	Type of Crest	H Ft.	$H_o = H + \frac{v^2}{2g}$	α and tan α	Q c.f.s.	Q* per ft. width	$h_{cr} = \sqrt[3]{\frac{k_d Q^2}{g}}$ **	Observed h in feet	$C = \frac{Q}{H^{3/2}}$
1		0.115	0.115	6°-31' 0.114	0.177	0.108	0.075	0.066	2.76 (b)
2	See Fig.29	0.164	0.164	6°-31' 0.114	0.283	0.172	0.100	0.098	2.59 (b)
3	See Fig. 30	0.213	0.214	5°-43' 0.100	0.424	0.258	0.131	0.131	2.60 (b)
4	See Fig.31	0.246	0.256	5°-00' 0.080	0.600	0.366	0.166	0.148	2.97
5		0.107	0.107	5°-00' 0.080	0.177	0.108	0.075	0.03 (a)	3.02
6		0.148	0.148	5°-00' 0.080	0.212	0.172	0.216	0.082 (a)	3.01

(a) In spite of the impermeable diaphragm installed a greater percentage of discharge passes through body of dam than in previous experiments owing to a lower elevation of downstream pool.

(b) Value of C is decreased by the accumulation of a ridge of stones along crest of weir.

* Width of flume 50 cm = 1.64 feet.

** k_d = a correction applied to the velocity-head to compensate for non-uniform distribution of velocities in cross-section. ($k_d > 1.0$)

It appears, therefore, that for this stage, depending on the form of the crest,

$$C_4 = 3.13 \text{ to } 3.60$$

The value $C_4 = 3.60$, certainly may be applied in the case where the crest is so perfect that it may, from the standpoint of hydraulics, approach the average type of ogee crests found in practice, and since this value is the maximum value encountered it may be taken as the upper limit of C_4. However, under field conditions of dropping the stones it is reasonable to assume that C_4 would not exceed the value of 3.20.

In conclusion Table 9 is presented as a summary of experimental coefficients of discharge for submerged dams.

TABLE 8

Experimental Results - Determination of Coefficient C for Fourth Stage.
(Broad-crested Weir of Curvilinear Profile --Free Overflow)
Date of Experiments: Sept. 23 - Oct. 1, 1930, See Fig. 32, 33.

#	H Ft.	$H_o = H + \frac{V^2}{2g}$	α and tan α	Q c.f.s.	Q Per Foot Width	$h^*_{cr} = \sqrt[3]{\frac{k_d Q^2}{g}}$	Observed h in feet	$C = Q/H^{3/2}$
3	0.211	0.213	(a) 8^o-16' 0,145	0.508	0.310	0.148	0.115	3.12
4	0.171	0.172	(a) 11^o-30' 0.200	0.455	0.279	0.138	0.098	3.90

(a) Obtained from Chapter III based on percolation and overflow.

* k_d = a correction applied to the velocity head to compensate for non-uniform distribution of velocities in cross-section ($k_d > 1.0$)

TABLE 9

Summary of values of C for various stages of construction.

Stage of Construction	Shape of Crest	Coefficient C for Free Overflow
I	Triangular	3.60
II	Curvilinear	3.69
III	Broad crested (Free overflow type)	2.54 to 2.81
IV	Curvilinear (Free overflow type)	3.12 to 3.60

CHAPTER III

ROUGHNESS COEFFICIENT IN ZONE OF FREE OVERFLOW

SECTION 24. Scope and Technique of Experiments.

In order to secure an accurate evaluation of the effect of geometrical size on the roughness coefficient, and to eliminate the influence of losses due to percolation flow, it was dediced to make the downstream face of the submerged dam an impermeable surface and peace on it a uniform layer of cubes (a=0.945"), in accordance with Figure 34.

Since in actual conditions the downstream face of the dam would be a surface with numerous depressions and elevations owing to washing out of the stones, the arrangement used for the initial experiments was not considered suitable for simulating actual conditions. Rows of cubes were therefore inserted normal to the flow and at a fixed distance apart. The model was also equipped with three hook gages to measure depth on the downstream face, and discharge measurements were made by means of a Thomson V-notch weir. Thirty-four tests were made using different hydraulic radii, fourteen being conducted with a smooth downstream face and twenty with a roughened face.

SECTION 25. Method of Evaluating Experimental Data.

Although the energy loss along the rough surface of the downstream face of the submerged dam under conditions of low hydraulic radius must be of different order than the surface friction loss usually contemplated by the coefficient C, we shall attempt to deal only with the determination of the coefficient of roughness as ordinarily defined.

The well-known equation of non-uniform flow

$$\Delta_y = k_d \frac{\left(v_2^2 - v_1^2\right)}{2g} + \left(\frac{v_{av}^2}{C_{av}^2 R_{av}}\right) \Delta_s$$

will be used to determine the roughness coefficient. Figure 34 shows the relationship between terms of this equation and the model, the letters T indicating the location of hook gages. In the following section the coefficient of roughness of the model is determined using the formulas of Bazin, Manning, and Forchheimer.

SECTION 26. Coefficients of Roughness Obtained from Experiments.

The tabulated results of experiments to determine the roughness coefficient appear below. In these the hydraulic radium has been varied between 0.354" and 2.123" for both smooth and roughened faces.

It should be noted that for the very small values of hydraulic radius, particularly those approaching the size of individual stones, the formula for coefficient C gives questionable results since it fails to take account of the actual phenomena. Recalculation of the model roughness coefficient to agree with values obtained under full-scale conditions was made by assuming equality of Chezy coefficients for model and prototype.** This assumption combined with that of increasing the model hydraulic radius to the prototype hydraulic radius by means of the scale ratio, furnished a basis for recalculation. Recalculated data are given in Tables #12 and #13 for both smooth and roughened faces, based on concrete cubes, having a = 1.18', and weighing about 220 pounds. The model scale ratio used was 1:15. It will be noted from the tables that there is considerable variation in the experimental roughness coefficient, as well as in the recalculated prototype. It will also be noted that the introduction of additional ridges causes but a comparatively small increase in the computed roughness coefficient. In recalculating from model to prototype account should be taken of the difference in character of flow (different amount of air in solution, etc.), which results from the increase in velocities in the prototype compared with the model. In computing C for cases of shooting flow over surfaces of great roughness, it is obviously necessary to use another formula in which an additional compensating factor appears for greater slopes and which differs substantially from the formula usually applied to open channels. For these reasons it is not considered sufficient to limit the discussion solely to the analysis coefficients computed in routine fashion, when data is available on roughness coefficients obtained under conditions similar to those occurring on the downstream face of submerged dams.

P. D. Morosov* made field measurements of the relation of cross-sectional areas to discharges on reaches of mountainous rivers in the Kuban district. Using the Chezy formula he computed C for various conditions and later, by using the Ganguillet and Kutter formula, computed the corresponding coefficients of roughness. These data are shown in Table 14. It is evident from this table as well as from the foregoing experimental results that the roughness coefficient as computed by the usual empirical formula may vary within wide limits. Also, because of the difference in character of flow between the model and prototype, the maximum values of the roughness coefficient, stepped up from model experiments to prototype condit ons, correspond to the minimum values in nature.

* "Transactions of the First All Russian Hydrological Convention," 1925.

** This assumption is usually proposed in current literature (see, for example, L. Engels "Die Wasserhaulaboratorien Europas," 1926 or Esconde-Etude theoretique et experimentale sur la similitude des fluides incompressibles," 1929).

Maximum values of the roughness coefficient in nature may exceed by almost five times values obtained by recalculation of the results of model experiments. This is seen by comparison of Tables #12 and #13 with Table #14. Consideration of these points leads to the selection of the following values for roughness coefficient corresponding to flow along the downstream face of a submerged dam constructed of 220 pound stones:

Manning's n = 0.04 Bazin's m = 3.17

As the above are minimum values for natural mountain streams, in a large majority of cases they will also hold true in the case of rock dams.

In concluding this chapter attention is directed to the importance of the coefficient of roughness in determining the velocity along the downstream face of the rockfill, and the consequent effect on the size of the stones to be used. The values recommended above may be considered as having been stopped up from model tests and are therefore conservative. A comparison of the stepped up model values against the full-scale prototype will undoubtedly give larger roughness coefficients, and result in a very substantial decrease in the required size of stone.*

* See Chapter VI

TABLE 10

EXPERIMENTAL VALUE OF ROUGHNESS COEFFICIENT

FLOW AT CRITICAL DEPTH OR LOWER (SHOOTING FLOW)

Smooth downstream face. Concrete cubes (a = 0.945")

Exp	Chezy Coeff. C	Hydr. Radius in feet	Roughness Coefficient (Dimensions in feet)		Remarks
			n according to Manning	m according to Bazin	
1	48.5	0.0673	0.0195	0.581	All odd numbered experiments are calculated with length of the shooting stream surface equal to 32.85 in.
2	57.0	0.0705	0.0167	0.464	
3	42.7	0.787	0.0227	0.755	
4.	47.3	0.0820	0.0207	0.668	
5	46.7	0.0840	0.0210	0.688	
6	52.7	0.0850	0.0187	0.580	
7	45.8	0.0906	0.0216	0.733	All even numbered experiments are calculated with length of shooting stream surface equal to 16.42 inches.
8	48.9	0.0912	0.0203	0.672	
9	50.7	0.1020	0.0200	0.674	
10	52.9	0.0971	0.0190	0.618	
11	55.1	0.1070	0.0186	0.610	
12	63.2	0.1001	0.0160	0.473	
13	90.19	0.0489	0.0100	0.166	(Translator's Note: The column showing values of n according to Forchhiemer has been omitted owing to lack of sufficient data to permit transformation of the Forchhiemer formula from metric to English units.)
14		0.0463			
15	95.4	0.0374	0.009	0.126	
16		0.0358			
17	49.6	0.1785	0.0224	0.922	
18	49.3	0.1640	0.0223	0.893	
19	47.1	0.0915	0.0211	0.710	
20	48.4	0.0860	0.0204	0.663	

Manning Formula (English units) = $C = \frac{1.486}{n} R^{\frac{1}{6}}$

Bazin Formula (English units) = $C = \frac{157.6}{1 + \frac{m}{\sqrt{R}}}$

TABLE 11

EXPERIMENTAL VALUE OF ROUGHNESS COEFFICIENT

FLOW AT CRITICAL DEPTH OR LOWER (SHOOTING FLOW)

(Downstream face roughened by introducing 4 ridges of cubes)

Exp No.	Chezy Coeff. C	Hydr. Radius in feet	Roughness Coefficient (Dimension in Feet)		Remarks
			n according to Manning	m according to Bazin	
1	90.9	0.0404	0.0095	0.1349	All odd numbered experiments are calculated with length of the shooting stream surface equal to 32.85 inches.
2	54.5	0.0423	0.0160	0.3894	
3	47.8	0.0564	0.0192	0.5433	
4	51.4	0.0541	0.0177	0.5542	
5	45.5	0.0712	0.0210	0.6592	
6	49.6	0.0712	0.0192	0.5795	
7	40.7	0.0912	0.0244	0.8657	All even numbered experiments are calculated with length of the shooting stream surface equal to 16.42 inches. (Translator's Note: The column showing values of n according to Forchheimer has been omitted owing to lack of sufficient data to permit transformation of the Forchheimer formula from metric to English units.)
8	42.2	0.0919	0.0236	0.8276	
9	47.1	0.1096	0.0217	0.7769	
10	47.6	0.0696	0.0293	0.7407	
11	44.9	0.1247	0.0234	0.8838	
12	36.4	0.1102	0.0282	1.1047	
13	38.4	0.2090	0.0298	1.4126	
14	33.1	0.1762	0.0336	1.5756	

Manning Formula (English units) $C = \frac{1.486}{n} R^{\frac{1}{6}}$

Bazin Formula (English units) $C = \frac{157.6}{1 + \frac{m}{\sqrt{R}}}$

TABLE 12

COMPUTED VALUE OF ROUGHNESS COEFFICIENT

FLOW AT CRITICAL DEPTH OR LOWER (SHOOTING FLOW)

(Recalculated from Table 10 for cubes of a = 1.18')

Exp. No.	Chezy Coeff. C	Hydr. Radius in feet	Roughness Coefficient (Dimensions in Feet)		Remarks
			n according to Manning	m according to Bazin	
1	48.5	1.010	0.0306	2.2583	Experiments # 13 and #15 are doubtful; #14 and #16 are missing.
2	57.0	1.040	0.0262	1.8092	
3	42.7	1.181	0.0357	2.9338	
4	47.3	1.230	0.0325	2.5915	
5	43.1	1.260	0.0330	2.6730	Translator's Note: The column showing the value of n according to Forchheimer has been omitted owing to lack of sufficient data to permit transformation of the Forchheimer formula from metric to English units.)
6	52.7	1.276	0.0294	2.2493	
7	45.8	1.358	0.0339	2.8451	
8	48.9	1.368	0.0319	2.6078	
9	50.7	1.532	0.0314	2.6169	
10	52.9	1.457	0.0298	2.3978	
11	55.1	1.604	0.0292	2.3724	
12	63.2	1.503	0.0252	1.8364	
13	90.2	0.735	0.0157	2.4539	
14		0.696			
15	95.4	0.561	0.0141	0.4890	
16		0.538			
17	49.6	2.667	0.0352	3.5749	
18	49.6	2.461	0.0350	3.4626	
19	47.1	1.375	0.0332	2.7527	
20	48.4	1.289	0.0320	2.5716	
Mean arithmetic values Excluding #13 and #15			0.0315	2.5970	

Manning Formula (English Units) $C = \frac{1.486}{n} R^{\frac{1}{6}}$

Bazin Formula (English Units) $C = \frac{157.6}{1 + \frac{m}{\sqrt{R}}}$

TABLE 13

COMPUTED VALUE OF ROUGHNESS COEFFICIENT

FLOW AT CRITICAL DEPTH OR LOWER (SHOOTING FLOW)

(Recalculated from Table 11 for cubes of a = 1.81')

Exp. No.	Chezy Coeff. C	Hydr. Radius in feet	Roughness Coefficient (Dimension in Feet)		REMARKS
			n according to Manning	m according to Bazin	
1	90.9	0.607	0.0149	0.523	(Translator's Note: The column showing the values of n according to Forchheimer has been omitted owing to lack or sufficient data to permit transformation of the Forchheimer formula from metric to English units).
2	54.7	0.636	0.0251	1.512	
3	47.8	0.846	0.0302	2.110	
4	51.4	0.814	0.0278	2.151	
5	45.5	1.070	0.0330	2.554	
6	45.5	1.070	0.0302	2.251	
7	40.7	1.368	0.0384	3.359	
8	42.2	1.380	0.0370	3.211	
9	47.1	1.644	0.0342	3.015	
10	47.6	1.539	0.0334	2.879	
11	49	1.870	0.0368	3.441	
12	36.4	1.654	0.0443	4.288	
13	38.4	3.133	0.0468	5.487	
14	33.1	2.641	0.0336	6.121	
Mean arithmetic value			0.0335	2.934	

Manning Formula (English Units) $C = \frac{1.486}{n} R^{\frac{1}{6}}$

Bazin Formula (English Units) $C = \frac{157.6}{1 + \frac{m}{\sqrt{R}}}$

TABLE 14

Date of Measurement	Q c.f.s.	Area Sq. Ft	Ave. velocity Ft. per sec.	Hyd. Rad. Ft.	Surface Slope	Roughness Coefficient	
						n	Y
			River Oullov - Kam (near confluence)				
8/23/19	1070	196.7	5.45	3.77	0.0249	0.118	15.34
8/27/19	1042	210.6	4.89	3.97	0.0244	0.102	17.26
9/ 4/19	968	192.0	5.02	3.64	0.0248	0.104	16.06
11/1/19	219	112.4	1.97	2.17	0.0230	0.186	24.79
2/21/20	109	74.2	1.48	4.95	0.0240	0.200	28.12
			River Teberda (near confluence)				
7/5/19	3814	550.7	6.86	4.89	0.0046	0.032	5.43
7/13/19	6304	635.3	9.84	5.09	0.0052	0.040	3.64
8/8/19	4520	488.7	9.22	4.63	0.0074	0.048	4.64
9/4/19	533	217.0	2.46	5.38	0.0052	0.074	8.29
2/18/19	205	127.0	1.61	1.74	0.0046	0.086	10.18
			River Kouban (before condluence with River Teberda)				
7/5/19	7346	789.2	9.28	4.89	0.008	0.051	5.20
7/13/19	10072	899.2	11.12	5.58	0.008	0.048	4.71
8/8/19	4715	550.8	8.40	4.13	0.0082	0.050	4.93
9/4/19	671	166.2	3.97	1.31	0.0103	0.062	4.11

TABLE 15

Form of Stone	Dimension of Stone Feet	% of Volume	Specific Weight	Porosity
Rounded Pebbles	0.056	11.76		
	0.052	11.70		
	0.047	23.52	2.62	37%
	0.040	47.05		
	0.033	5.97		
Concrete Cubes 1:13	0.079	100	2.31	48.5%

CHAPTER IV.

PERCOLATION FLOW THROUGH SUBMERGED ROCK FILL DAMS

SECTION 27. Scope and Technique of Experiments.

Two experiments were performed investigating in detail the percolation flow through a rockfilled dam; one using stones of rounded shape and a variable rate of discharge; the other with concrete cubes and a constant rate of discharge. From these it was sought to determine (a) the distri bution of flow through and over the dam referred to the vertical plane through the axis of crest, (b) streamlines and equipotential lines in the body of the dam and, (c) the magnitude of velocities over the top and on the downstream face.

The velocity over the top of the dam was determined by traverses with a Pitot-Rehbock universal tube. The average velocity through the voids of the rock fill was determined by introducing coloring matter at the upstream face and observing its time of passage through the rock fill. * The direction of flow lines was also established by this method. The pressure under the base of the dam was measured by piezometers inserted through the floor of the flume, while the pressure on the crest was observed with piezemeters acting as siphons over the flume wall. In Table 15 are given data regarding the size and shape of stones used in the model. Accurate determination of the cross-section could not be made because of the irregular surface of the crest. Pitot-Rehbock tube measurements of velocities taken close to stones projecting from the downstream face were much affected by deflection of the flow lines around these stones. The two latter conditions tend to decrease the accuracy of the measurements.

Tests on the permeability of materials used in the model were made with apparatus of the Darcy type (diameter 9 and 20 cm.). From the data so obtained curves were plotted (Figures 35 and 36) showing percolation velocity against gradient. The exponent of the velocity in the formula $v^m = KI$, was found to be $m=\pm 1.5$ for rounded pebbles and $m= \pm 1.85$ for cubes.

SECTION 28. Summary of Results Using Rounded Stones.

In summarizing the results of percolation flow through the body of a submerged dam constructed of rounded stones, reference is made to Figures 37 and 38. Figure 37 shows a cross-section on which the paths of free overflow and percolation were obtained by observing the movement of dye; Figure 38 shows the same cross-

* Observed values were checked by computing percolation velocities from the relation of gradient to percolation flow.

section on which lines of equal pressure are plotted. In Figure 37 the lines of percolation flow are seen to start from the upstream face B'-E. Below line B'-B the magnitude of the percolation velocities is considerably smaller than in the region above. This is explained by the fact that the zone A-B is one of equal pressures, corresponding to the tailwater elevation. A particle of water entering at point B' follows the path of least resistance, that is B'B rather than B'A. Above the line B'-B the direction of the percolation flow line is definitely influenced by the suction effect of discharge over the crest and the downstream face B-E. The tendency of the percolation zone to become established above the line B'-B and that of the overflow discharge to pull the percolation flow into the zone BEB' will be accentuated when the rational method of dumping is used (see Section 19) The use of this method would place finer, more impervious material in the lower part of the dam and would reach its maximum effect when a fill more impervious than the rockfill itself, such as a cofferdam, was used. It will also be seen that the filtration flow lines sub-divide the upstream face EB' and the downstream face into zones, which are approximately proportional, so that for example $\frac{Eb}{Eb'} = \frac{EB'}{ED'}$.

The point B of the line BD is located approximately at mid-height of the submerged dam.

It is also seen that the somewhat smaller distance between lines of equal pressure in the upper part of the submerged dam indicate that the most intensive "pushing out" pressure caused by filtration flow must be expected on the downstream face close to the top of the dam. This zone, being subjected simultaneously to the impulse action of the flow over the crest as well as the most intensive percolation flow is the most highly taxed zone of the entire structure. A considerable part of the percolation flow comes to the surface in this zone, increasing the amount moving along the face. The surface velocities plotted on Figure 37 are typical of the surface flow along the face B-E.

In Figure 39 are shown data observed on a model of the first stage, from which it can be seen that the attraction of the percolation flow lines into the upper zone of the dam occurs even during the initial construction.

Table 16 is a summary of experimental data on percolation flow through the body of the dam. With rounded fragments in which d = 0.63 to 0.71 inches, the percolation discharge across a vertical plane taken normal to the flow, amounts to 9.25% of the total for the first stage and 30% at the end of third stage. The important part played by percolation flow in reducing the amount passing over the crest is, therefore, readily apparent.

SECTION 29. Summary of results using cubes.

In general, the results obtained using cubes substantiate the conclusions drawn in Section 28. Two of the models investigated under this heading are shown in Figures 40a and 40b, the average velocities of percolation flow observed by use of the color injection being indicated. Owing to the turbulence in the rockfill and the short time interval required for passage of the color, these measurements can not be considered accurate. However, they may be considered sufficiently reliable to confirm the statement that for the given profile of the rockfill, the average percolation velocities along the different flow lines in the zone above B'-B differ but slightly, the exception being found in the zone near the crest where suction produced by the overflowing discharge increases the velocity of percolation.

Table 17 contains a summary of observations on flow through and over the dam. It will be seen that the percentage of total discharge passing the dam by percolation is higher for cubes than for rounded stones. This is due to the greater void percentage (about 47.5%) of the dam constructed cubes. Constituting 26% of the total discharge for the first stage of construction, the percolation exceeds 60% for the subsequent profiles. This again emphasizes the significance of percolation through the rockfill dam.

SECTION 30. Method of calculating percolation flow.

The fundamental considerations in studies of percolation through coarse-grained materials are set forth in my paper "Filtration in Coarse-Grained Materials." * In this treatise the partial expression for the generalized Chezy formula applicable to dumping stones in flowing water is given as:

$$V_p = C_o\, p \sqrt{dI} \qquad (8)$$

in which V_p = the percolation velocity in feet per second.

C_o = a generalized Checy coefficient depending on permeability, roughness, and dimensions of the rockfill.

p = the natural porosity or void percentage of the rockfill (magnitude $\ll 1$)

d = the diameter of stone, reduced to an equivalent sphere, in feet.

I = the percolation gradient, i.e. the ratio of head to length of layer.

* See "Transactions of Scientific-Research Institute of Hydraulics," Volume 1, October 1931.

TABLE 16

SUMMARY OF RESULTS OF EXPERIMENTS FOR INVESTIGATION OF PERCOLATION FLOW IN the body of a submerged rockfill dam made of rounded fragments, and of bottom velocities on the face.
(Experiments from Sept. 28 to Dec. 1, 1930)

Date of Experiment	No. of Experiment	Total discharge $q\ell$ measured by weir. c.f.s.	Overflow discharge q, from velocity measured by pitot tube and measurement of depth below water surface. c.f.s.	Percolation discharge $q\ell$ calculated from velocity in voids. c.f.s.	Percolation Discharge $q\ell$ in % of q	Error in measurement (relative to q as basis) x100	Maximum bottom velocity obtained by Pitot tube. Ft./sec.	Cross-section of the overflow. Sq. Ft.
Sep.28	1(1)	0.752	0.710	0.069	9.25	103.8	1.96	0.161
"	2	0.727	0.709	0.078	10.73	103.0	2.51	0.308
"	3	0.606	0.510	0.101	16.50	100.6	2.63	0.205
Dec.1	4	0.606	0.472	0.152	23.50	103.0	2.48	0.217
"	5(2)	0.519	0.498(3)	0.141	27.0	123.0	1.96	0.215
"	6	0.519	0.353	0.156	30.00	98.0	2.08	

(1) Corresponding to Figure 39

(2) Corresponding to Figures 37 & 38

(3) Undoubted error in measurements. The value obtained, 14.10 was discounted in the analysis of results.

TABLE 17

Summary of discharge; Distribution into portions passing over and through the body of submerged dam made by dumping cubes.
(Referred to the vertical cross-section through the axis of crest)

Combined Discharge per foot width = 0.360 c.f.s.

Date of Experiment	No. of Experiment.	Calculated percolation discharge through the dam			
		According to velocity of percolation V_p		According to velocity in voids.	
		c.f.s.	% of total flow	c.f.s.	% of total flow
Nov. 14	1	0.094	26.0	0.107	29.7
"	2*	0.121	33.7	0.121	33.5
Nov. 17	5	0.140	38.8	0.136	37.7
"	6	0.140	38.8	0.136	37.7
"	6	0.155	42.9	0.146	40.5
Nov. 18	7	0.196	54.3	0.154	42.7
"	8	0.228	63.6	0.169	47.0
Nov. 19	9	0.228	63.3	0.163	45.2
Nov. 22	10	0.235	65.5	0.192	53.5
Nov. 23	11	0.242	67.4	0.201	55.9
"	13**	0.272	75.6	0.211	58.7

* Corresponding to Figure 40a (upper profile)
** Corresponding to Figure 40b (lower profile)

TABLE 17 (Continued)

Date of Experiment	Calculated discharge over the dam (by subtracting from the total discharge)			
	According to velocity of percolation V		According to velocity in voids	
	c.f.s.	% of total flow	c.f.s.	% of total flow
Nov. 14	0.266	74.0	0.264	70.3
"	0.239	66.3	0.250	66.5
Nov. 17	0.220	61.2	0.235	62.3
"	0.220	61.2	0.235	62.3
"	0.205	57.1	0.225	59.5
Nov. 18	0.164	45.7	0.217	57.3
"	0.131	36.4	0.208	53.0
Nov. 19	0.132	36.7	0.208	54.8
Nov. 22	0.123	34.5	0.178	46.5
Nov. 23	0.117	32.6	0.170	44.1
"	0.088	24.4	0.159	41.3

For homogeneous rounded stones having an equivalent spherical diameter $d \geq 0.0023$ feet, and a range of gradients $0.10 < I < 1.00$, the magnitude of the generalized Chezy coefficient may be calculated by the formula:

$$C_o = 3.623 - \frac{0.0832}{d} \quad \text{where d is in feet.} \qquad (9)$$

A laboratory check was made on this formula using stones with equivalent spherical diameters up to 0.188 feet.* For stones of larger size the results may be extrapolated.

The method of attacking the problem of themagnitude of percolation flow through the body of a rockfill dam will now be summarized. The results of experiments, as discussed in Sections 28 and 29, furnish a basis for presenting the theory of percolation flow in the following way. Let the line K-l-m-n-o-p (Figure 41) represent the free surface of the flow over the submerged dam with the line l-c parallel to the downstream face BE. This line, then, represents the direction of uniform flow along the face. Let the points B and F be connected by a straight line of length $l\phi$ representing the general direction of percolation flow between B and F. Divide the lines BE and EF into any convenient number of equal lengths and connect corresponding points. If the lines thus drawn (DD', CC', etc.) are assumed to represent stream lines of percolation, which according to the data of the experiments is particularly intensive in the zone BEF, then it is easily shown that all elementary tubes of flow, having these lines as axes, have equal hydraulic gradients. From the similarity of triangles DED' and CEC' on one side, and triangles non' and mom' on the other:

$$\frac{DE}{CE} = \frac{DD'}{CC'} \quad \text{and} \quad \frac{on}{om} = \frac{nn'}{mm'}$$

From the quality of DE and on on one side and CE and om on the other

$$\frac{nn'}{mm'} = \frac{DD'}{CC'}$$

and finally

$$\frac{nn'}{DD'} = \frac{mm'}{CC'} = \frac{h}{l\phi} = I = \text{constant.}$$

For the average size of stone having an equivalent spherical diameter d, and average porosity p, the condition of constant gradient derived above, gives rise to constant velocities of percolation along the elementary tubes of flow, or:

$$V_p = C_o p \sqrt{DI} = \text{constant}$$

* It is hoped additional experimental data using stones of larger size will be available in the near future.

which coincides in general with the results of observations (see Sections 27 and 28). Continuing the calculations on the per foot of width of dam basis, measured in the direction perpendicular to the plane of the drawing, and denoting the thickness of an elementary tube by Δ_n (Figure 41), there is obtained the following expression for the elementary percolation flow through the tube:

$$\Delta_q = \Delta_n \quad V_p$$

from which the total discharge per foot of submerged dam is:

$$q_p = - V_p \cdot \Sigma \cdot n$$

where n is as shown on Figure 41 and Σ represents a coefficient establishing transition from the schematic flow of Figure 41 to the actual. For the majority of cases we may assume from experimental data that :

$$\Sigma \cdot n = H$$

This equation accounts for that part of the discharge filtering through the dam above the line B F. Substituting the value of $\Sigma \cdot n$ in the previous equation for discharge:

$$q_p = v_p \cdot H \qquad (10)$$

The terms in this equation are found from the following expression:

$$V_p = C_o \; p\sqrt{dI} \qquad \text{(in feet per second)} \qquad (8)$$

$$C_o = 3.623 - \frac{0.6832}{d} \qquad \text{(for d in feet)} \qquad (9)$$

$$I = \frac{Z_o}{l\phi} \qquad \text{(See Figure 47)}$$

$$l\phi = \sqrt{h_t^2 + \left(H + \frac{Z_o}{i}\right)^2} \qquad (11)$$

$$H = h_t + Z_o \qquad (12)$$

$$L_o = 1.25 \, (h_t + Z_o + h_t) + \frac{Z_o}{i} \qquad (13)$$

The last three equations above are obtained geometrically from Figure 47.

Referring to Figure 42 and using the corresponding notation we may write:

$$l\phi = \sqrt{(0.5m_1 + m_2)^2 + 0.25h_1^2}$$

where $m_1 = h_1 \cot.\alpha_1$, and $m_2 = h_1 \cot.\alpha_2$. For the usual slopes $m_1 = 1.25h_1$ (approx.) and $m_2 = 1.00h_1$ (approx.), so that

$$l\phi = 1.72 \, h_1 \qquad (14)$$

Table 18 shows the comparison between data obtained from model experiments and data calculated from observations on a full size dam built of 175# to 210# stones. The full scale equivalents of model test values were obtained by means of the scale transference relations given in Table 19.

TABLE 18

No. of Experiment	Percolation discharge from laboratory experiments in & of total	Percolation discharge calculated from observations on full size structure in % of total	Difference between full scale and experimental discharge in %	Remarks
1	9.25	10.5	+11.4	See Fig. 39
2	27	26.1	- 3	See Fig. 38
3	30	32.5	+ 8	

TABLE 19

No.	Quantity	Scale transference relation λ = scale Ratio
1	Length	$L = \lambda_C$
2	Areas	$\Omega = \lambda_w^2$
3	Volumes	$W = \lambda_w^3$
4	Velocities	$V = \lambda^{0.5}\, v$
5	Pressures (in the height of fluid column)	$H + \frac{V2}{2g} = \lambda\,(H + \frac{v2}{2g})$
6	Time	$T = \lambda^{0.5}\, t$
7	Discharge	$Q = \lambda^{2.5}\, q$
8	Stress	$P = \lambda^{3}\, p$
9	Inclines	$I = i$

CHAPTER V

LAWS OF HYDRAULIC SIMILITUDE AS APPLIED TO ROCKFILL DAMS

SECTION 31. General Remarks.

Extension and development of the laws governing the application of the principles of hydraulic similitude have not kept pace with the requirements of problems arising in the field of experimental hydraulics. This situation was discussed at the 15th International Navigation Congress in Venice (September, 1931) at which many highly theoretical investigations and reports of involved laboratory tests were presented, but no extension of the laws of hydraulic similitude was proposed to cover the many new fields in which model study could be applied to advantage. One such field receiving attention in the hydro-technical laboratories of U.S.S.R. is that of stability of models of dams of the mass type. On the one hand we find expert dam designers insisting that such problems are not susceptible to study by models; while on the other reputable scientists often attempt to perform laboratory experiments of bewildering complexity before seriously analyzing the limits within which the present laws of similitude may be applied. These technicians do not stop to determine the scale transference relations in advance but proceed hurriedly to model experimentation. For the above reasons, the purpose of the following remarks is to discuss some problems I have met in my experimental work, to bring to the attention of the workers in hydraulic laboratories the fact that each new project undertaken should be accompanied by an attempt to add to the neglected theory of hydraulic similitude.

SECTION 32. Fundamental Considerations.

As has already been indicated, all experiments made in reference to the problem under investigation are fundamentally hydraulic. The questions of strength of material used, stresses in the submerged dam and, settlement under superimposed load could not be investigated on small models in hydraulic laboratories and are therefore not considered in this study. The law of hydraulic similitude, strictly true for a heavy ideal fluid, and for brevity and convenience referred to as Froude's law,* is given in detail in Table 20. In this table the capital letters refer to prototype dimensions and the small letters to model dimensions; λ is the scale ratio, and the fluid is assumed to be the same in model and prototype. It is well known that these rules may be applied without correction with an accuracy sufficient for practical pruposes in cases where the fundamental role is played by

* This name is frequently found in German literature on model study. Froude, an engineer and ship-architect, first applied the relation that the prototype velocity is equal to the model velocity multiplied by the square root of the scale ratio to investigations of ship models in 1872.

the force of gravity* and where it is possible to neglect the forces caused by fluid viscosity and molecular attraction. However, in cases where fluid viscosity (or molecular forces) are an important consideration it is necessary, in transferring from dimensions of the model to those of the prototype, to establish correction coefficients to Froude's law.

Owing to the complexity of the hydraulic phenomena accompanying the construction of rockfill dams it will be necessary to study the action of each separate variable by itself. Consequently it will also be necessary to establish an expression for the correction coefficients of each main variable, showing whether transference relations based on Froude's law, give results too large or too small compared to full-scale conditions. It is highly desirable, where possible, to establish the order of magnitude of those coefficients within certain limits.** The final step is to combine the separate component corrective coefficients into an integrated coefficient that will summarize the total effect and facilitate making the transition from model to prototype. This integrated coefficient will be the resultant of the individual tendencies of the separate components, some of which will be positive in algebraic sign and some negative. Because of this compensating cancellation of individual component effects, the resultant action as observed in experiment often differs both qualitatively and quantitively from the action of any single factor taken alone.

The last remarks hold true for the theory of hydraulic similitude as a whole, since it is necessary always to remember that the transition from small models to large ones (and consequently to the prototype) may be accompanied by very substantial quantitative changes in the character of the phenomena, which in turn may complicate the scale transference relations and in many cases require the use of supplementary correction factors.

Having recognized the general necessity for considering the individual tendency of each of the component factors in the hydraulic phenomena occurring in a rockfill dam, let us consider a specific case. Using the same classification as was given in Section 4, the following topics will be studied from the viewpoint of hydraulic similitude:

(a) The impulse action of the overflow over the submerged dam upon stones lying on the downstream slope.
(b) The movement of water on the overflow section of the downstream face.
(c) The percolation flow through the body of the dam and the upward pressure produced on the stones by this flow.

** A detailed determination of the numerical values of coefficients for some model studies would involve a separate scientific investigation which is beyond the scope of this paper.

* This rule is sometimes referred to in French literature as "the law of gravitational similarity" (la loi de similitude gravitationelle).

SECTION 33. Law of Hydraulic Similitude for Impulse Forces Acting on a Stone Lying on the Downstream Face.

By the use of Froude's law it can be shown that the unit impulse pressures acting upon the stones in the prototype are equal to those in the model multiplied by the first power of the scale ratio. (see Table 20). This is expressed in the simplest form of Airy's Law: $\frac{v^2}{2g} = \epsilon d$

from which - $$\frac{\frac{v_p^2}{2g}}{\frac{v_m^2}{2g}} = \frac{\epsilon_p d_p}{\epsilon_m d_m} = \lambda \text{ since } d_p = \lambda d_m \text{ when } \epsilon_p = \epsilon_m$$

the subscripts p and m in this case denoting prototype and model respectively. The results obtained above show that Froude rules may be applied directly to the case under consideration without corrective coefficients. In foreign laboratory practice the above rule is expressed as follows: To preserve similarity with respect to stability of individual stones against displacement by the impulse ofthe overflow, in both model and prototype, it is necessary only to decrease the linear dimensions of the stone according to the first power of the model scale ratio. For example, the investigation of Professor Smrcek with reference to the stability of rockfill dams subjected to overflow, is an example of the application of this rule of similitude. From the data available on American practice, may be mentioned the laboratory investigations of B. F. Groat* and the analysis of those data by A. C. Chick**. It is important to note that these experiments were made on a scale of only 1:100 and were not checked subsequently against full scale conditions. However a series of experiments at larger scale, performed by Rehbock at Karlsruhe and by Thysse at Delft in connection with the closure dams for the Zuyder-Zee Reclamation in Holland, were checked to some extent against the full scale prototype subsequent to construction. Detailed consideration of these tests is somewhat beyond the scope of this paper and consequently discussion will be limited to an abstract of the above program by R. Seifert.***

To obtain a comparison between model and prototype conditions for the deposition of rockfill on woven mattresses for protecting the unfinished Zuyder-Zee Dam against washout, a mattress built to natural scale was sunk in the flood channel of the Meuse Dam at Ruremond. By manipulation of the bottom gates

***This data was reviewed by me in a paper entitled, "Investigation of the Effect of Scale Ratio Upon Transference Relations for Model Tests Conducted at the Hydrotechnical Laboratory."

* The Canadian Engineer, Vol. 39, Nov. 25, 1920, P. 551.

** Hydraulic Laboratory Practice, 1929, New York, P. 798

OF THE FLOODWAY VELOCITIES OF FROM 20 TO 26 FEET PER SECOND WERE obtained, equal to those expected during a storm tide at closure. The depth of overflow was from 2 to 4 feet. At about the same time, in the laboratory at Delft (l'Universite Technique de Delft), a model of Mouse Dam was tested on a scale of 1:21. Notwithstanding the action of the piers in the floodway in disturbing uniform velocity distribution in both model and prototype, "the transfer from model to full scale quantities in accordance with Froude's law, showed that at corresponding velocities, the flow moved the predicted amount of stone." This statement is confirmed by photographs and tabular comparisons. From this data R. Seifert, Professor and Director of an important German government scientific institution, concludes that "gravitational laws of similarity may be applied in developing scale transference relations for the transportation of material along stream beds in a case similar to that described above"* The above data are sufficiently convincing to justify the use of the Froude rule in transferring from model to prototype quantities when the scale ratio is of the magnitude of 1:20 or (to less than 20) and large stones are used in the prototype. One question however still remains: within what limits may one decrease the size of models, compared with 1:20 as is sometimes necessary when simulating structures of large dimensions. For instance, are scale ratio of the order of 1:100, such as have been used by Smrcek and Great admissible and, if so, will the transference of results from such small scale models according to Froude's law involve error on the side of increased stability or will the model tests indicate a greater factory of safety than actually exists in the full scale prototype.

In the foreign literature mentioned above no answer is found to this important question and we will therefore attempt to supply one, using the splendid work of M. A. Velicanov** in checking and more accurately restating the Airy law.

Professor Velicanov states in a general way the conditions for equilibrium of a solid body of cubical form, having the basic dimension, d:

$$\frac{1}{gd^2}\int_0^d v_i^2\, dy = \frac{\frac{\Delta s}{\Delta w} - 1}{K} = \text{a constant.} \quad (15)$$

where Δ_s = weight of unit volume of stone particle.

Δ_w = weight of unit volume of water.

K = a constant summarizing friction and streamlining effects. Assuming the following law of distribution of velocities

* The investigation of critical transporting velocities.

** The notation given by Velicanov has been changed to conform to that adopted in this volume.

in turbulent flow: $$V_i = V \left(\frac{V}{H}\right)^{\frac{1}{n}}$$

where n is variable, increasing as shown by the experiments of Nicouradze, with the increase of Reynolds' number, the following expression is derived:

$$\frac{v^2}{gd}\left(\frac{d}{H}\right)^{\frac{2}{n}}\left[1 + \frac{1}{n^2+2n}\right] = \frac{\frac{\Delta_s}{\Delta_w} - 1}{K} \qquad (16)$$

This expression of Velicanov's will be taken as basic on considering the problem of similitude. For convenience let:

$S = \frac{d}{H}$ = the coefficient of submergence of the stone.

$p = \frac{\Delta_s}{\Delta_w} - 1$ = a coefficient pertaining to the unit weight of the stone.

$E = 1 + \frac{1}{n^2 + 2n}$ = a numerical coefficient.

Expression (16) then becomes

$$V^2 = \frac{dgp}{KE\,(s)^{\frac{2}{n}}}$$

Designating the elements of the model by the subscript 2, and those of the prototype by the subscript 1, the following expression is obtained:

$$\frac{V_1^2}{V_2^2} = \frac{d_1 g p_1}{K_1 E_1 (s_1)^{\frac{2}{n_1}}} \Big/ \frac{d_2 g p_2}{K_2 E_2 (s_2)^{\frac{2}{n_2}}}$$

from which, with $d_1 = \lambda d_2$ and $s_2 = s_1 = s$

$$\frac{V_1^2}{V_2^2} = \lambda \frac{p_1 K E_2}{p_2 K E_1} S^2 \left(\frac{1}{n_2} - \frac{1}{n_1}\right)$$

Comparing this expression with

$\frac{V_1^2}{V_2^2} = \lambda$, obtained directly from the Froude's law, it can be seen that the expression by Velicanov gives the same transference rule if

$$\frac{p_1}{p_2} \cdot \frac{K_2}{K_1} \cdot \frac{E_2}{E_1} \cdot S^2 \left(\frac{1}{n_2} - \frac{1}{n}\right) = 1 \qquad (17)$$

Thus, in general, the corrective coefficient to Froude's law will depend upon the ratio of the the natural properties p (specific weights of liquids and of stones), the ratio of coefficients K(dealing primarily with shapes of fragments), the degree of submergence of stones S, and upon factors which are related to the values of Reynolds' number in model and prototype.

As has been stated previously, it is necessary to consider separately the influence exerted by each individual component on the integrated value of the corrective coefficient. For simplification of the discussion let the same fluid, water, and fragments of the same shape and specific weight be assumed in the model and prototype, since these conditions can practically be assured in the laboratory. With the same fluid used in model and prototype the Reynolds' number in the model decreases very substantially as compared with the prototype because v and d in the expression $N=\frac{vd}{\upsilon}$ ** are decreasing simultaneously.*

According to Nicouradze's experiments the magnitude of n is in some cases increased more than tenfold by an increase in Reynolds' number. According to Velicanov n will decrease, and may even reach its minimum limiting value n = 2, with a decrease in Reynolds' number. With these data as a guide we may determine whether some of the factors in equation (17) are larger or smaller than unity. Since, for a decrease in Reynolds' number in the model, the magnitude of n_2 decreases:

$$n_2 < n_1$$

where n_1 refers to prototype conditions. Based on the above expression, the exponent to the coefficient of stone submergence s,

$$2\left(\frac{1}{n_2} - \frac{1}{n_1}\right)$$

will always be positive, and since s itself is always less than unity,

$$s^2 \left(\frac{1}{n_2} - \frac{1}{n_1}\right) < 1 \qquad (18)$$

It also follows from the expression $n_2 > n$, that:

$$1 + \frac{1}{n_2^2 + 2n_2} > 1 + \frac{1}{n_1^2 + 2n_1}$$

or in other words

$$E_2 > E_1$$

* For this reason it is necessary to check small scale models to be sure that the character of flow (laminar or turbulent) remains the same in model and prototype.

** υ = the kinematic viscosity of the liquid.

from which $\frac{E_2}{E_1} > 1$

The coefficients K depend primarily on the shape of the stones and to a lesser degree upon some other factors. With fragments of the same shape used in both model and prototype it can be assumed for a first approximation that $\frac{K_2}{K_1}$ is approximately equal to 1.

Finally, for the coefficients of natural properties of stone and fluid P_2 and P_1, it can be shown that with the same weight per unit volume Δ_s in both model and prototype the increased velocities encountered in the prototype will cause an increase in the amount of air dissolved in the fluid, and consequently the weight per unit volume of fluid Δ_{w_1} in the prototype will be decreased as compared with Δ_{w_2} in the model or in general:

$$\Delta_{w_2} > \Delta_{w_1}$$

from which $$\left(\frac{\Delta_s}{\Delta_{w_2}} - 1\right) < \left(\frac{\Delta_s}{\Delta_{w_1}} - 1\right)$$

or $p_2 < p_1$, from which $\frac{p_1}{p_2} > 1$. It should be noted that only the fundamental tendency of this relation is established. Practically, the magnitude of departure of the ratio $\frac{p_1}{p_2}$ from unity is for many cases, as for instance in the case of stones differing in roughness, almost imperceptible. In the case where high velocities are encountered at comparatively shallow depth accompanied by great roughness, such as occurs in the zone of shooting flow on the downstream face of the dam, the difference between $\frac{p_1}{p_2}$ and unity may be quite appreciable. To summarize the above discussion, we may rewrite Equation (17) in the following schematic form, so that the parentheses forming the right hand member of the equation correspond in order to the algebraic factors in parentheses forming the left hand member, and showing in the same respective order whether any given factor taken individually tends to make the final integrated value of the corrective coefficient to Froude's law greater or less than unity:

$$\left(\frac{p_1}{p_2}\right)\left(\frac{K_2}{K_1}\right)\left(\frac{E_2}{E_1}\right)^{s^2\left(\frac{1}{n_2} - \frac{1}{n_1}\right)} = (>1)\ (\sim 1)\ (>1)\ (<1) = A_a \quad (19)$$

To judge whether the magnitude of the integrated corrective coefficient is smaller or larger than unity, let us turn to the report of laboratory experiments made under the direction of M. A. Velicanov for the purpose checking and more accurately restating the Airy law. The degree of precision with which the separate factors may be evaluated is shown by following case. The experiments were preformed in a horizontal rectangular channel 1.64 x 0.82 feet in cross-section and 30 feet long.

Weight per unit volume of material forming grains Δ_s = 165 pounds per cubic feet (sand alone-no voids)
Form of grains = rounded
Diameter of fragments, reduced to equivalent sphere = 0.017 to 0.0003 feet.
Coefficient of submergence S - 1/15 to 1/325
Average velocities V = 0.67 to 2.15 feet per second
Reynolds' number = 3000 to 76,000 (dimensionless)

From these data it is seen that same relative shape and unit weight of fragments were used, that the velocities and Reynolds' number were small and that the submergence s is relatively small. Therefore the ratios $\frac{p_1}{p_2}$ and $\frac{K_2}{K_1}$ are practically equal to unity.

The more exact expression of the Airy law obtained by Velicanov from these experiments is

$$\frac{V^2}{g} = \alpha d + \beta \qquad (20)$$

the value of the parameters α and β obtained by experiment being:

$$\beta = 0.0197 \text{ feet}; \alpha = 151$$

It is seen from equation (20) that with pebbles of 0.013 feet diameter the influence of the factor β is only about one percent. With stones of dimensions approaching those used in the prototype the influence of β becomes totally insignificant and the Airy formula may be rewritten:

$$\frac{V^2}{g} = \alpha d$$

and will give sufficiently accurate results.*
From the relations

$$\frac{V_1^2}{V_2^2} = \frac{\alpha d_1}{\alpha d_2 + \beta} \quad \text{and} \quad d_1 = \lambda d_2$$

* See also p. 28 of Seifert's paper.

$$\frac{V_1^2}{V_2^2} = \lambda \frac{\varphi^{d_2}}{\varphi^{d_2} + \beta} = \lambda \frac{\varphi}{\varphi + \frac{\beta}{d_2}}$$ from which we obtain:

$$A_a = \frac{\varphi}{\varphi + \frac{\beta}{d_2}} < 1 \qquad (21)$$

Thus the integrated corrective coefficient for Froude's law, as obtained from the data of Velicanov's experiments, is smaller than unity.

Returning to formula (19) it can be seen from the experimental data that final value of the integrated coefficient A_a is materially affected by the factor

$$S^2 \left(\frac{1}{n_2} \quad \frac{1}{n_1}\right)$$

which is itself dependent upon the degree of submergence of the stone. For the factor $\frac{K_2}{K_1}$ pertaining to the shapes of the stones A_a is practically equal to unity. The influence of the ratio $\frac{p_1}{p^2}$ might possibly be great enough to cancel out opposing tendencies and finally make the integrated value of A_a greater than 1.

From the expression $V_1^2 = \lambda A_a V_2$, where V_1 and V_2 are critical transporting velocities for prototype and model respecitively, and taking into account the inequality expressed in (21), it is concluded that the direct use of Froude's law (that istaking $A_a = 1$) would give larger values of velocity at which washout is incipient, than would be true underprototype conditions. In other words, using small scale models and transferring results to full scale by Froude's law only, there would be obtained computed safe prototype velocities which would be higher than those actually safe in nature for a given size stone. This indicates that care should be exercised in applying the results of small scale model data on stone sizes to prototype structures.* As will be seen in the following this caution is particularly necessary in the cases in which the structure to be investigated is of such type that the friction losses along its length are insignificant.

* As for example experiments of Smrcek and Croat on scale models of 1:100

SECTION 34. Laws of Similitude for Discharge over the Top of a Submerged Dam.

Here, as in the previous section, Froude's rule may be used. As an illustration of the tendency and the degree of accuracy obtained in the transference of model discharge values according to Froude's law, a family of curves is given in Figure 43 relating to a comparative test of four models of the Pouchabon dam. (France)**

The values as plotted have been recalculated from model to prototype scale, and illustrate the tendency toward diminishing magnitudes of recalculated prototype discharges due to the influence of viscosity as the model scale grows smaller. To correct this false indication it is necessary to introduce in the discharge formula the corrective coefficient

$$Q = \lambda^{2.5} A_b q \qquad \text{where } A_b > 1$$

Usually this coefficient is interpreted as a factor of safety in the sense that the discharge capacity of the prototype crest will be higher than as shown by the values recalculated from models. In the present case, however, the purpose of the submerged dam is to raise the water level as high as possible, and in the model this level will therefore be disproportionately higher than in actual conditions. It should be noted, however, that with a scale ratio of 1:300 (such as was used for Figure 43) the error in discharge is only 10%. On the other hand, the crest of the submerged dam is very irregular in shape and measurements of its profile may introduce an error in the coefficient of discharge of 10 to 15%. It appears, therefore that for practical purposes in the case of rock filled weirs A_b is substantially = 1

SECTION 35. Flow on the Downstream Face of the Submerged Dam.

Discussion here will be limited to the area of uniform flow at the lower end of the downstream face. Apply the Chezy formual for prototype and model conditions respectively we have

$$V_1 = C_1 \sqrt{R_1 i_1} \quad \text{and} \quad V_2 = C_2 \sqrt{R_2 i_2}$$

With $R_1 = \lambda R_2$ and $i_1 = i_2 = 1$

$$\frac{V_1}{V_2} = \frac{C}{C_2} \lambda^{0.5}$$

** M. S. Esconde. "Etude theoretique et experimentale sur la similitude de fluides incompressible." - Revue Generale de l'Electricite.

from which $A_c = \frac{C_1}{C_2}$

Formulas for C by different authors give different values for this coefficient and if a formula of the exponential type is used the general case may be written

$$A_c = \frac{n_1}{n_2} \lambda^m \qquad (22)$$

where n is the roughness coefficient. From this it may be seen that A_c is dependent upon the ratio of roughness coefficients in prototype and the model scale. Therefore, for different combinations of these relations

$$A_c = \text{maybe} > 1 \text{ or} < 1.$$

As the values of scale reduction in hydraulic laboratories are rarely outside the limits 1:20 to 1:250, and as λ^m in equation (22) has values of the order of 1.8 to 3.0, then by direct numerical calculation using tables of roughness coefficients, the following is true:

(1) Between the limits of moderate roughness and smooth surfaces in the prototype, and within the usual range of model scales we may write:

$$A_c > 1$$

(2) With great roughness and considerable water surface slope in the prototype and within the usual range of model scales simulating this roughness, it is probable that:

$$A_c < 1$$

Only in the zone of shooting flow along the downstream face of the submerged dam do we encounter the conditions of the second group. This statement is also confirmed by the experimental and field data given in Chapter III. It was shown that the maximum values of roughness coefficients, transformed to full-scale conditions of geometrically similar roughnesses, gave only minimum values of roughness coefficient for the prototype.

The discussion has been limited to the above points owing to lack of data on the phenomena of shooting flow over areas of great roughness. It is evidently necessary to develop a special formula for the Chezy coefficient C, differing from all previous formulas applied to open channels, and containing terms involving the factors of steeper slopes and amount of air in solution in the overflow. Since the solution of this problem in its entirety is hindered by lack of systematically arranged experimental data, the necessity for a series of pertinent full-scale experiments is manifest.

SECTION 36. Law of Similitude for Percolation Flow through the Body of Submerged Rockfill Dam.

The generalized Chezy formula submitted by me in the paper entitled "Percolation in Coarse Grained Materials,"* can well be applied here as it is equally applicable to laminar, transitional, or turbulent percolation flow. The formula and explanation of its terms are as follows:

$$V_p = C_o^1 \; p \; \sqrt[m]{\sigma^{m-2} \; d^{3-m} \; I} \qquad (23)$$

V_p = the percolation velocity per square unit of area.

C_o^1 = a generalized Chezy coefficient in the original form.

p = the natural porosity of material, that is, the ratio of volume of voids to the entire volume (magnitude < 1).

d = the equivalent spherical diameter of individual stones.

I = the hydraulic gradient, that is, the ratio of head to the length of percolation path.

$\sqrt{\sigma}$ = the numerical value of kinematic viscosity in C.G.S. units (for water at 10°C - $\sqrt{\sigma} = 0.013$.

m = a variable exponent.

$\sqrt{\sigma}$ is also equal to 1000μ where μ is a coefficient of viscosity of the fluid and Δ is the Δweight of the fluid per unit volume.

$$C_o = C_o' \; (1000)^{\frac{2-m}{m}} \quad \text{or} \quad C_o' = (0.001)^{\frac{2-m}{m}} \; C_o$$

where C_o = a generalized Chezy coefficient corresponding to turbulent flow conditions.

Under the actual conditions of placing a rockfill of large stones in flowing water, the formula for turbulent flow may be written:

$$V_p = C_o \; p \; \sqrt{d \; I}$$

In laboratory investigations turbulent percolation flow is likely to exist in large models, transitional flow in average size models, and laminar flow in very small models. Formula (23), therefore, is probably the most applicable to percolation flow in models. Using, as before, the subscript 2 for model elements and the subscript 1 for prototype elements, we may write

* Transactions of Scientific Research Institute of Hydraulics, Vol. I, pg. 1.

$$\frac{Vp_1}{Vp_2} = \frac{Co_1 p_1 \sqrt{d_1 I_1}}{\left[0.001^{\frac{2-m}{m}}\right] Co_2 p_2 \sqrt[m]{\nu_0^{m-2} d_2^{3-m}}\, I_2} \qquad (24)$$

For similarity in model and prototype $I_1 = I_2$. It is also not difficult to obtain equality of porosity in the model and in the prototype so that

$$p_1 = p_2$$

and finally, according to Froude's rule

$$d_1 = \lambda d_2$$

Substituting these three relations in formula (24) we obtain:

$$\frac{Vp_1}{Vp_2} = \frac{Co_1 \lambda^{0.5} d_2^{0.5} I_1^{0.5}}{\left[0.001^{\frac{2-m}{2}}\right] Co_2 \cdot \sqrt{\nu_0^{\frac{m-2}{m}}} \cdot d^{\frac{3-m}{m}} \cdot I^{\frac{1}{m}}}$$

$$= \lambda^{0.5} \frac{C_{o_1} \left(d_2\right)^{\frac{1.5m-3}{m}} \cdot \left(I\right)^{\frac{0.5m-1}{m}}}{\left[0.001^{\frac{2-m}{m}}\right] \cdot C_{o_2} \sqrt{}^{\frac{m-2}{m}}}$$

from which $A_p = \dfrac{C_{o_1} \left(d_2\right)^{\frac{1.5m-3}{m}} \cdot \left(I\right)^{\frac{0.5m-1}{m}}}{\left[0.001^{\frac{2-m}{m}}\right] \cdot C_{o_2} \sqrt{o}^{\frac{m-2}{m}}}$

The possibility of arbitrarily varying many of the factors in this equation, immediately becomes apparent as well as the consequent difficulties encountered in applying it to the general case. Three specific cases will therefore be considered.

(a) If in the submerged dam model the percolation flow is laminar, what will be the predominating influence due to small scale or small percolation gradients. Placing m=1, in expression (25) we obtain:

$$A_p = \frac{C_{o_1} \sqrt{o}}{0.001\, C_{o_2} \left(d\right)^{1.5} \cdot \left(I\right)^{0.5}}$$

Based on previously performed laboratory experiments and using metric units:

$$C_{o_1} = 20 \qquad \sqrt{o} = 0.013 \qquad C_{o_2} = 0.22 \text{ to } 4.00$$

$$d_2 = 0.01 \text{ to } 1.00, \quad I < 1$$

with these conditions it is seen that $A_p > 1$

(b) Percolation flow in the model is transitional from laminar to turbulent - a case which occurs frequently in laboratory practice using average model scale ratios. In this case

Equation (25) still applies, and for uniformly round pebbles with a diameter of 0.70 cms, and a range of percolation gradients of $0.10 < I < 1.00$ the following empirical relations obtain (in cms)

$$m = 2 - \frac{0.34}{d_2^2} \qquad C_{o_2} = 20 - \frac{14}{d_2}$$

and, as before, $C_{o_1} = 20$

Under these conditions $A_p > 1$

(c) Filtration flow in the model is turbulent. This condition occurs with very large scale models in which the range of gradient is $0.10 < I < 1.00$ and pebbles are rounded with $d > 6$ cms. Assuming as before in equation (25) $m = 2$ we obtain as the correction coefficient for this case

$$A_p = \frac{C_{o_1}}{C_{o_2}}$$

and its calculated value becomes

$$A_p > 1$$

which closely approaches unity as the model scale increases and reaches this value when $\lambda = 1$.

The above discussion may be summarized as follows: Using only Froude's law, percolation flows stepped up from model conditions will be less than those actually obtained in nature, and will be found more in error as the model grows smaller. Also, for geometrically similar rockfills and equal effective percolation gradients, the percentage of discharge going through the body of the sumberged dam will show a larger stepped up value as the model becomes larger. In other words, the prototype percolation discharge in nature will always be higher than the vlaue obtained by stepping up the model discharge.

SECTION 37. Law of Similitude for the Uplift due to Percolation Flow.

Let us consider only an isolated part of the surface of the downstream face (Figure 44) of a submerged dam consisting of small cubes with the dimension of side b, assuming that the transition to any other form of stone may affect the absolute values of coefficients but not the form of their interdependent relationship.

Upon any cube located on the surface of the face of the dam (for example, that shown in Figure 44, detail A) the following forces will act when the direction of the percolation flow is vertically upward:

(a) The downward pressure of the water $\Delta_w h\, b^2$ acting on the lower side of the cube - where Δ_w = the weight of water per unit volume.

(b) The upward pressure $\Delta_w (h + bI)b^2$, due to the gradient I in the space nearest to the cube, acting on the lower side of the cube.

(c) The upward pressure $\Delta_w K b^2 \frac{V_v^2}{2g}$ due to the impulse of percolation velocity, in which K is a coefficient depending on the flow around the stones, V_v is the actual velocity in the voids which for the general case may be obtained from the formula:

$$V_v = \frac{V_p}{p} = C_o' \sqrt[m]{\sqrt{d^{m-2}}\, l^{3-m}}$$

(d) The uplift due to percolation flow, or its pushing out action upon the stones T, where

$$T = \Delta_w (h + bI)b^2 - \Delta_w h b^2 + K b^2 \frac{\Delta_w V_v^2}{2g}$$

$$= \Delta_w \left(Ib^3 + K b^2 \frac{V_v^2}{2g}\right)$$

$$= b^3 \Delta_w \left(I + K \frac{V_v^2}{2gb}\right)$$

With the above discussion as a basis let us now turn to the fundamental problem of this chapter - that of establishing the law of hydraulic similitude for the uplift due to percolation flow.

The relation of model to prototype elements for uplift pressure may be written

$$\frac{T_1}{T_2} = \frac{b_1^3 \Delta_{w_1} \left(I_1 + K_1 \frac{V_{v_1}^2}{2gb_1}\right)}{b_2^3 \Delta_{w_2} \left(I_2 + K_2 \frac{V_{v_2}^2}{2gb_2}\right)}$$

For geometrical similarity $b_1^3 = \lambda^3 b_2^3$, for the same fluid in model and prototype ($\Delta_{w_1} = \Delta_{w_2}$) and for the same gradient $I_1 = I_2$*, therefore:

$$\frac{T_1}{T_2} = \lambda^3 \frac{\left(I_1 + K_1 \frac{V_{v_1}^2}{2bg_1}\right)}{\left(I_2 + K_2 \frac{V_v^2}{2gb_2}\right)} \qquad (26)$$

Direct use of the Froude rule shows the uplift in the model and prototype to vary as the cube root of the scale ratio (see Table 19(, that is:

$$\frac{T_1}{T_2} \text{ varies as } \lambda^3$$

It is therefore evident that the corrective coefficient to be applied to the Froude rule in this case would be

$$A_t = \frac{1+K_1\left(\frac{V_{v_I}^2}{2gb_1 I_1}\right)}{1+K_2\left(\frac{V_{v_2}^2}{2gb_2 I_2}\right)} \qquad (27)$$

If the magnitudes of flow factors are approximately equal** and the porosity coefficients are also approximately equal,

$$K_1 = K_2 \text{ and } p_1 = p_2$$

it may be seen that

$$A_t > 1$$

* It is to be noted that this equality, even for geometrically similar structures and heads, may be accepted only if the form of the stream lines and equipotential lines is the same in model and prototype.

** To assure this being the case it is necessary that the shape of fragments be essentially the same in model and prototype.

A_t will be equal to unity only if the velocities in the voids are in the ratio of Froude's rule, that is

$$V_{v_1}^2 = \lambda V_{v_2}^2 \quad \text{also} \quad b_1 = \lambda b_2 \quad \text{and} \quad V_{v_1} = \lambda^{0.5} V_{v_2} \qquad (28)$$

If this were the case,

$$K_1 \frac{V_{v_1}^2}{2gb_1 I_1} = K_2 \frac{V_{v_2}^2}{2gb_2 I_2}$$

and A_t would equal unity.

But as shown in the previous section

$$V_{p_1} = \lambda^{0.5} A_f V_{p_2} \qquad (29)$$

whence $A_f > 1$

and consequently, instead of equation (28) we obtain for actual velocity in the voids,

$$V_{v_1} = \frac{V_{p_1}}{p_1} \quad \text{and} \quad V_{v_2} = \frac{V_{p_2}}{p_2}$$

when $p_1 = p_2$

$$V_{v_1} = \lambda^{0.5} A_f V_{v_2}$$

From which, taking into account expression (29) it is clear that

$$K_1 \frac{V_{v_1}^2}{2gb_1 I_1} > K_2 \frac{V_{v_2}^2}{2gb_2 I_2}$$

and consequently $A_t > 1$.

The condition

$$T_1 = \lambda^3 A_t T_2$$

may be expressed as follows:

With the same effective gradients, form of stones, and porosity, as well as the same fluid percolating with the same character of flow through geometrically similar rockfill, the uplift due to percolation flow in the prototype will be larger than that stepped up from the model according to Froude's rule. It is clear therefore that stepped-up values indicate greater stability of stones against flotation by percolation than is actually obtained in the prototype. To show the extent of this false excess stability let us consider a case in which the percolation flow is laminar in the model and turbulent in the prototype. Referring to Equation (27) we see that the factor

$$\frac{K_2 V_{v_2}^2}{2gb_2}$$

may be neglected as compared owing to the small velocities encountered in laminar flow. The magnitude of

$$V_{v_1}^2 = \frac{V_{p_1}^2}{p_1^2}$$

corresponding to turbulent percolation flow may be obtained from the equation $V_p = p C_o \sqrt{bI}$ in which $V_v^2 = \frac{V_p^2}{p^2} = C_o^2 bI$.

Using the above two considerations in Equation (27) we obtain

$$A_t = 1 + K\left(\frac{C_o^2}{2g}\right)$$

With $C_o = 20$ and $K = 1$, as was mentioned in the previous section,

$$A_t = 1 + \frac{20^2}{2 \times 981} = 1.20 \quad \text{(metric units)}$$

It should be noted that in many cases the value of A_t given above will be considerably increased owing to the fact that with small scales, the forces of cohesion in the material, which are not taken into account, and which may be developed in the model, will increase the stability of stones in the model against flotation by percolation flow while the presence of vacuum in the prototype, also not taken into account in this example, will increase the uplift in full-scale conditions and, therefore, the surface fragments may be pushed out of the prototype even when the corresponding model tests indicate A_t less than unity.

SECTION 38. Summary.

In Table 20 is presented a summary of data obtained in this chapter. Referring to that part of the table dealing with phenomenon #1, it is seenthat the values of critical transporting velocity

stepped up to full-scale conditions from small -scale models by Froude's rule alone, will show higher displacement velocities than those which actually occur in the prototype, and hence the corresponding value of A_a must be <1. However, for larger models (1:15 or 1:10) the values stepped up by Froude's rule alone will equal the prototype values or $A_a = 1$. Phenomenon #2 does not appreciably effect the transference made in accordance with Froude's law. Phenomena #3 and #4 introduce an error on the side of safety in recalculating prototype values from small-scale models in accordance with Froud's law. In transferring results from small -scale models to the prototype, the actual prototype volocity of water moving along the face of the full-scale dam is less than the value recalculated from the model tests by use of Froude's rule ($A_c < 1$). Also, the actual percolation flow is greater than the stepped -up value ($A_f > 1$) which means that the velocities of water moving along the face of the prototype dam in nature will be less than obtained from model tests and stepped up by Froude's rule alone. Phenomenon #5 , however, operates to reduce the factor of safety, since, the values of uplift indicated by stepped up small scale model tests in accordance with Froude's law, are smaller than those actually occurring in nature; in other words $A_t > 1$.

The resultant effect of these various individual phenomena upon the stability of the submerged dam thus depends largely upon the interaction of the three following tendencies: Phenomena #3 and #4 tend to give more stable prototype structures when transference is made from the model according to Froude's rule. Phenomena #5 has the opposite effect. The predominating effect may be found for any particular scale ratio and for any definite profile either by means of the methods presented in Chapter V (taking into account the corrective coefficient A), or by means of experimental investigation of the effect of scale upon the phenomena as a whole. In this paper only the results of the latter method will be given.

SECTION 39. Experimental Investigation of the Effect of Scale upon the Phenomena as a Whole.

Experiments were performed upon these models at scale ratios of 1:1, 1:2.4, and 1:4.5. Laboratory conditions were maintained the same for all experiments, that is the same flume and the same method of depositing the stones were used. The experiments were performed by the author with the assistance of J. G. Satylnjikov. Concrete cubes were used to insure strict geometric similarity, and the discharges passing the cube fill were held to those computed by Froude's rule for the given dimension of cube used.

The results of the experiments, stepped-up by Froude's rule to the same prototype scale, having the cross-sections of the submerged dam plotted as abscissas, and water rise in the upper pool as ordinates, are shown in Figure 45. From this chart the cross-sections corresponding to different scale ratios at any given head may be otained. A horizontal line drawn from some predetermined value of head, intersects the curves of scale ratios at abscissa values corresponding to the area different cross -sections.

TABLE 20

CORRECTION COEFFICIENTS TO FROUDE'S LAW FOR THE TRANSFERENCE OF MODEL TEST VALUES

No.	Variable to be Investigated	Formula for Transfer	Expression for Correction Coefficient
1	Impulse force of overflow on individual stones.	$V_1^2 = A_a V_2^2$	$A_a = \left(\frac{p_1}{p_2}\right)\left(\frac{K_2}{K_1}\right)\left(\frac{E_2}{E_1}\right) S^2\left(\frac{1}{n_2} - \frac{1}{n_1}\right)$
2	Discharge over top of dam	$q_1 = \lambda^{2.5} A_b q_2$	$A_b > 1$
3	Velocity of overflow over top of dam.	$V_1 = \lambda^{0.5} A_c V_2$	$A_c = \frac{C_1}{C_2}$
4	Percolation velocity through rockfill dam	$V_{p_1} = \lambda^{0.5} A_f V_{p_2}$	$A_p = \frac{Co_1 \left(d_2\right)^{\frac{1.5m-3}{m}} \left(I\right)^{\frac{0.5m-1}{m}}}{\left[0.001^{\frac{2-m}{m}}\right] C_o \frac{m-2}{m}}$
5	Percolation uplift force on individual stones on surface of downstream slope.	$T_1 = \lambda^3 A_t T_2$	$A_t = \frac{\left(\frac{V_{v_1}^2}{2gb_1 I_1}\right)^{1+K_1}}{\left(\frac{V_{v_2}^2}{2gb_2 I_2}\right)^{1+K_2}}$

Subscript 1 denotes prototype; subscript 2 denotes model
Geometric similarity is presupposed for dam profile, surface roughness and shape of constituent stones.

TABLE 20 (CONTINUED)

Magnitude of A compared to unity	Remarks
$A_a < 1$	For λ = 20 and moderate velocities in full-scale prototype.
$A_a = 1$	For λ = 20 and high velocities in full-scale prototype.
$A_a > 1$	At very high velocities in prototype and high dissolved air content.
A_b slightly greater than 1	Practically no correction to Froude scale ratio Necessary.
$A_c > 1$	For small models and comparatively rough surface in prototype.
$A_c < 1$	For large models, steep downstream slopes and rough surface in prototype
$A_p > 1$	A_p approaches unity when $\lambda = 1$.
$A_t > 1$	$A_t > 1$ for all model scales except 1:1.

It is seen that the maximum value of cross-section will be obtained, for any given head, from the intersection with curve C, i.e. at the smallest scale. In passing to larger models, that is, in the transition from model to prototype, the cross-sections indicated are smaller. This proves that with recalculation from model to prototype conditions in accordance with Froude's rule, the results of model investigations on dumping stones in flowing water would give a safety factor, i.e. in reality the volume of prototype dumping will prove to be somewhat smaller than one obtained by recalculation from models according to Froude's rule.

It is now clear which of the five phenomena have greatest influence in the transition from model to prototype. These are phenomena #3 and #4; phenomena #1 and #2 are neutral, while phenomenon #5 is apparently counteracted by #3 or #4.

This knowledge gives a more exact basis for recalculation. It also shows the necessity in constructing models of increasing or at least maintaing, the relative roughness of the shooting flow area and of also increasing or maintaining the relative percolation flow through the submerged dam.

It is seen that the curves intersect near their extremities. The experiments show this to correspond to elongated base widths and it may be explained by the decreased percolation flow encountered on elongated profiles with a consequent weakening of the influence of phenomenon #4. Abrupt changes in the slope of the curve are due to a downstream mass movement of the stones when the existing slopes become unstable. Following this downstream movement the cross-section increases rapidly with little correspond ing increase in head. However, as this phenomena is common to models of any scale whatever it need not be further considered here.

CHAPTER VI

CALCULATIONS FOR ROCKFILL DAM DESIGN

SECTION 40. The Fundamental Problem.

The basic problem in rockfill dam design is to determine the profile corresponding to the following given data:

Equivalent spherical diameter of available stone = d feet.
Unit weight of available stone = Δ_s pounds per cubic foot.
Discharge of stream per foot width = q_t c.f.s. per foot.
Original depth of stream = h_t feet.
Required difference in headwater and tailwater elevation subsequent to construction = Z_s feet.

At certain sites it is necessary to limit the base width of the profile to a certain predetermined value L_o, in which case the required equivalent spherical diameter of stone becomes the basic variable to be determined.

On many projects a side-channel spillway or by-pass tunnel is provided to handle part of the stream discharge during construction, and in such instances the unit main channel discharge q_t decreases as the reservoir level rises, owing to the increased capacity of the by-pass. However the two detailed modifications given, as well as several others, are all included in the basic problem as stated initially.

The hydraulic features controlling any particular design are themselves very largely influenced by the following factors:

(a) The effective width of river measured along the crest of dam, taking into account the actual distribution of stream velocities in determining the proper value of q_t.

(b) The determination of the stream discharges to be expected during the construction period, including estimates of duration.

(c) The composition and grading of stones available at the site.

(d) The necessity for passing ice during construction.

(3) The construction schedule and machinery to be employed for handling and dumping material.

As would naturally be expected from the earlier portions of the text, the procedure in designing will be separated into two steps corresponding to the two basic hydraulic conditions, the submerged flow condition and the free-overflow condition. In addition a number of simplifying assumptions will be introduced

to reduce the labor of calculation.

At the stage of submerged flow, the critical transporting velocities occur on the top or crest surface of the partially completed cross-section and consequently desing calcuations for this stage will be limited to consideration of the top horizontal surface.

At the stage of free overflow the critical transporting velocities occur on the downstream slope; but, as will be shown subsequently, the practical effect of changes in angle of downstream face is so slight that it may be neglected in calculating the coefficient of stone stability, Y.

Since, as previously outlined, very little is known regarding the energy loss in channels of great roughness and large slope, a very conservative value, n = 0.04, will be selected as the coef ficient of roughness in the Manning formula, and as an additional factor of safety, the dissipation of energy resulting from the impact of percolation discharge and overflowing nappe will be neglected.

In Section 46, a detailed comparison will be made between profiles for a specific job, as determined by calculation and by laboratory experiments.

SECTION 41. Notation.

The following notation (Figures 46 and 47) will be used as a basis for developing design computations:

q_t = the combined percolation and overflow discharge in cubic feet per second per foot length of dam crest. (Deducting any portion of natural discharge carried by by-pass structures).

q_p = the total percolation discharge in cubic feet persecond per foot length of dam crest.

$q = q_t - q_p$ = The net overflow discharge in cubic feet per second per foot length of dam crest.

$V_q = \frac{q_t}{h_t}$ = the original natural discharte velocity of the stream below the dam in feet per second, corrected if necessary to include the effect of by-passing structures.

h_t = the depth of tailwater above the channel bottom in feet.

V = the velocity of flow acting on the individual stones of the dam, in feet per second.

V_a = the velocity of approach in feet per second.

V_p = the velocity of percolation flow in feet per second.

z_o = the difference in head and tailwater elevation for the free overflow condition in feet.

Z_s = the difference in head and tailwater elevation for the submerged flow condition in feet.

h_t = the height of the downstream edge of crest above the channel bottom in feet.

h_s = the difference in elevation in feet between the tailwater surface and the downstream edge of dam crest.

$S = \frac{h_s}{h_t}$ = the ratio between the head on the downstream edge of crest and the tailwater depth h_t.

H = the maximum height of dam in feet.

L_o = the base width of dam in feet.

i_o = the slope of crest for the free overflow condition or tangent α.

l_p = the length of percolation for the free overflow condition in feet.

l'_p = the length of percolation path for the submerged flow condition in feet.

d = the size of stone reduced to the diameter of an equivalent sphere in feet.

Δ_s = the unit weight of stone in pounds per cubic foot.

Δ_w = the unit weight of water in pounds per cubic foot.

I = the average hydraulic gradient for percolation flow.

p = the natural porosity or void ratio of the rockfill.

C_o = a generalized coefficient of the Chezy type, modified and adapted to apply to percolation flow.

ϕ = the broad-crested weir coefficient for the submerged condition in formula $q = \phi\, h_c \sqrt{2g(h_c + Z_s + \frac{v_a^2}{2g})}$

SECTION 42. The Analytical Method of Calculation.

The first step in the analytical method of calculation is to determine the maximum limiting height of dam section at which the character of the overflow will still be submerged rather than free, remembering that the critical velocity for transporting component individual stones on the crest for the submerged stage is from Section 6:

$$v_t = Y_t \psi \sqrt{d}$$ in which

Y_1 = from 0.86 to 0.90 and $\psi = \sqrt{2g\ \left(\frac{\Delta_s - \Delta_w}{\Delta_w}\right)}$ (2)

Assuming the unit percolation discharge equal to q_p we find that:

$$q = q_t = q_p$$

From Equation (2) above:

$\frac{q}{h_s}$ must be less than v_1 .

Since the so-called critical flow depth marks the lower limit of the submerged flow condition, it appears that for this stage:

h_s must be greater than $0.6\ (h_s + Z + \frac{v_a^2}{2g})$

Now q may be expressed in terms of h_s and Z_s by applying the Berneuilli equation to sections 1-1 and 2-2, Figure 46, as follows:

$$q = \phi\, h_s \sqrt{2g\ (Z_s + \frac{v_a^2}{2g})} \qquad (30)$$

Values of h_s and Z_s may be determined from the above formula by the method of trial and error.

Then the required height h_1, is obviously

$$h_1 = h_t - h_s$$

Now since we know from Section 30 that

$$l_p' = 1.7\ h_1$$

and also

$$I = \frac{Z_s}{l_p'}$$

We may next revise the assumed value of percolation flow q_p in accordance with the formula $q_p = v_p h_1$, in which $v_p = C_o p \sqrt{dI}$ and $C_o = 3.623 - \frac{0.0832}{d}$, the stone dimension d being expressed in feet. If the assumed value of q_p differs appreciably from the value obtained by substitution in the above formula it will be necessary to repeat the entire calculation using the latter value. In this way h_1 may be determined to the desired degree of accuracy by the method of successive approximations.

For the free overflow condition it is necessary to make computations for successive stages of the construction, using the head and tailwater conditions that are critical at each particular stage. This first step is, as in the previous case, to assume a value for the percolation flow and then compute:

$$q = q_t - q_p$$

The maximum permissible transporting velocity v_3, may then be computed from the relation:

$$v_3 = y_3 \psi \sqrt{d}$$

in which Y_3 = from 1.10 to 1.20 and $\psi = \sqrt{2g \left(\frac{\Delta_s - \Delta_w}{\Delta_w} \right)}$

Also, (Figure 17)

$$h_o = \frac{q}{v} \quad \text{or} \quad v = \frac{q}{h_o} \tag{31}$$

According to the Chezy formula

$$v = C \sqrt{Ri}$$

or for all practical purposes, since in the case of a wide river, R is substantially equal to h_o,

$$v = C \sqrt{h_o i} \tag{32}$$

Using the well-known Manning formula, the coefficient C may be expressed:

$$C = \frac{1.486}{n} R^{1/6} = \frac{1.486\, h_o^{1/6}}{n} \tag{33}$$

in which n is the roughness coefficient.

Combining equations (31), (32), and (33):

$$\frac{q}{h} = \frac{1.486}{n} h_o^{1/6} h_o^{\frac{1}{2}} i^{\frac{1}{2}} = \frac{1.486}{n} \cdot h_o^{2/3} i^{\frac{1}{2}}$$

or

$$h_o = \left[\frac{n\, q}{1.486\, i^{\frac{1}{2}}} \right]^{0.6} \tag{34}$$

and

$$i = \frac{n^2 q^2}{2.21\, h_o^{3.33}} \tag{35}$$

Taking n = 0.04 (a conservative low value).

$$h_o = \left[\frac{.026q}{i^{0.5}} \right]^{0.6} \tag{36}$$

and

$$i = \frac{.0007\, q^2}{h_o^{3.33}} \tag{37}$$

Using Equation (37) we may calculate i from q and h_o; then assuming a difference Z_o between head and tailwater levels, we may calculate the base width of dam, L_o, from the expression

$$L_o = 1.25 \left(h_1 + h_t + Z_o - h_o\right) + \frac{Z_o}{i} \qquad (13)$$

Equation 13 being readily obtained from the geometry of Figure 47. Now also according to the geometry of Figure 47:

$$l_p = \sqrt{h_1^2 + \left(H + \frac{Z_o}{i}\right)^2} \qquad (11)$$

In which $H = h_t + Z_o - h_o$

The percolation gradient I may then be found from the relation:

$$I = \frac{Z_o}{l_p}$$

The assumed percolation flow may now be checked from the formula

$$q_p = v_p H$$

in which

$$v_p = C_{op} \sqrt{dI}$$

If there is any appreciable difference between the assumed and calculated percolation flows, the calculation should be repeated and the desired degree of accuracy obtained by the method of successive approximations as in the case of the submerged flow stage.

SECTION 43. Development of Charts.

To save the time and labor required in making trial and error computations the following series of graphical charts has been prepared:

Graph I, Figure 48, has been prepared for determining the critical transporting velocities for displacing rounded stones of diameter d feet, having unit weights, Δs, or 175, 165, and 155 pounds per cubic feet. The critical velocities for the stage of submerged flow have been calculated from the formula:

$$V_1 = Y_1 \psi \sqrt{d}$$

in which $Y_1 = 0.86$ and $\psi = \sqrt{2g\left(\frac{\Delta_s - \Delta_w}{\Delta_s}\right)}$

The corresponding critical velocities for the stage of free overflow have been computed from the equation:

$$V_3 = Y_3 \psi \sqrt{d}$$

in which $Y_3 = 1.20$ and $\psi = \sqrt{2g \left(\frac{\Delta_s - \Delta_w}{\Delta_s} \right)}$

For convenience in designing, an additional curve has been plotted giving the total weight of stones in this for various diameters.

Graphs II and III, Figures 49 and 50, have been prepared to facilitate computations for the stage of submerged flow. Dividing both sides of Equation (30):

$$q = \phi h_s \sqrt{2g \left(Z_s + \frac{V_a^2}{2g} \right)} \qquad (30)$$

By h_t, we obtain:

$$\frac{q}{h_t} = \phi \frac{h_s}{h_t} \sqrt{2g \left(Z_s + \frac{V_a^2}{2g} \right)}$$

Now denote $\frac{q}{h_t}$ by v_q - the average unit "filament velocity" below the dam; based on the net discharge only, that is with percolation flow deducted in obtaining q.

And let $s = \frac{h_s}{h_t}$ = the ratio between the head on the downstream edge of crest and the tailwater depth h_t.

Equation 30 may then be rewritten as follows:

$$V_q = \phi s \sqrt{2g \left(Z_s + \frac{V_a^2}{2g} \right)}$$

whence $$Z_o = \frac{V_q^2}{2gs^2 \phi^2} - \frac{V_a^2}{2g}$$

Furthermore, since the coefficient ϕ has a value of the order of 0.90 and since, in addition, the percolation discharges for the submerged flow condition are on the average about 10 per cent of the total discharges, we may safely assume that for V_q in the range between 1 and 12 feet per second:

$$V_q = \phi V_a$$

Then: $$Z_s = \frac{V_q^2}{2gs^2 \phi^2} - \frac{V_q^2}{2g\phi^2} = \frac{V_q^2}{2g\phi^2} \left(\frac{1}{s^2} - 1 \right)$$

Using an average value of $\phi = 0.92$ we obtain:

$$\Sigma_s = 0.0183\, v_q^2 \left(\frac{1}{S^2} - 1\right)$$

GRAPHICAL CHART II, Figure 49, has been prepared from the above formula by assigning various values to the velocity v_q and the ratio $S = \frac{h_s}{h_t}$

Then by assuming that the flow over the crest is at the critical depth:

$$h_s = 0.6 \left(h_s + \Sigma_s + \frac{v_q^2}{2g\phi^2} \right)$$

and since h_s may be replaced by sh_t

$$h_t = \frac{1.5\,\Sigma_s + 0.0273\, v_q^2}{s}$$

Now on any given curve of the v_q family, we may spot the position of any selected integral value of h_t by successive trial and error substitutions of Σ_s and s in the above expression. The family of curves for various selected integral values of h_t was plotted in this way.

Since the lower limiting position of tailwater elevation for the submerged state is marked by the water surface elevation for overflow at the critical depth on the crest, it is evident that only such v lues of Σ_s and s as lie below the curve of h_t for the case in question, will be included in the submerged flow state.

For example, if the given original depth of river be h_t = 15 feet, we may use only that part of the chart lying below the curve marked $h_t = 15$.

To summarize, Graphical Chart II consists of two families of intersecting curves, plotted against Σ_s and s as coordinates. The first family corresponds to different constant values of v_q and the second to different constant values of h_t.

For given values of v_q, h_t, and s the value of h_s, the head in the downstream edge of crest, and v, the velocity acting on the individual stones, may easily be calculated from the equations:

$$h_s = s\, h_t \qquad q = v_q h_t \text{ and } v = \frac{q}{h_s}$$

Graphical Chart III, Figure 50, has been prepared for the submerged condition from the above equations by plotting the velocities acting upon the individual stones at the top of the dam as ordinates against the coefficients ($s = \frac{h_s}{h_t}$) as abscissas.

This chart also consists of two families of intersecting curves, the first of which corresponds to different constant values of v_q and the second of which corresponds to the lower limiting constant values of h_t for the submerged conditions, exactly as explained for Chart II. In other words if h_t = 15 feet, we may use only the portion of the chart lying below the curve marked h_t=15.

Graphical Chart IV, Figure 51 has been plotted from the expression:

$$vp = C\ p\ \sqrt{d\ I}$$

using v_p and d as coordinates, taking the void ratio, p, at 35 per cent, and assuming I constant for various selected values of percolation gradient.

Graphical Chart V, Figure 52, has been constructed for the state of free overflow in accordance with Equation (36):

$$h = \left(\frac{.026q}{i^{0.5}}\right)^{0.6} \qquad (36)$$

for values of q from 3 to 500 c.f.s. and for values of i from 0.04 to 0.40.

SECTION 44. Calculation by means of Charts.

To illustrate the use of the graphical charts, assume that Δ_s, d, q_t, and h_t are given and that it is required to determine the dimensions of the submerged dam.

For the submerged flow condition with d and Δ_s given, we find the maximum permissible velocity v from Graphical Chart I. Assuming a value for the percolation discharge q_p, we calculate:

$$q = q_t - q_p \text{ and } v_q = \frac{q}{h_t}$$

Now entering Chart III on the ordinate corresponding to the limiting velocity v, we draw a horizontal line over to intersect with the curve corresponding to v_q. If the point of intersection lies below the h_t curve for the given value of h_t, then the vertical drawn downward through the point of intersection gives the proper value of s directly. If however, the point of intersection of the horizontal line through v with the corresponding v_q curve lies above the h_t curve, corresponding to the given value of h_t, it is necessary to lower the horizontal line until the point of intersection with the v_q curve comes to meet the proper h_t curve, which in this case will determine the proper value of s.

After determining s, we find by calculation:

$$h_s = s\ h_t\ ;\ h_c = h_t - h_c\ ;\ l'_p = 1.7h_c$$

Now entering Chart II with the above value of s we determine the value of Z_s and substitute in the equation:

$$I = \frac{Z_s}{q_p}$$

Then using Chart IV, with the given stone size d, and the above value of I we determine the permissible velocity V_p and recalculate the corresponding percolation discharge.

$$q_p = V_p h,$$

If q_p agrees substantially with the assumed value, no further calculation is required for the submerged stage. If any appreciable difference exists between the assumed and calculated values of q_p, the computations must be repeated using the new value of q_p until the repeated trials show a reasonable agreement. In this way it is possible to obtain the value h_o to any desired degree of refinement.

For the stage of free overflow, the method of procedure is to make a separate calculation for each pertinent value of Z_o, the difference in elevation between the head and tailwater.

Assuming a value for the percolation dishcarge q_p, we determine by calculation:

$$q = q_t - q_p$$

We next determine from Chart I the value of the limiting transporting velocity V, for the given vlaues of d and Δ_s. Then by calcuation

$$h_o = \frac{q}{v}$$

Using Chart V and drawing a horizontal line from the above value of h_o over to intersect the curve corresponding to q, we find the correct abscissa i by projecting down form the intersection.

Using the assumed value Z_o, we find the height of dam H from thr relation

$$H = h_t + Z_o - h_o$$

Also

$$l_p = \sqrt{h_t^2 + \left[H + \frac{z_o}{i}\right]^2} \quad \text{and} \quad I = \frac{z_o}{l_p}$$

From the above value of I and the given stone size, the permissible percolation velocity V_p, may be determined by means of Chart IV, and the assumed value of percolation discharge checked by substitution in the formula

$$q_p = V_p H$$

If there is good practical agreement between the assumed and computed values of percolation discharge, the computation may be completed by determining the base width of dam from the relation:

$$L_o = 1.25 (h_t + h_t + z_o - h_o) + \frac{z_o}{i}$$

If however, there is any appreciable difference between the assumed and computed value of percolation discharge, it will be necessary to continue the trial computations until satisfactory agreement is reached.

The method of calculation will be made clearer by the following numerical example.

SECTION 45. Numerical example of calculation of dam profile.

Given a stone of rounded shape having an equivalent spherical diameter of 1.38 feet and having a unit weight of 166 pounds per cubic foot.

Required to determine the dimensions of the submerged dam constructed by dumping the above material into a stream having a natural depth h_t = 19.7 feet, so as to create a difference in elevation of 12.1 feet between headwater and tailwater for a discharge of q = 57.5 c.f.s. per foot width of stream. A by-pass tunnel is provided having the discharge capacities shown by Table 21.

The sequence of computation will be the same as outlined in the previous paragraph.

Submerged Flow Condition - Chart I

For d = 1.38 feet and Δ_s = 166 lb. per cu. ft., the weight of individual stone W = 200 lb. and the corresponding maximum permissible velocity = 10.6 feet per second.

Now as a trial value assume a percolation flow equal to 10% of the river discharge, which is given as q_t = 57.5 per ft. width of river bed, or

$$q_p = 0.10 \times q_t = 0.10 \times 57.5 = 5.75 \text{ c.f.s./ft.}$$

$$q = q_t - q_p = 57.5 - 5.75 = 51.75 \text{ c.f.s./ft.}$$

$$v = \frac{51.75}{19.70} = 2.63 \text{ f.p.s.}$$

Entering Chart III with V = 10.6 f.p.s. we draw a horizontal line over to intersect the curve corresponding to V_{q_t} = 2.63 f.p.s. (by interpolation between curves marked v_q = 2 and v_q = 3). Dropping a vertical from this point, we read on the axis of abscissas:

$$S = 0.25$$

As the above intersection is located below the curve marked h_t + 19.70 the given conditions correspond to the submerged flow state and Chart I is applicable.

By substitution:

$$h_c = sh_t \; ; \; 0.25 \times 19.70 = 4.93 \text{ ft.}$$

$$h_1 = h_t - h_c = 19.70 - 4.93 = 14.77 \text{ ft.}$$

$$l_p = 1.7 \, h_1 = 1.7 \times 14.77 = 25.10 \text{ ft.}$$

Entering Chart II with s = 0.25 we erect a vertical up to intersect with the curve corresponding to v_q = 2.63 f.p.s. (by interpolation between curves marked v_q = 2 and v_q = 3). Drawing a horizontal line from the point of intersection over to the axis of ordinates we find

$$Z_s = 1.97 \text{ feet}$$

As the intersection with the curve for v = 2.63 lies below the curve h_t = 19.70, the conditions conform to the submerged flow state.

Checking back against the discharge rating table for the tunnel by pass we find that since Z_s = 1.97 feet is less than 4.10 feet. the discharge through the by pass is zero.

With Z known we can compute

$$I = \frac{Z_s}{lp} = \frac{1.97}{25.10} = 0.08$$

Also, using, Chart IV, for d = 1.38 feet and I = 0.08 we find

$$V = 0.43 \text{ f.p.s.}$$

and $q_p = V_p h_1 = 0.43 \times 14.77 = 6.35$ c.f.s.
Since q_p was assumed equal to 5.75 c.f.s. it will not be necessary to make a second trial computation.

Free Overflow Condition - Using Chart I we find that for d = 1.38 feet and Δ_s = 165 lb. per cu. ft., the maximum permissible velocity

$$V = 14.75 \text{ f.p.s.}$$

Let us now consider 6 stages of construction corresponding to 6 specific differences in elevation between headwater and tailwater as given in Table 21, showing the distribution of discharge between the river bed and by-pass.

Head Difference No. 1

Z_o = 4.10 feet $\qquad\qquad$ q_t = 57.5 c.f.s./ft.

Assuming the filtration flow as 12% of the river discharge

$$q_p = 0.12 \times 57.5 = 6.90 \text{ c.f.s./ft.}$$

$$q = q_t - q_p = 57.5 - 6.90 = 50.6 \text{ c.f.s./ft.}$$

$$h_o = \frac{q}{v} = \frac{50.6}{14.75} = 3.43 \text{ ft.}$$

Entering Chart V with h_o = 3.43 feet and q = 50.6 c.f.s./ft. we find

$$i = 0.031$$

Aslo $\quad H = h_t + Z_o - h_o = 19.70 + 4.10 - 3.43 = 20.37$ ft.

Then

$$l_p = \sqrt{h_1^2 + \left[H + \frac{Z_o}{i}\right]^2} = \sqrt{14.77^2 + \left[20.37 + \frac{4.10}{0.031}\right]^2} = 153 \text{ ft.}$$

$$I = \frac{Z_o}{l_p} = \frac{4.10}{153.0} = 0.0268$$

Entering Chart IV with d = 1.38 feet and I = 0.0268 we obtain V_p = 0.30 feet per second from which we obtain:

$$q_p = V_p H = 0.30 \times 20.37 = 6.11 \text{ c.f.s./ft.}$$

The discrepancy between the assumed percolation flow q_p = 6.90 c.f.s./ft. and the calculated value q_q = 6.11 c.f.s./ft. is about

10%, which is within the desired limit of accuracy so that no second trial computation is necessary. We may now compute the base width of dam.

$$L_o = 1.25\ (h_t + h_1 + Z_o - h_o) + \frac{Z_o}{i}$$

$$= 1.25\ (19.70 + 14.77 + 4.10 - 3.43) + \frac{4.10}{0.031} = 176 \text{ ft.}$$

Head Difference No. 2

$Z_o = 5.90$ feet $\qquad\qquad$ $q = 49.50$ c.f.s./ft.

Assuming a percolation flow of 20%

$$q_p = 0.20 \times 49.50 = 9.90 \text{ c.f.s./ft.}$$

and $q = q_t - q_p = 49.50 - 9.90 = 39.60$ c.f.s./ft.

$$h_o = \frac{q}{v} = \frac{39.60}{14.75} = 2.68 \text{ ft.}$$

According to Chart V for $h_o = 2.68$ and $q = 39.60$

$$i = 0.045$$

Hence $H = h_t + Z_o - h_o = 19.70 + 5.90 - 2.68 = 22.92$ feet

$$l_p = \sqrt{h_1^2 + \left[H + \frac{Z_o}{i}\right]^2} = \sqrt{\frac{}{14.77}^2 + \left[22.92 + \frac{5.90}{0.045}\right]^2} = 155 \text{ feet}$$

and $$I = \frac{Z_o}{i_p} = \frac{5.90}{155} = 0.04$$

According to Chart IV; for $I = 0.04$ and $d = 1.33$ feet, $v = 0.30$ feet per second and $q_p = v_p H = 0.30 \times 22.94 = 6.90$ c.f.s./ft.

The discrepancy between the assumed value of percolation flow $q_p = 9.90$ and the computed value $q_p = 6.90$ is in this case about 40% so that a second trial computation will be necessary.

Assuming $q_p = 15\%$ of q_t

$$q_p = 0.15 \times 49.50 = 7.45 \text{ c.f.s./ft.}$$

and $q = q_t - q_p = 49.50 - 7.43 = 42.07$ c.f.s./ft.

and $$h_o = \frac{q}{v} = \frac{42.07}{14.75} = 2.85 \text{ feet}$$

According to Chart V for $h_o = 2.85$ and $q = 42.07$,

$$i = 0.04$$

Then $H = h_t + Z_o - h_o = 19.70 + 5.90 - 2.85 = 22.75$ feet

$$l_p = \sqrt{h_1^2 + \left[H + \frac{Z_o}{i}\right]^2} = \sqrt{14.77^2 + \left[22.75 + \frac{5.90}{0.04}\right]^2} = 171 \text{ feet}$$

$$I = \frac{Z_o}{l_p} = \frac{5.90}{171} = 0.035$$

According to Chart IV for $I = 0.035$ and $d = 1.38$ feet

$$V_p = 0.30 \text{ feet per second}$$

and $q_p = V_p H = 0.30 \times 22.75 = 6.85$ c.f.s./ft.

In the case of this second trial the discrepancy between the assumed percolation flow $q_p = 7.43$ and the computed percolation flow $q_p = 6.85$ is about 10% which is within the desired limits of accuracy.

$$L_o = 1.25 (h_t + h_1 + Z_o - h_o) + \frac{Z_o}{i} = 1.25 (19.70 + 14.77 + 5.90 - 2.85)$$

$$+ \frac{5.90}{0.04} = 194 \text{ feet}$$

The above value of 194 feet is greater than the base width for the first head difference, 176 feet. In other words the submerged dam continues to widen.

Head Difference No. 3

$Z_o = 6.56$ $\qquad$ $q_t = 40.7$ c.f.s./ft.

Assuming a percolation flow of 20%

$$q = q_t - q_p = 40.7 - 0.20 \times 40.7 = 32.55 \text{ c.f.s./ft.}$$

$$h_o = \frac{q}{V} = \frac{32.55}{14.75} = 2.20 \text{ feet}$$

Entering Chart V with $h_o = 2.20$ feet and $q = 32.55$ c.f.s./ft. we obtain

$$i = 0.055$$

Because of the comparatively steep slope obtained let us check the height and bottom width of the dam:

$$H = h_t + Z_o - h_o = 19.70 + 6.56 - 2.20 = 24.06 \text{ feet}$$

$$L_o = 1.25 (h_t + h_1 + Z_o - h_o) + \frac{Z_o}{i} = 1.25 (19.70 + 14.77 + 6.56 - 2.20)$$

$$+ \frac{6.56}{0.055} = 157 \text{ feet.}$$

In other words the base width corresponding to the third difference in water levels is less than the base width for the second difference. That is the slope of the downstream face steepens and consequently, to be on the conservative side, the percolation flow will be computed on the basis of the largest value of l_p previously obtained or l_p = 171 feet.

Thus:
$$I = \frac{Z_o}{l_p} = \frac{6.28}{171} = 0.04$$

Referring to Chart V for I = 0.04 and d = 1.38 feet,

$$V_p = 0.30 \text{ feet per second}$$

and $q_p = V_p H = 0.30 \times 24.06 = 7.22$ c.f.s./ft.

As the discrepancy between the assumed percolation discharge q_p = 8.17 c.f.s./ft. and the computed percolation discharge q_p = 7.22 c.f.s./ft. is about 10%, a second trial computation will not be necessary.

4th Difference in Water Surface Elevations

Z_o = 8.20 feet and q_t = 33.1 c.f.s./ft.

Assuming the percolation flow at 30%:

$$q_p = 0.30 \times 33.1 = 9.95 \text{ c.f.s./ft.}$$

and $q = q_t - q_p = 33.2 - 9.95 = 23.25$ c.f.s./ft.

$$h_o = \frac{q}{V} = \frac{23.25}{14.75} = 1.58 \text{ feet}$$

Entering Chart V with h_o = 1.58 feet and q = 23.25 c.f.s./ft. we obtain i = 0.085

from which $H = (h_t + Z_o - h_o) = (19.70 + 8.20 - 1.58) = 26.32$ feet

and $$I = \frac{Z_o}{l_p} = \frac{8.20}{171} = 0.05$$

Entering Chart IV with I = 0.05 and d = 1.38 feet

$$V_p = 0.33 \text{ ft. per second}$$

and $q_p = V_p H = 0.33 \times 26.32 = 8.70$ c.f.s./ft.

As the discrepancy between the assumed value of the percolation flow q_p = 10 c.f.s./ft. and the computed value q_p = 8.70

is of the order of 10%, a second trial computation will not be necessary. The corresponding base width of the dam will be

$$L_o = 1.25\ (h_t + h_1 + Z_o - h_o) + \frac{Z_o}{i} =$$

$1.25\ (19.70 + 14.77 + 8.20 - 1.58) + \frac{8.20}{0.085} = 148$ feet which is less than the value for the second head difference $L_o = 194$ feet.

5th Difference in Water Surface Elevation

$Z_o = 9.85$ feet $\qquad q_t = 24.30$ c.f.s./ft.

Assume percolation flow = 50%

Then $q = 0.50 \times 24.20 = 12.10$ c.f.s./ft.

$$q = q_t - q_p = 24.20 - 12.10 = 12.10 \text{ c.f.s./ft.}$$

$$h_o = \frac{q}{V} = \frac{12.10}{14.75} = 0.82$$

Entering Chart V with $h_o = 0.82$ and $q = 12.10$

$$i = 0.165$$

$$H = (h_t + Z_o - h_c) = 19.70 + 9.85 - 0.82 = 28.73 \text{ feet}$$

and $I = \frac{Z_o}{l_p} = \frac{9.85}{171} = 0.06$

Entering Chart IV and $I = 0.06$ and $d = 1.38$ feet we obtain

$$V_p = 0.36 \text{ feet per second}$$

and $q_p = V_p H = 0.36 \times 28.73 = 10.35$ which agrees closely enough with the assumed percolation value $q_p = 12.10$ c.f.s./ft.

L_o will obviously be less than for the second difference in in water surface elevation.

6th Difference in Water Surface Elevations.

$Z_o = 11.80$ feet and $q_t = 19.30$ c.f.s./ft.

Assuming a percolation discharge of 70%

$$q_p = 0.70 \times 19.25 = 13.50 \text{ c.f.s./ft.}$$

and $q = q_t - q_p = 19.25 - 13.50 = 5.75$ c.f.s./ft.

$$h_o = \frac{q}{V} = \frac{5.75}{14.75} = 0.39 \text{ feet}$$

Entering Chart V with h_o = 0.39 feet and q = 5.75 c.f.s./ft. we obtain

$$i = 0.33$$

Then $H = h_t + Z_o - h_o = 19.70 + 11.80 - 0.39 = 31.11$ feet

$$\text{and } I = \frac{Z_o}{l_f} = \frac{11.80}{170} = 0.07$$

Entering Chart IV with I = 0.07 and d = 1.38 feet we read

$$V_p = 0.40 \text{ feet per second}$$

and $q_p = V_p H = 0.40 \times 31.11 = 12.45$ c.f.s./ft. which agrees closely enough with the assumed percolation discharge $q_p = 13.50$ c.f.s./ft.

7th Difference in Water Surface Elevations

$Z_o = 12.30$ and q = 8.90 c.f.s./ft.

Since in the computation for the 6th water surface difference $q_p = 12.45$ is greater than q = 8.92 c.f.s. it follows that the dam profile came out above the water surface.

SECTION 46. Additional Comments on Calculation. It is apparent from the calculations of the previous paragraph and substantiated by model tests, that a rockfill dam constructed by dumping stones in flowing water goes through a critical stage during which transition is made from the condition of submerged flow to the condition of free overflow. During the critical stage the impulse of the overflow velocity against the individual stones is quite large; but the percolation discharge is still quite small. In addition the portion of the discharge handled by the by-pass tunnel is very small. This stage of construction is well termed "critical", because, it is just at this time that the base width L reaches its maximum value.

As previously noted, the critical stage is readily identified in laboratory model tests. The experiments usually show a slight increase in base width even after the critical stage owing principally to the effect of a few isolated stones not finding anchorage for interlocking and consequently rolling along the downstream face of dam to the toe.

It is particularly important at the critical stage to insure uniform dumping of material along the entire length of dam, and to employ for the most part large stones of similar size to insure interlocking capacity and stability against displacement by the overflow.

In conclusion it may be instructive to compare the results of the previous numerical calculation with the results of 1/25 scale model studies, for the typical stages of submerged flow and free overflow. (See Table 22)

TABLE 21

Number	Difference in Elevation, Headwater & tailwater-feet.	Discharge c.f.s. per ft. width of dam		Summary
		Overflow Plus percolation flow	Discharge through By-pass tunnel	
1	4.10	57.5	0	57.5
2	5.90	49.5	8.0	57.5
3	6.56	40.7	16.8	57.5
4	8.20	33.1	24.4	57.5
5	9.85	24.3	33.2	57.5
6	11.80	19.3	38.2	57.5
7	12.30	8.9	48.6	57.5

TABLE 22

Profile	Height of Dam Feet		Difference in Elevation Headwater and Tailwater Feet		Base Width of dam Feet	
	Calcul.	Exper.	Calculated	Experimental	Calcul.	Exper.
Submerged Flow Condition	14.75	14.60	1.97	1.97		
Free Overflow Condition	31.10	30.20	11.80	11.80	199	135

The difference in headwater and tailwater levels at which the dam profile appears above the water is practically the same whether determined by computation or by model experiments.

The experimental values have been transformed to full scale quantities using the Froude Scale ratio modified in accordance with the principles outlined in Chapter V.

As can readily be seen from Table 22, the agreement between calculated and experimental results is quite satisfactory except for the bottom width of dam L_o, the calculated bottom width (based on an assumed coefficient of roughness n = 0.04 in the Manning formula) being 50% larger than the base width determined by experiment and transferred to full scale values using the Froude scale ratio with proper corrective coefficients. It is believed that this excess base length may be traced to the selection of a very conservative roughness coefficient n = 0.04 and consequently calculations using this value may be considered as limiting maximum values. If the roughness coefficient were assumed as n = 0.06 the resultant profile could probably be considered as having the limiting minimum base width.

After fixing the limiting values of base width as outlined, the selection of the proper intermediate value will depend largely upon the character and size of the particular project. In the case of the larger structures the expense of constructing a laboratory model to check computations would appear to be well warranted.

SECTION 47. Sealing Blanket Construction. An investigation of sealing blanket design and construction should naturally be included in any treatise on rockfill dams, but owing to the complexity of the subject we shall be forced to limit our descussion to the most elementary data as derived from use of the previously described laboratory tests.

Using a model scale of 1 to 100, a purely qualitative study was conducted relative to depositing graded material on the upstream face of dam to serve as a support for, and prevent washing out of the clay or similar colloidal material employed for effecting a final water-tight seal. The basic dimensions of the model are shown by Figure 53.

Without giving any further attention to the mechanism by which sealing is gradually accomplished or to the effect of the air dissolved in the water upon the accuracy of laboratory determinations, we shall proceed at once to the study of position of percolation gradients during the construction of the sealing blanket and the supporting layers of graded material.

In Figure 54, line #1 denotes the position of the percolation gradient for the rockfill only, while line #2 shows the change in position of saturation line after a layer of spalls has been deposited on the upstream face. As can readily be seen from the figure, the layer of spalls has only a negligible effect on the position of the gradient. Line #3 shows a very pronounced dropping of the gradient, due to the addition of a layer of sand upon the upstream face, while the subsequent addition of three layers of clay, as shown by lines #4, #5, and #6 cause the percolation gradient to drop almost to the tailwater level.

It is important to note that the effectiveness of the sealing blanket is not uniform from top to bottom of dam, the sections at the low head having the least effectiveness and the sections deposited near the top causing the percolation gradient to drop sharply, indicating that the major portion of the percolation discharg flows through the upper section of the upstream face.

The above experiment serves chiefly as a visual information of a well-known method of sealing rock-fill dams, it being obvious that the detailed analysis of the effect of clays and graded fines could not be attempted on the small scale of 1 to 100, as the problem deals principally with the movement of sedimentary material. Leading engineering organizations recognize that the movement of colloidal material in percolation flow is one of the most vital of present day hydraulic problems and one on which information is markedly lacking.

The basis for analysing this complex and interesting problem will be developed from my experience with different construction organizations. A paper entitled "The Movement of Colloidal Clays in Percolation through Rockfill Dams", prepared under my direction serves to summarize the principles most useful in actual construction. To show the method of approach, the deduction of the law of permeability will be abstracted from the above work.

Referring to Figure 55, let us consider an isolated cylinder abcd, having the length L, and the cross sectional area A, and consisting of some isotropic material saturated with water, such as water saturated soil or concrete immersed in water. Also let the reduced pressure heads at sections ab and cd be H_1 and H_2 respectively and the limiting head, with reference to datum plance 0-0, at which the layer of material of thickness t is still impervious, be H_{cr} the so-called "critical" head.

We seek to find, for any fluid any material, the law connecting the critical head H_{cr} with the thickness of layer L, in other words the fundamental law of permeability.

Upon AB as an axis let us find the projections of the forces acting upon the fluid filling the pores of the material in the volume abcd:

(1) Forces due to pressures on cross-sections ab and cd.

$$p_A = \Delta h, \quad \text{and } p_B = \Delta h_2$$

in which Δ is the unit weight of fluid and the direction from A to B is taken as positive.

If the total area of the pores in the material is A_o and the coefficient of surface porosity

$$E_s = \frac{A_o}{A}, \text{ then the projection}$$

upon the axis AB of the total force of the hydrostatic pressure transmitted to the fluid in the pores is

$$P_{AB} = \Delta E_s A (H_{cr} - L\cos\alpha) = \Delta E_s AL (i_{cr} - \cos\alpha) \quad (38)$$

Also the projection upon the axis AB of the total hydrostatic pressure acting upon the material in the remainder of the cross-section

$$P'_{AB} = \Delta A (1 - E_s) (H_{cr} - L\cos\alpha) = \Delta AL (1 - E_s) (i_{cr} - \cos\alpha) \quad (39)$$

(2) Force due to the weight of fluid in the pores of the materials.

If X be the total cylindrical volume and X_o the volume of pores, then the volume coefficient of porosity

$$E = \frac{X_o}{X} \quad (40)$$

(3) Molecular forces due to the elastic resistance of water to shearing. Let T denote the projection of these forces upon the axis AB, and S the sum of the areas of the internal side surfaces of the material on which the elastic resistance to shearing is concentrated. Now let

$$S = t\,AL \qquad \text{from which we may write}$$

$$t = \frac{S}{AL} \quad (41)$$

The quantity t, as a quantity referred to the unit of volume may be called the specific surface of the elastic resistance. Then quantity t, having the dimesion $feet^{-1}$, depends principally upon the stucture of the material.

At the instant of limiting equilibrium of the fluid in the pores of the soil, the sum of the projections of active forces and resistance forces is equal to zero and hence:

$$\Delta E_s A (H_{cr} - L\cos\alpha) + \Delta E_v AL\cos\alpha - T = 0 \quad (42)$$

or $$T = \Delta A \left[F_s (H_{cr} - L\cos\alpha) + E_v L\cos\alpha\right]$$

When $E_s = E_v = E$

$$T = \Delta AE \left[H_{cr} - L\cos\alpha + L\cos\alpha\right] = \Delta AEH_{cr} \quad (43)$$

as is well known, the energy of elastic deformation of shearing (within the limits of applicability of Hooke's law) stored during the gradual increase of load starting from zero is expressed, per unit volume of the body, by

$$\frac{P^2}{2G}t$$

in which P_t = the unit tangential or shearing stress
and G = the shearing modulus of elasticity.

For the total volume of fluid in the pores of the material, the magnitude of the energy of elastic deformation will be

$$A_y = \frac{P_t^2}{2G} X_o = \frac{P_t^2}{2G} E_v AL \qquad (44)$$

At the instant of limiting equilibrium this elastic energy will be completely converted into potential energy and the latter may be easily determined for the water included in the pores of the material.

Finally, if the molecular or capillary forces were released, the water in the pores of the soil would be able to produce work equal to

$$A_p = \Delta AE_v LH_{cr} \qquad (45)$$

Equating expressions (44) and (45):

$$\frac{P_t^2}{2G} E_v AL = \Delta AE_v LH_{cr}$$

Whence $$H_{cr} = \frac{P_t^2}{2\Delta G} \qquad (46)$$

From Equations (42) and (43):

$$P_t = \frac{T}{S} = \frac{\Delta AE_v Hcr}{tAL} = \Delta \frac{E_v}{t} \frac{Hcr}{L} = \Delta \frac{E_v}{t} i_{cr} \qquad (47)$$

Substituting the value of P_t from Equation (47) in Equation (46)

$$H_{cr} = \frac{\Delta^2 E_v^2 H_{cr}^2}{2\Delta G t^2 L^2} = \frac{\Delta^2 E_v^2 i_{cr}^2}{2\Delta G t^2} \qquad (48)$$

From which finally the fundamental law of permeability may be written for saturated isotropic material, for the case of a gradual increase of head from 0 to H_{cr}, as follows:

$$H_{cr} = \frac{2GL^2 t^2}{\Delta E_v^2} \qquad (49)$$

or as a general case:

$$H_{cr} = \nabla I^2 \qquad (50)$$

In other words, the critical head is proportional to the square of the thickness of the layer. The coefficient ∇ may be called the permeability coefficient and is determined experimentally by testing samples in the laboratory.

The connection between the permeability coefficient, the shearing modulus of elasticity for the fluid in the pores of the material, the specific area t, the coefficient of porosity E_v and the weight of the fluid per unit of volume Δ, may be expressed

$$\nabla = \frac{2Gt^2}{\Delta E_v^2} \qquad (51)$$

Formula (50) shows how the thickness of blanket should be changed for various heads to give the same degree of imperviousness throughout all parts of the entire structure.

Formula (51) indicates that in general imperviousness is secured by

(a) Selecting a fluid for filling the pores of the material such that there will be maximum cohesion between the material and the fluid so as to obtain a high value of G (For instance the combination of asphalt filling in the pores of a sand blanket).

(b) For any fixed selection of fluid and material, by ramming or packing, as packing tends to decrease E_v and simultaneously increase t. In other words the ratio $\frac{t^2}{E_v^2}$ and consequently the degree of imperviousness is increased very materially by ramming.

SECTION 48. The limits of applicability of the method of Dumping.

The limiting height to which a rockfill dam may be carried using a given slope can readily be determined by detailed calculation, but in many cases it is useful to have at least an approximate advance figure for estimating.

The solid line in Figure 56 represents the profile of a dam constructed in flowing water by the dumping method. The heavy dotted line represents the limiting profile that may be obtained if desired by dumping additional material up to crest height H_{min}, using the same side slopes and the same base width. It is evident that it would be possible to construct a still larger dam with crest height at H_1, using the same side slopes but widening the base width; as shown by the light dotted line in Figure 56. In order that the designing engineer may not waste stone during the initial dumping process, it is essential to determine H_{min} in advance.

TABLE 23

Basic dimensions and data for typical rockfill dams

No by-pass provided

No.	Model Scale	Stone Size feet	Stone Weight tons	Original depth stream h_t feet	Discharge per foot width c.f.s.	Original stream velocity V f.p.s.	Height at which rock-fill emerges feet	Base width L_o feet	Difference in Elevation Headwater, Tailwater feet	Ratio $\frac{L_o}{Z}$	Height to finished crest H_m feet
1	1:15	1.18	0.10	11.80	21.00	1.77	17.20	69.00	5.60	12.3	23.0
2	1:25	1.97	0.48	19.70	45.70	2.33	28.70	115.00	9.35	12.3	37.8
3	1:40	3.15	1.95	31.50	92.50	2.95	45.60	184.00	14.95	12.3	59.0
4.	1:50	3.94	3.82	39.40	204.00	3.28	55.20	230.00	18.70	12.3	75.5

TABLE 24

Basic dimensions and data for typical rockfill dams

Tunnel by-pass provided

No.	Model Scale	Stone Size feet	Stone Weight tons	Original depth stream h_t feet.	Discharge per foot width c.f.s.	Original stream velocity V f.p.s.	Height at which rock-fill emerges feet	Base width L_o feet	Difference in Elevation Headwater, Tailwater feet	Ratio $\frac{L_o}{Z}$	Height to finished crest H_m feet
1	1:15	0.69	0.03	11.80	26.70	2.27	13.75	82.0	7.10	11.4	27.9
2	1:15	1.15	0.12	11.80	26.70	2.27	17.20	32.8	6.90	4.8	19.7
3	1:25	1.15	0.12	19.70	57.50	2.92	23.00	134.5	11.80	11.4	46.0
4	1:25	1.28	0.54	19.70	57.50	2.92	28.70	105.0	11.50	9.0	34.5
5	1:40	1.84	0.47	31.50	116.00	3.71	36.80	216.0	18.90	11.4	72.0
6	1:50	2.30	0.91	38.40	162.00	4.14	46.00	269.0	23.60	11.4	88.5
7	?	?	?	31.50	116.00	3.71	?	164.0	18.35	9.0	52.5

Table 23 applies to cases in which no by-pass tunnel or spillway has been provided. The data have been obtained from laboratory model tests and stepped up to full-scale values by the application of Froude's law. The individual stones for the dam were cubes made from concrete having a unit weight of 138 pounds per cubic foot.

Test #2 from this table refers to stone about 2 feet on a side weighing about 1/2 ton. The original depth of river is taken as 19.70 feet and the average original velocity 2.3 feet per second. The dam profile started to emerge from the water at a heightof 29 feet. It was found that the total heightof crest for the completed section with equal upstream and downstream slopes and a standard crest width was about 38 feet.

Table 24 covers the case in which a by-pass is provided, the invert of tunnel in this case being at the tailwater level and with a depth of 2/3 h over the invert, the tunnel is capable of accommodating the entire river discharge. The individual stones used were of the rounded form, having an average weight of 165 pounds per cubic foot.

The methods of design outlined in this book have been successfully applied to a full-scale structure in the case of the Svir #2 Dam, for which the original natural velocities were in some places as high as 10 feet per second. In spite of such severe conditions, the profile as constructed conformed closely to the calculated dimensions.

SECTION 49. The interest of engineers in the method.

I have several times presented the results of laboratory experiments on the stone dumping method to audiences of engineers, technicians and students in Moscow, and the interest in the subject was manifest from the character of the subsequent discussions.

In conclusion I will simply cite the resolutions adopted at the Convention of Hydrualic Engineers, regarding the construction of dams by this method:

(1) The Convention believes that steps should be taken to acquaint engineers with the necessary model testing and design procedure.

(2) Immediate steps should be taken toward the construction of a large scale experimental dam of this type.

(3) The method reduces the hazard and expense of winter construction.

(4) The method serves to eliminate cofferdams and reduce the expense of temporary construction.

APPENDIX

List of Figures

Fig. 1. Closure of the Island Narrows of the River Svir.

Fig. 2. Dehri Weir.

Fig. 3. Investigation of overflow over a partly completed model dam.

Fig. 4. Kolva River Dam.

Fig. 5. Rockfill Dam - Upper Svir.

Fig. 6. Dam #1 on the River Niva.

Fig. 7. Four schemes for Rockfill Dams.

Fig. 8. Sequence of Profiles of a Dam built by dumping rock into Flowing Water (with a by-pass).

Fig. 9. Sequence of Profiles of a Dam built by dumping composite cubical stones into Flowing Water (without a by-pass).

Fig. 10. to Fig. 15.Inc. Photographs of Model Tests.

Supplementary Explanation of Figures 16 to 41. 3 sheets.

Fig. 16. Summary of sequential Profiles of a Dam constructed by dumping stone into flowing water (by-pass provided).

Fig. 17. Summary of sequential profiles of a dam constructed by dumping stone into flowing water (no by-pass provided).

Fig. 18. Profile of a Dam showing Percolation Flow.

Fig. 19. Forces acting upon an Individual Stone at Apex A.

Fig. 20. Showing Area of Cross-section vs. Height of Dam.

Fig. 21.) Fig. 21a) Fig. 21b) 21c) Resistance of Individual Stones during the First, Second and Third Stages of Construction.

Fig. 22. Dam constructed of Sand Stones with an Auxiliary Dam of Large Stones. Sequence of Profiles. Main Characteristics of Dam Construction.

Fig. 23. Dam constructed of Alternate Portions of Small and Large Stones. Sequence of Profiles. Main Characteristics of Dam Construction.

Fig. 24. Dam constructed up to certain limit of small stones only; after that large stones only (recommended method). Sequence of Profiles. Main characteristics of Dam Construction.

Fig. 25. Dam constructed of Large Stones Only. Sequence of Profiles. Main Characteristics of Dam Construction.

Fig. 26. Comparative Summary of final profiles of Dams constructed by different methods of dumping. Curve of ratio of volumes. Volumes in cubic yards.

#1 Dam Constructed of small stones (71.4%) with an auxiliary dam of large stones (28.6%)
#2 Dam Constructed of alternate portions of small stones (64.6%) and large stones (35.4%).
#3 Up to certain limit small stones only (71.5%) After that large stones only (28.5%).
#4 Large stones only (100%).
#5 Small stones only (100%).

Fig.27-33 Profiles of a Dam - Illustrations to accompany tables.

Fig. 34. Investigation of rockfill for condition of free overflow.

Fig. 35. Relation between gradient I and the velocity of percolation for rounded pebbles.

Fig. 36. Experiment for determination of coefficient of percolation K and the exponent "m" of the percolation velocity for a submerged dam made of concrete cubes 23 x 24 x 25 mm.; porosity = 47.5%; $\Delta_1 = 2.21$ gr/cm^3.

Fig. 37. Rock fill at the stage of submerged overflow.

Fig. 38. The character of percolation flow in the body of a submerged model dam made of rounded stones.

Fig. 39. Rockfill at the stage of submerged flow.

Fig. 40a) 40b) Character of percolation flow in a submerged model dam made of small cubes.

Fig. 41. Percolation through submerged dam at the stage of free overflow.

Fig. 42. Percolation flow through a submerged dam at the stage of submerged flow.

Fig. 43. Investigation of the effect of model scale upon overflow.

Fig. 44. Model for studying uplift pressure of the percolation flow through a rockfill.

SUPPLEMENTARY EXPLANATION OF FIGURES 16 to 41 Sheet 1 of 3

In preparing the translation of the Russian text, data that might, in the opinion of the translator, be useful in making design computations, have been converted to the English system of measurement. Where the results of model tests are used only to illustrate comparative tendencies, the metric system has been retained.

Supplementary sheets 1 to 3 inclusive have been prepared to assist the reader in understanding the figures. They also present a convenient method for transfering the model data, given to full-scale conditions in either the metric or English system.

The results of hydraulic model experiments given in the Russian pamphlet were originally obtained for the report on the Kolva River Project (compare Figure 4), and are therefore directly applicable to conditions at that site.

The experiments were made in a flume of 50 cm (1.64 ft.) width. The model scale was 1:25, with exception of the tests shown in Figure 45.

The data for figures 16 to 41 are given in model dimensions, the units of measurement being summarized in the conversion table on supplementary sheet 3. It should be noted however that river bottom and water surface elevations are presented in these figures in metres for full-scale conditions. The length of rock-fill profiles in Figure 26 are also given in metres and converted to conditions in nature.

For plotting rockfill profiles a system of coordinates in centimetre spacing is used in the figures, this coordinate system having an equivalent spacing of 5 cm in model conditions. The stationing shown on the bottom of the profiles is the same as that used in the experiments. Stations are 5 cm apart in model dimens ions.

Figures 22 to 26

Data on model setting are given in full detail in the text. The following compilation shows test conditions and conversion to full scale, according to Froude's law.

Properties of stone fill used:
rounded stones, specific weight 2.64
percent of voids in stone fill 37 to 40%

	Model Dimensions	Actual Dimensions	
		Metric system	foot system
Small stones, diameter	14 mm	0.35 m	1.15 ft.
Large " "	24 "	0.60 "	1.97 "
Small " weight	5 g	80 kg	176 lbs
Large " "	30 g	480 "	1060 "
Depth of tailwater	24 cm	6.0 m	19.7 ft
Elevation of tailwater		El 200	
Depth of headwater	24 to 38 cm	6.0 to 9.5 m	19.7 to 31.2 ft
Elevation of headwater		El 200 to 203.5	
Original River Discharge (The original discharge decreases gradually with the rise in headwater owing to the action of the by-pass)	21.4 Ltr/sec for 50 cm width of model flume	600 m^3/sec for 112 m width or 5.35 m^3/sec/m	21200 cfs. for 367 ft width or 57.5 cfs./ft.

The test conditions for the remaining figures, 26 to 41 inclusive, are not given completely in the text. These figures serve only illustrations to theoretical considerations.

Figures 16, 17, 20 illustrate the gradual development of profiles of a rockfill dam built in flowing water, and the sequence of hydraulic phenomena accompanying the construction.

Figures 27 to 33 pertain to the determination of discharge coefficients, for successive stages of construction.

Figures 37, 38, 39, 40a, 40b are inserted to show the characteristics of percolation flow.

Conversion of model data to full-scale dimensions in the metric and the English foot systems, based on 1:25 model scale and on Froude's law.

	Unit of Model Dimensions	Equivalent full-scale dimensions metric system	English system
Linear Dimensions:			
Size of stones and sand grains, d	1.0 mm	0.025 m	0.082 ft
Height of rock-fill dam, H	1.0 cm	0.25 "	0.82 "
Increase of height of dam, Δh			
Depth of Headwater etc., h_{ul}			
Areas:			
Cross-section of rock-fill dam, Ω	1.0 dcm^2	6.25 m^2	67.2 ft^2
Increase of cross-section of dam, $\Delta\Omega$			
Weight:			
Weight of stones	1.0 g	15.6 kg	34.5 lbs
Velocities:			
Overflow velocities	1.0 m/sec	5.0 m/sec	16.4 ft/sec
Percolation velocities	1.0 cm/sec	0.05 "	0.164 "
Discharge:			
Overflow plus percolation flow, q_t	1.0 ltr/sec for 50 cm width	0.25m^3/sec/m	2.69 cfs/ft
Volume:			
in rockfill dam	1.0 ltr for 50 cm width	1.25 m^3/m	0.498 cyd/ft
Effectiveness of Dumping $\frac{\Delta h}{\Delta \Omega}$	1.0 $\frac{cm}{dcm^2}$	0.04 $\frac{m}{m^2}$	0.0122 $\frac{ft}{ft^2}$

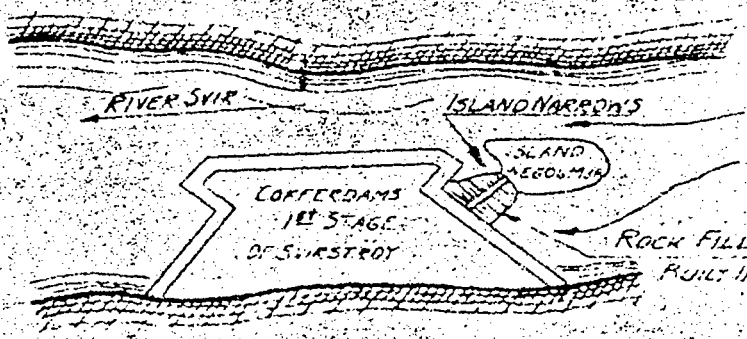

FIG 1. CLOSURE OF THE ISLAND NARROWS OF THE RIVER SVIR.

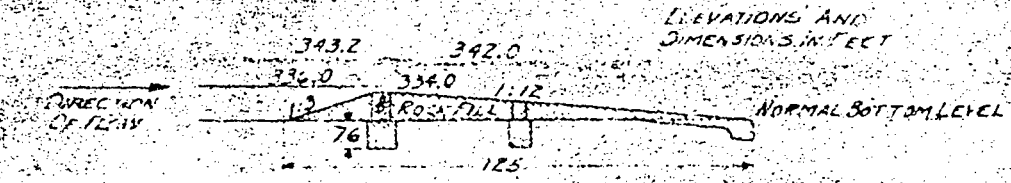

FIG. 2. DEHRI WEIR, LENGTH 1500 FT.

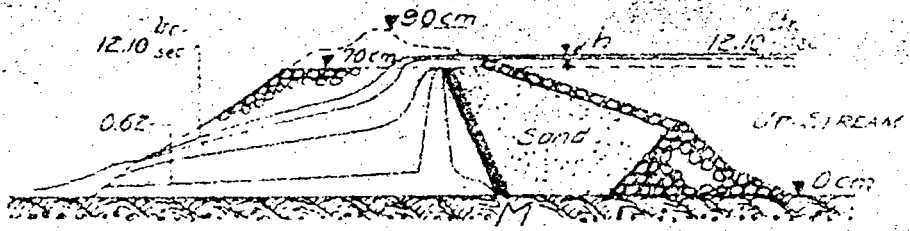

FIG 3 INVESTIGATION OF OVERFLOW OVER A PARTLY COMPLETED MODEL DAM
(MODEL DIMENSIONS IN C.M. MODEL SCALE 1:100)

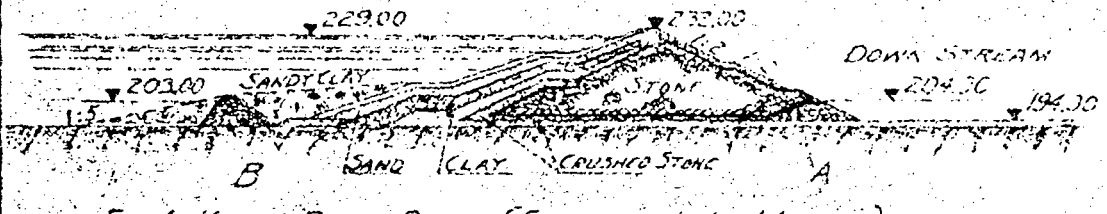

FIG 4. KOLVA RIVER DAM (ELEVATIONS IN METRES)

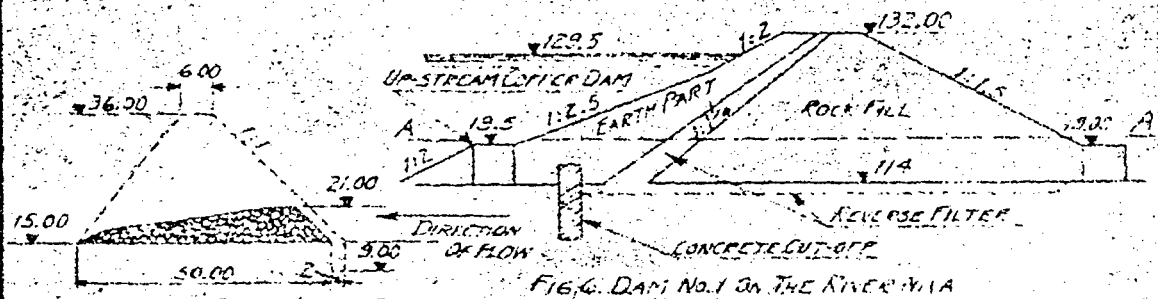

FIG. 5. ROCK FILL DAM - UPPER SVIR.
(ELEVATIONS IN METRES)

FIG. 6. DAM NO. 1 ON THE RIVER VIA
(ELEVATIONS IN METRES)

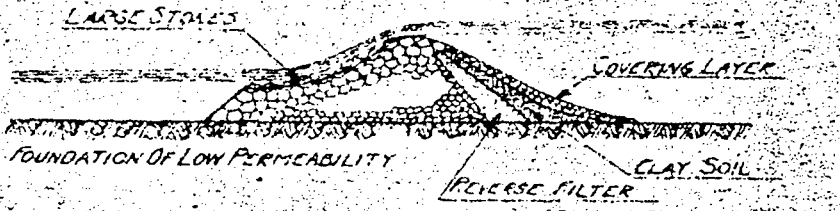

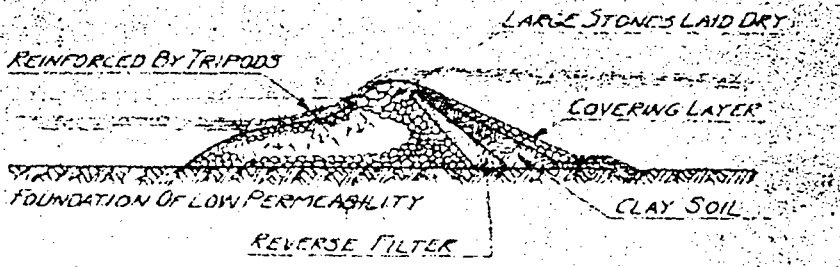

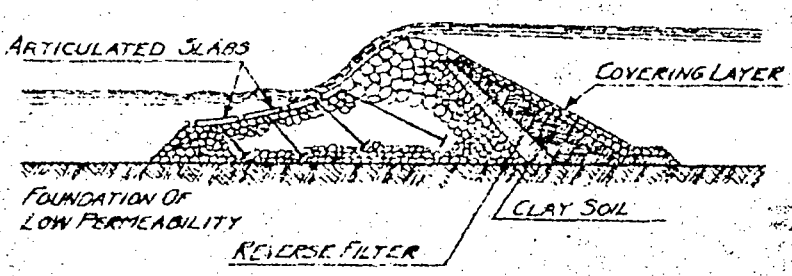

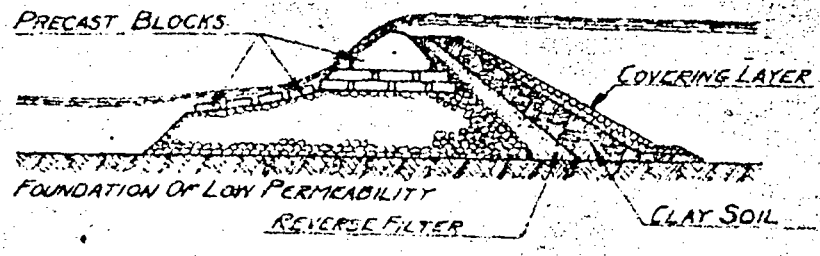

FIG. 7. FOUR SCHEMES FOR ROCK FILL DAMS

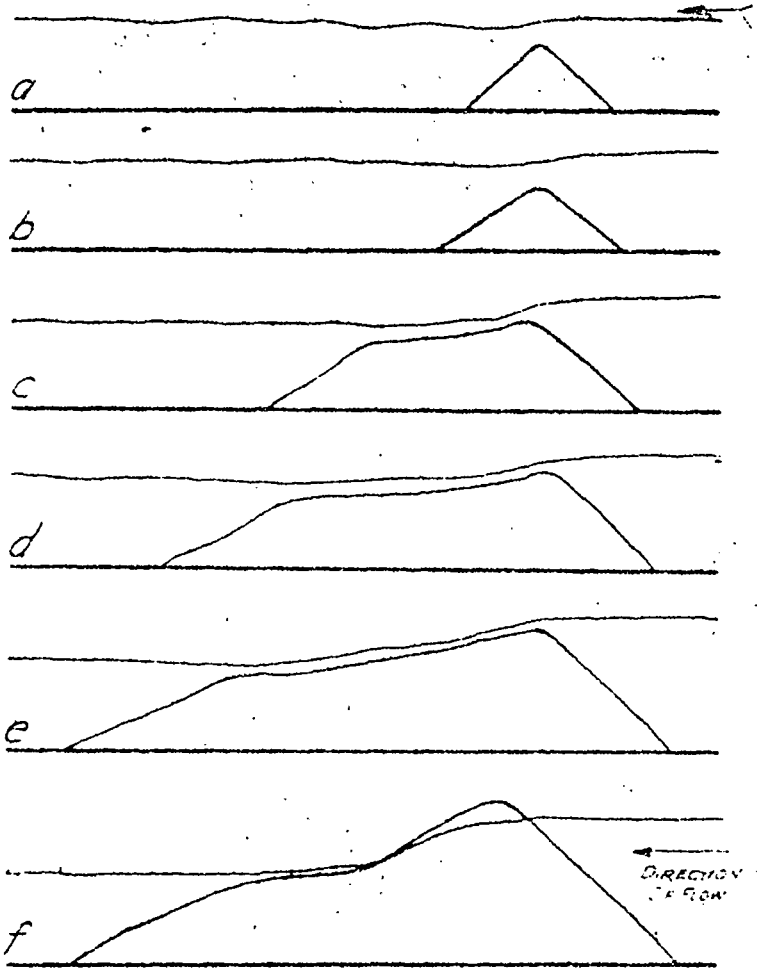

FIG. 8. SEQUENCE OF PROFILES OF A DAM CONSTRUCTED BY DUMPING ROCK INTO FLOWING WATER (WITH A BY-PASS)

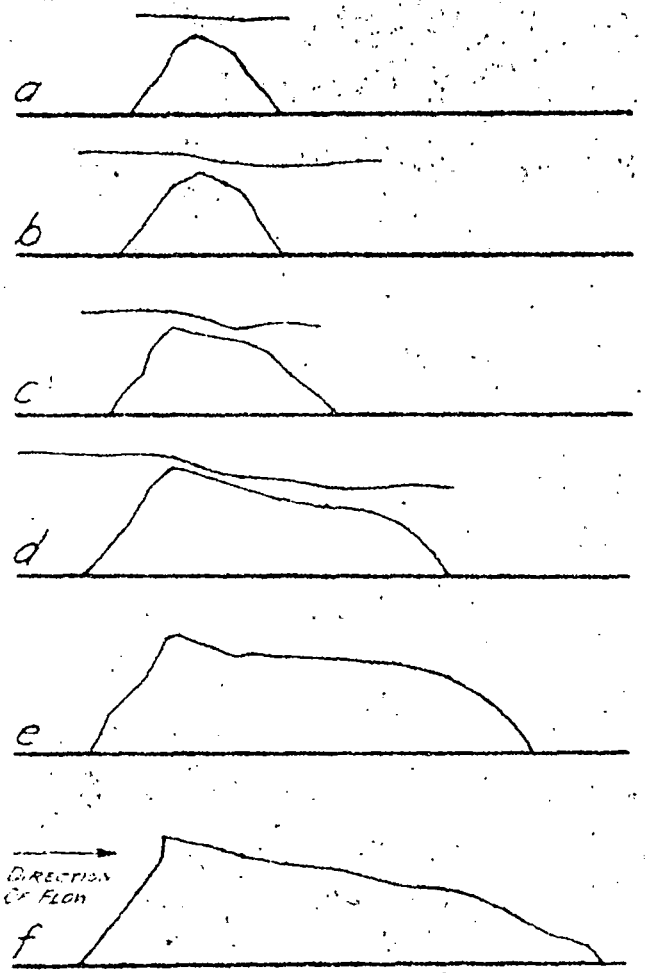

FIG 9. SEQUENCE OF PROFILES OF A DAM OBTAINED BY DUMPING PRECAST CUBICAL BLOCKS INTO FLOWING WATER (WITHOUT A BY-PASS)

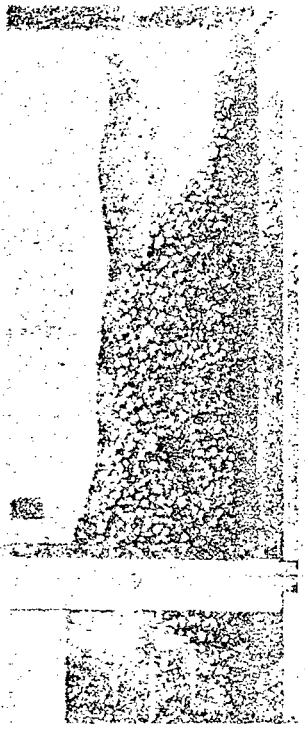

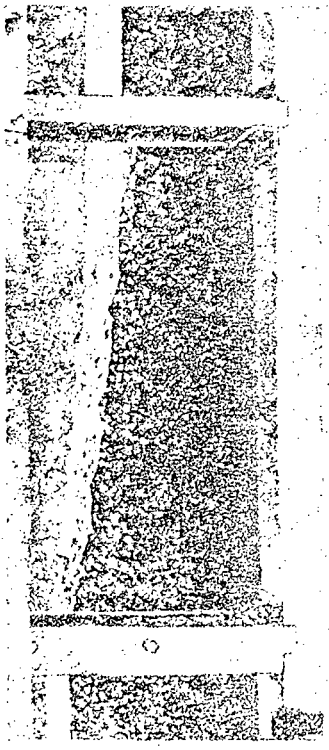

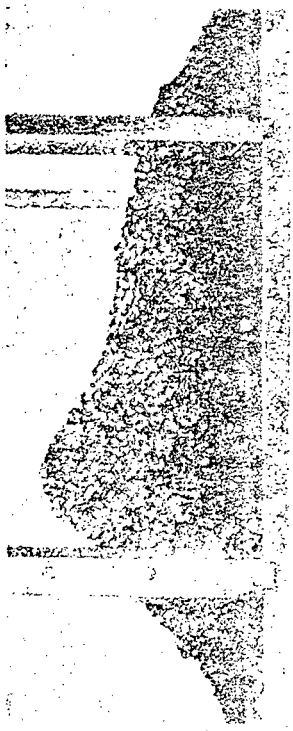

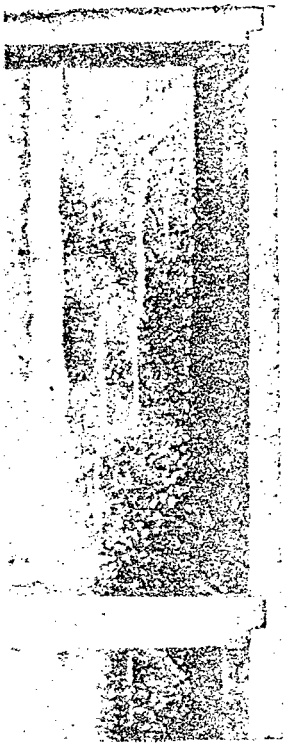

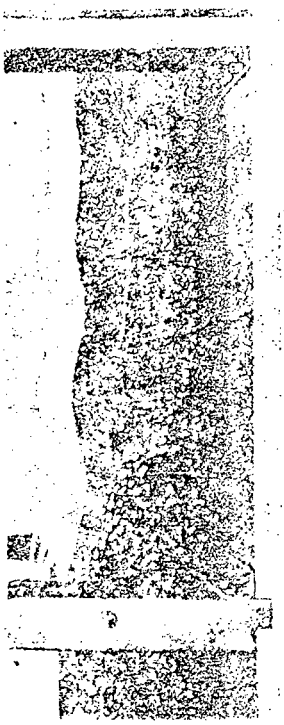

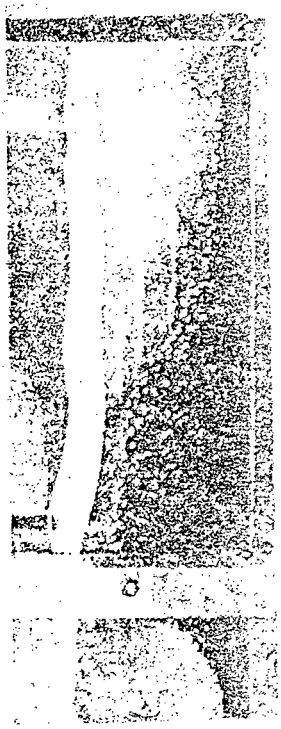

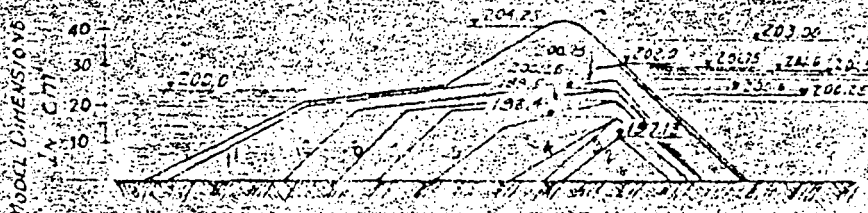

FIG. 16. SUMMARY OF SEQUENTIAL PROFILES OF A DAM CONSTRUCTED BY DUMPING STONE INTO FLOWING WATER (... BY-PASS PROVIDED)

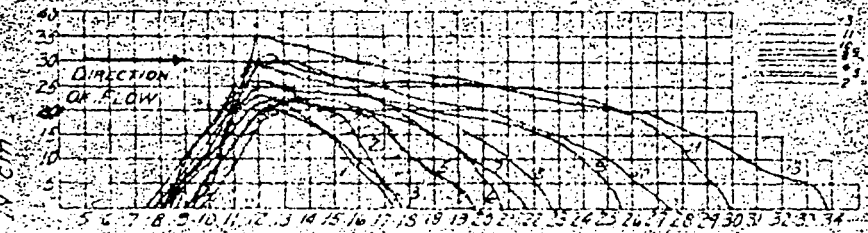

FIG. 17. SUMMARY OF SEQUENTIAL PROFILES OF A DAM CONSTRUCTED BY DUMPING STONE INTO FLOWING WATER (NO BY-PASS)

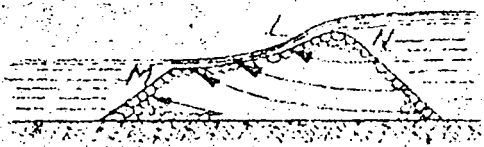

FIG. 18 PROFILE OF A DAMS SHOWING SECOLATION FLOW.

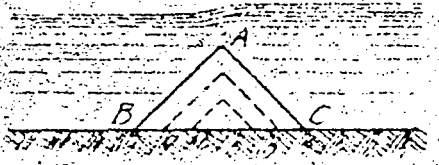

FIG. 19. FORCES ACTING UPON A STONE AT APEX A

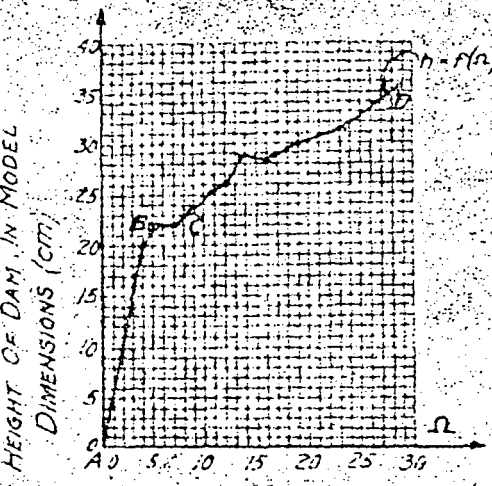

AREA OF DAM CROSS-SECTION IN MODEL DIMENSIONS (dcm^2)

FIG. 20. CURVE $h = f(\Omega)$

NOTE: FOR CONVERSION OF MODEL DATA TO FULL SCALE AND ENGLISH SYSTEM SEE SUPPLEMENTARY SHEETS 1 TO 3 INCL.

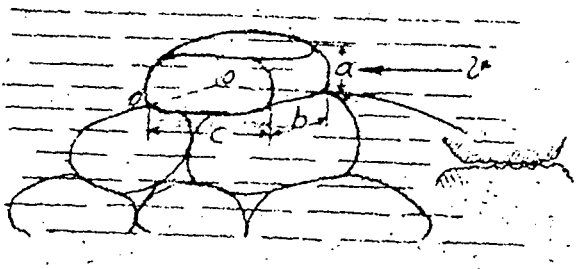

FIG. 21.

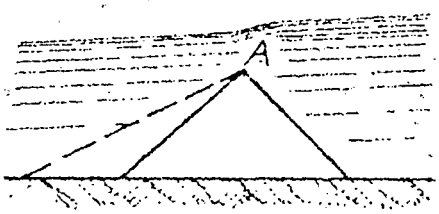

FIG. 21a.

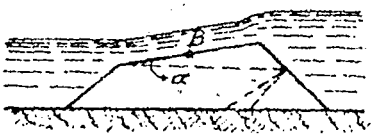

FIG. 21b.

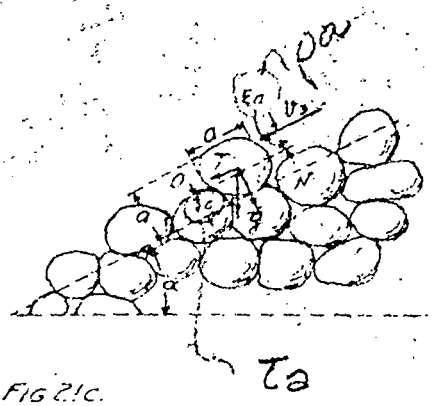

FIG 21c.

RESISTANCE OF INDIVIDUAL STONES DURING THE FIRST, SECOND, AND THIRD STAGES OF CONSTRUCTION

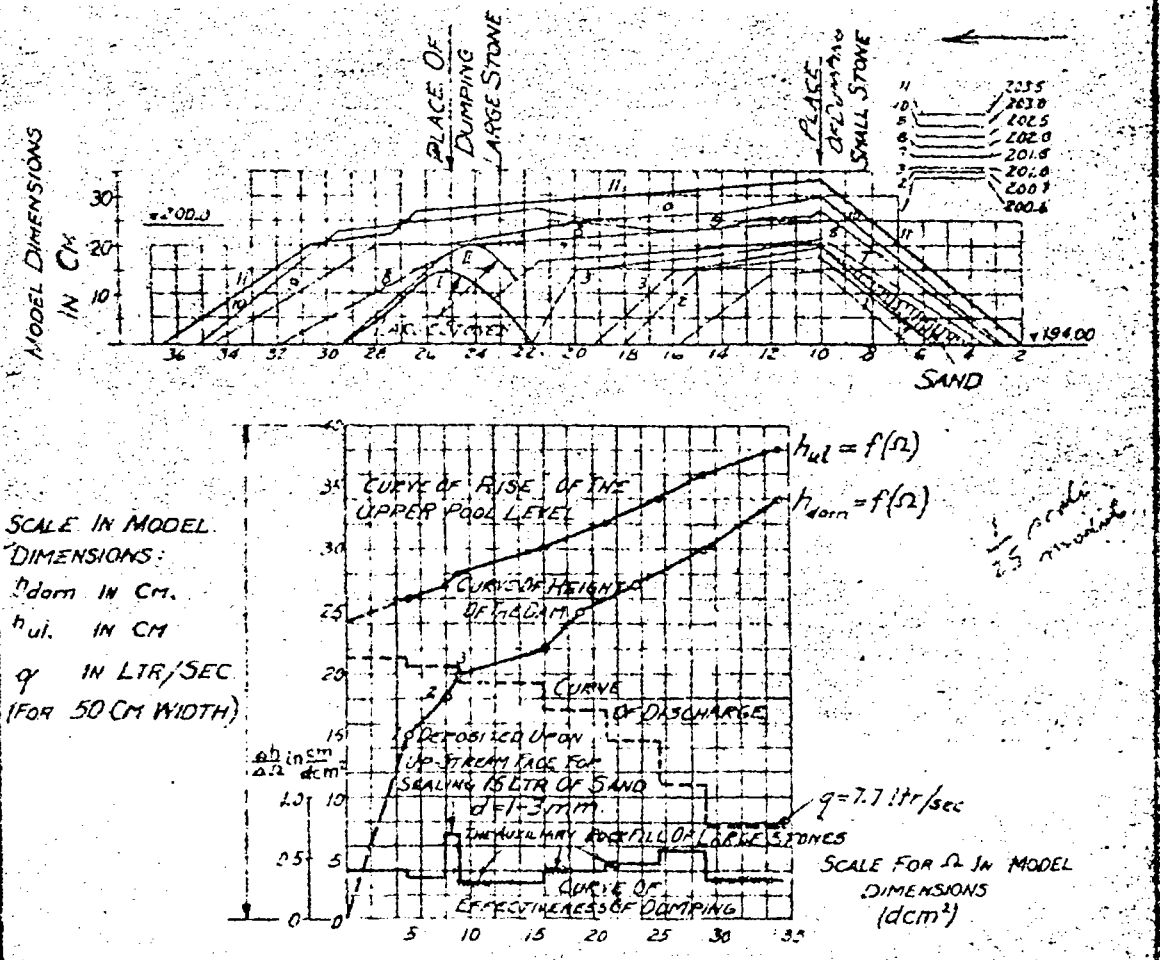

FIG 22. DAM CONSTRUCTED OF SMALL STONES WITH AN AUXILIARY DAM OF LARGE STONES SEQUENCE OF PROFILES. MAIN CHARACTERISTICS OF DAM CONSTRUCTION.

Sept 12

NOTE: For conversion of model data to full scale and English system see Supplementary Sheets 1 to 3 incl.

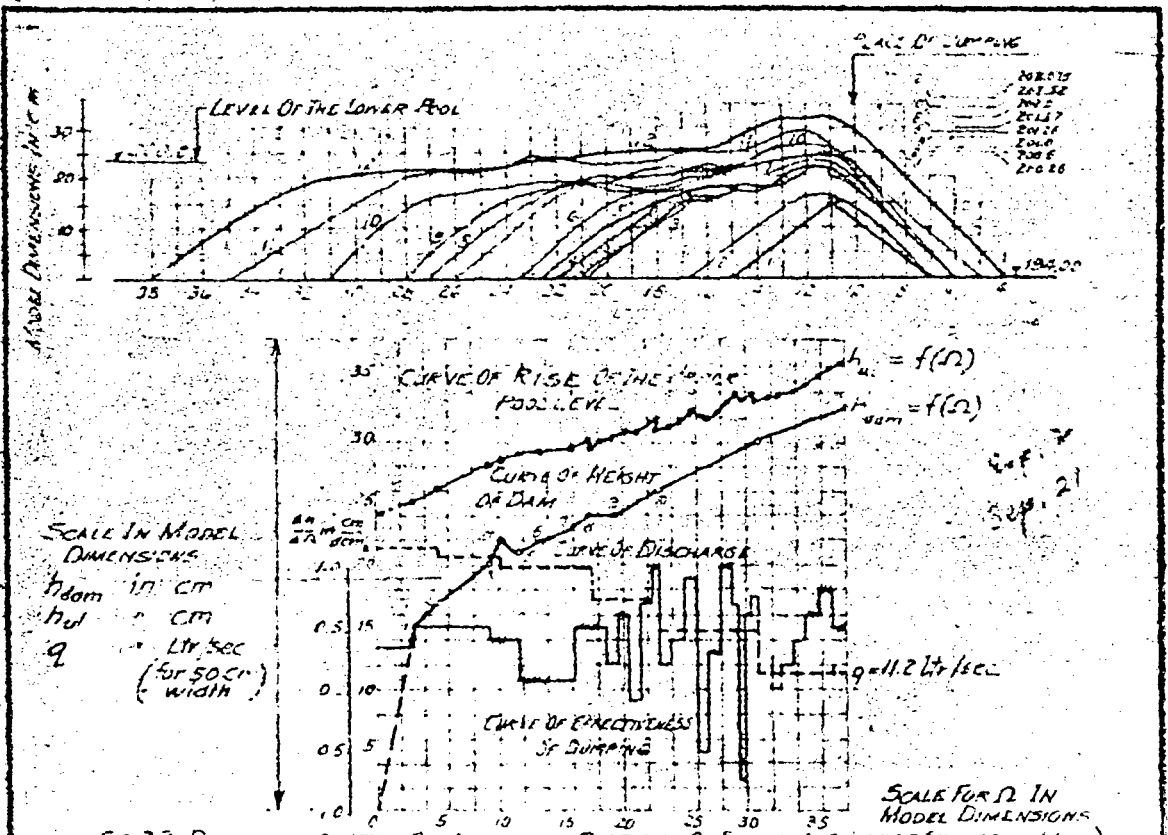

FIG 23 DAM CONSTRUCTED OF ALTERNATE PORTIONS OF SMALL AND LARGE STONES
SEQUENCE OF PROFILES. MAIN CHARACTERISTICS OF DAM CONSTRUCTION.

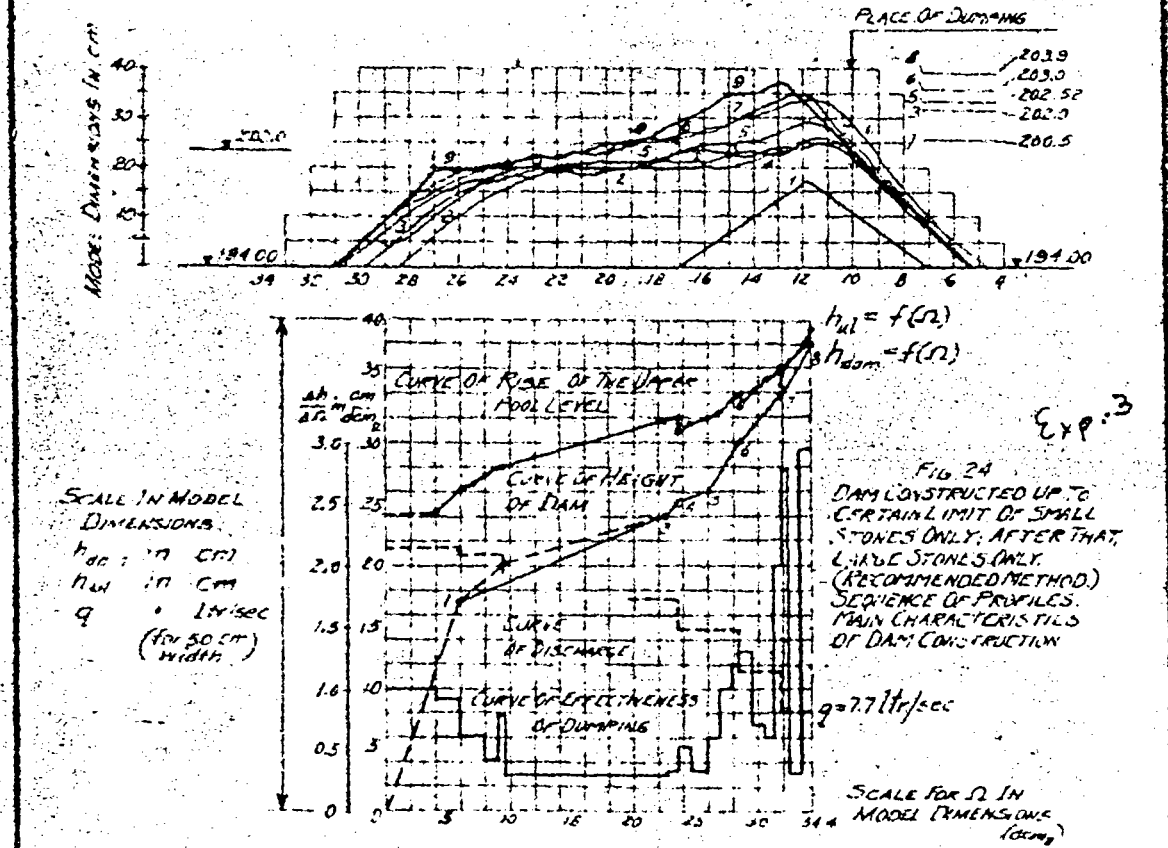

FIG 24
DAM CONSTRUCTED UP TO CERTAIN LIMIT OF SMALL STONES ONLY; AFTER THAT, LARGE STONES ONLY. (RECOMMENDED METHOD.)
SEQUENCE OF PROFILES. MAIN CHARACTERISTICS OF DAM CONSTRUCTION

NOTE FOR CONVERSION OF MODEL DATA TO FULL SCALE AND ENGLISH SYSTEM SEE SUPPLEMENTARY SHEETS 1 TO 3 INCL.

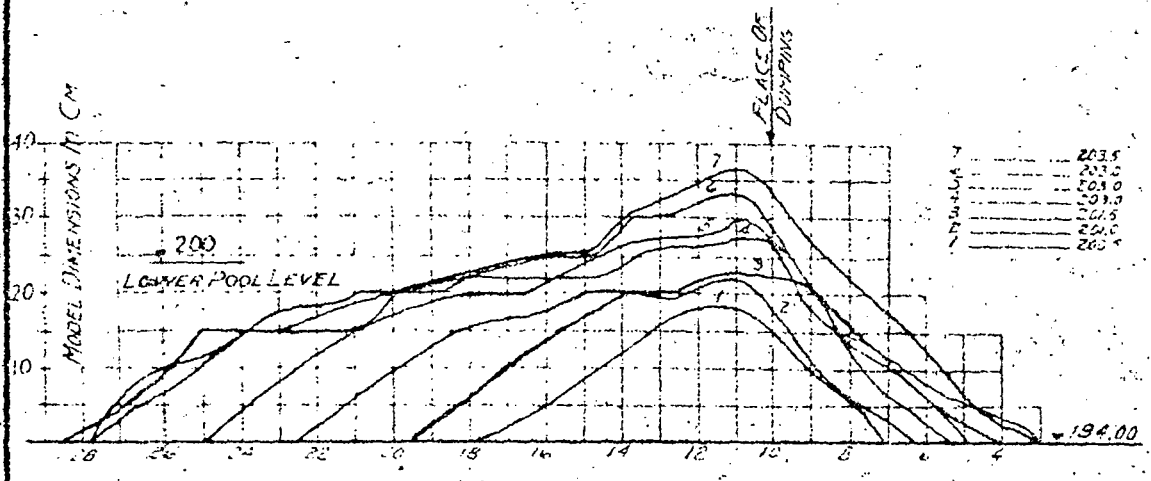

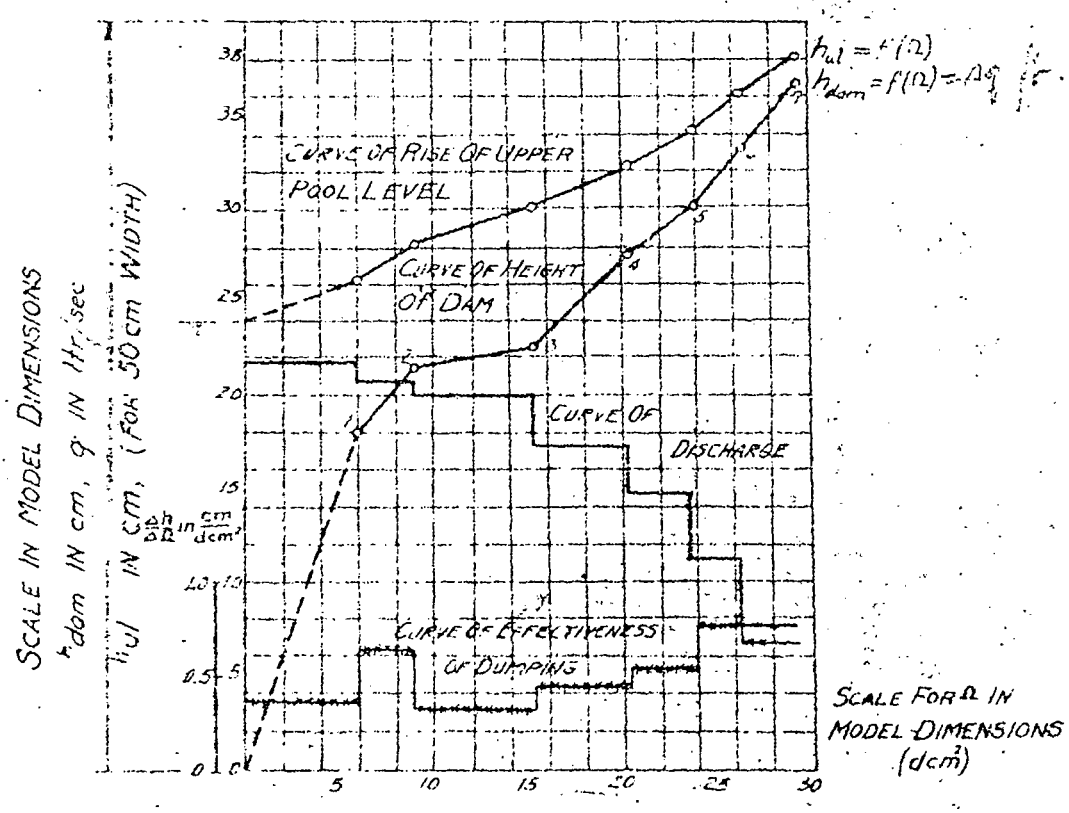

FIG. 25. DAM CONSTRUCTED OF LARGE STONES ONLY.
SEQUENCE OF PROFILES.
MAIN CHARACTERISTICS OF DAM CONSTRUCTION.

NOTE: FOR conversion of model data to full scale and English system see supplementary sheets 1 to 3 incl.

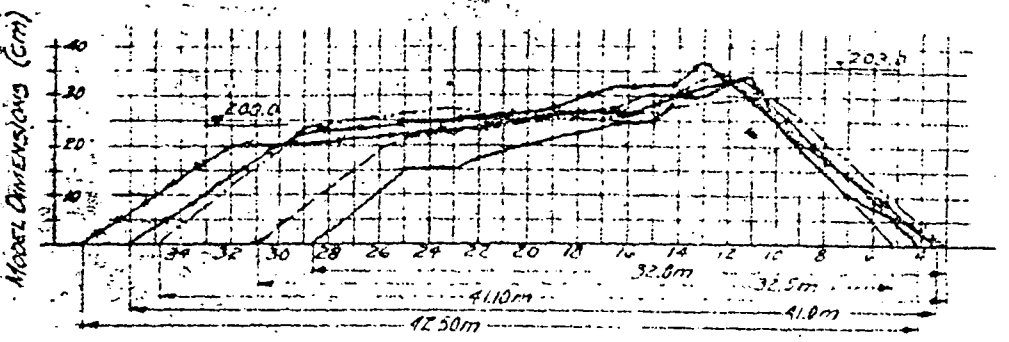

Length Of Profiles Given In Metres And Full Scale

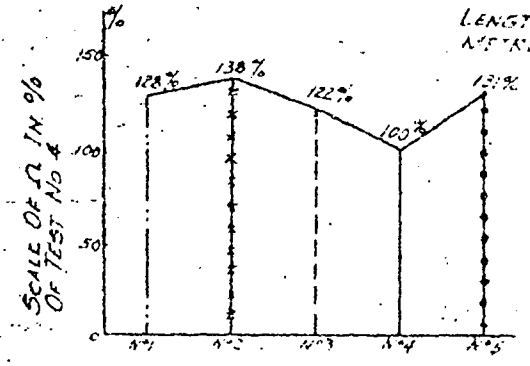

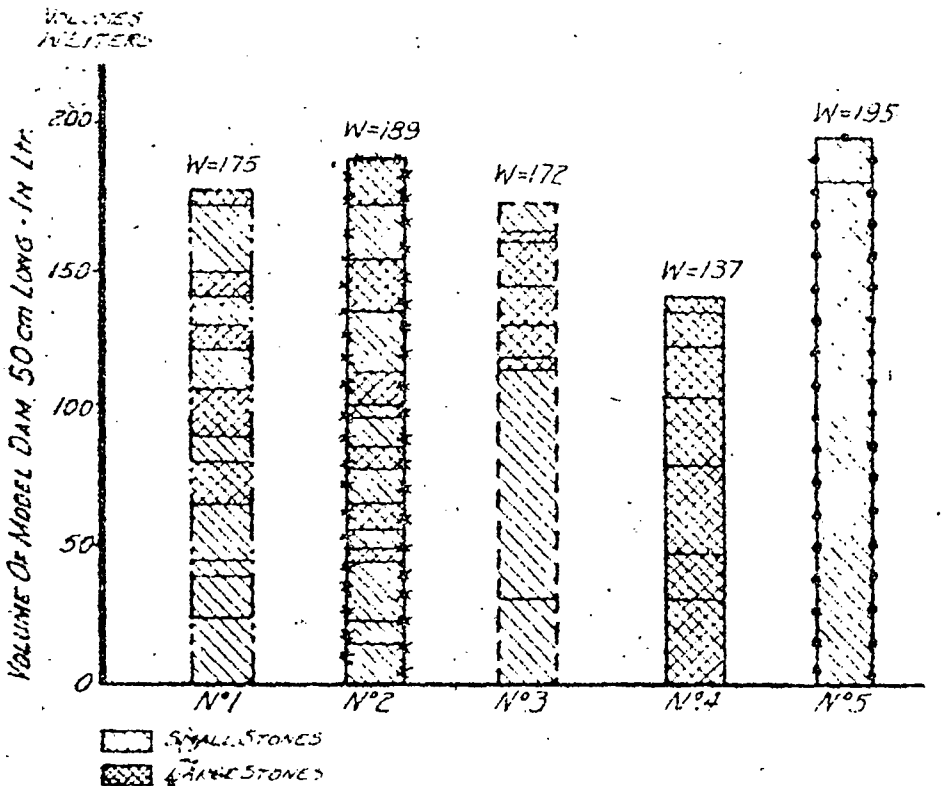

Fig. 26. Comparative Summary Of Final Profiles Of Dams Constructed By Different Methods Of Dumping; Curve Of Ratio Of Volumes; Graphical Comparison Of Volumes.
No.1. Dam Constructed Of Small Stones (71.4 %) With An Auxiliary Dam Of Large Stones (28.6 %).
No.2. Dam Constructed Of Alternate Portions Of Small Stones (64.6 %) And Large Stones (35.4 %).
No.3. Up To Certain Limit Small Stones Only (71.5 %). After That, Large Stones Only (28.5 %).
No.4. Large Stones Only (100 %).
No.5. Small Stones Only (100 %).
W = Volumes In Liters.

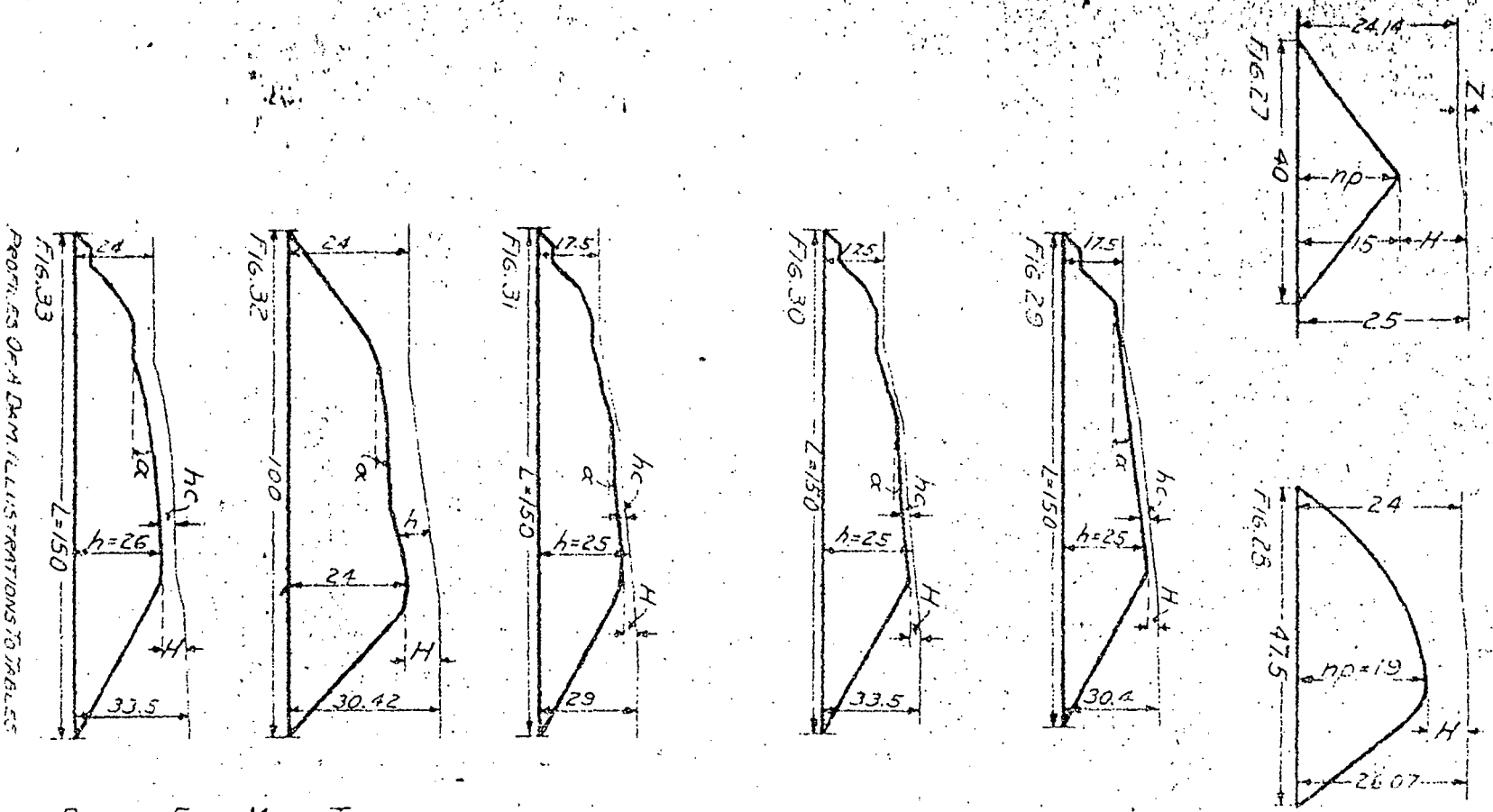

PROFILES FROM MODEL TESTS
MODEL SCALE 1:25
MODEL DIMENSIONS IN cm. FOR CONVERSION OF MODEL DATA TO FULL SCALE AND ENGLISH SYSTEM SEE SUPPLEMENTARY SHEETS 1 TO 3 INCL.

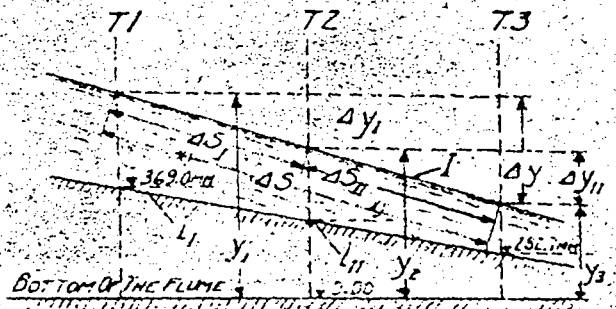

FIG. 34. INVESTIGATION OF ROCK FILL FOR SHOOTING FLOW.

$\Delta S_I = \Delta S_{II} = 0.4175\,m.$; $\Delta S = 0.835\,m.$
$i_I = \tan 6°12' = 0.1088$; $i_{II} = \tan 5°35' = 0.0977$

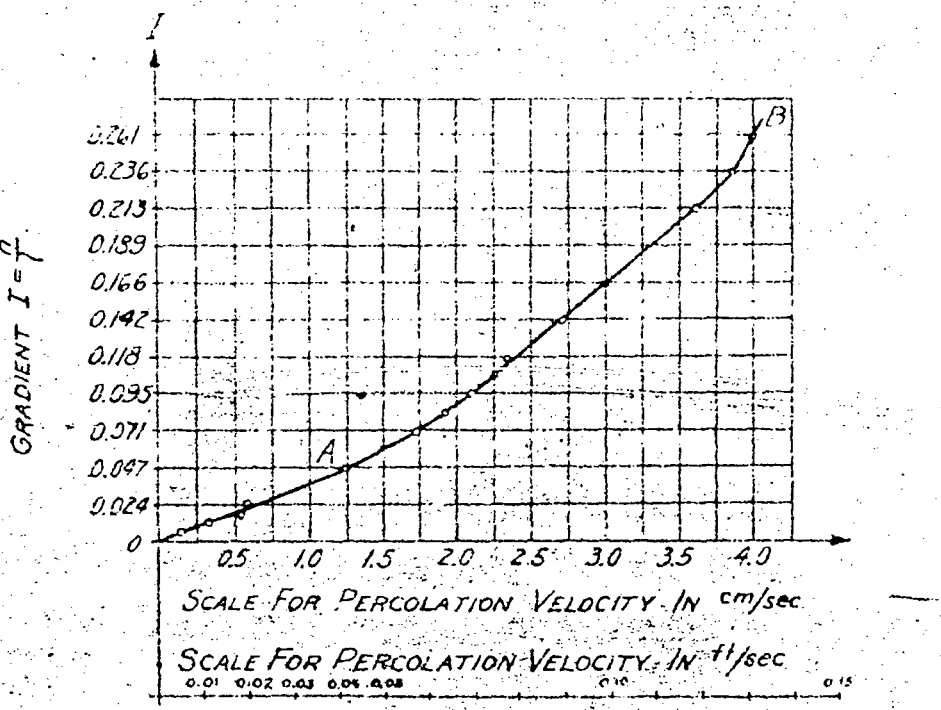

FIG. 35 RELATION BETWEEN GRADIENT I AND THE PERCOLATION VELOCITY; DARCY TYPE TEST WITH "PEBBLE" MATERIAL.

NOTE: THE ODD SCALE FOR THE GRADIENT PROBABLY RESULTS FROM A CORRECTION APPLIED TO THE DATA AFTER COMPLETION OF PLOTTING TRANSLATOR)

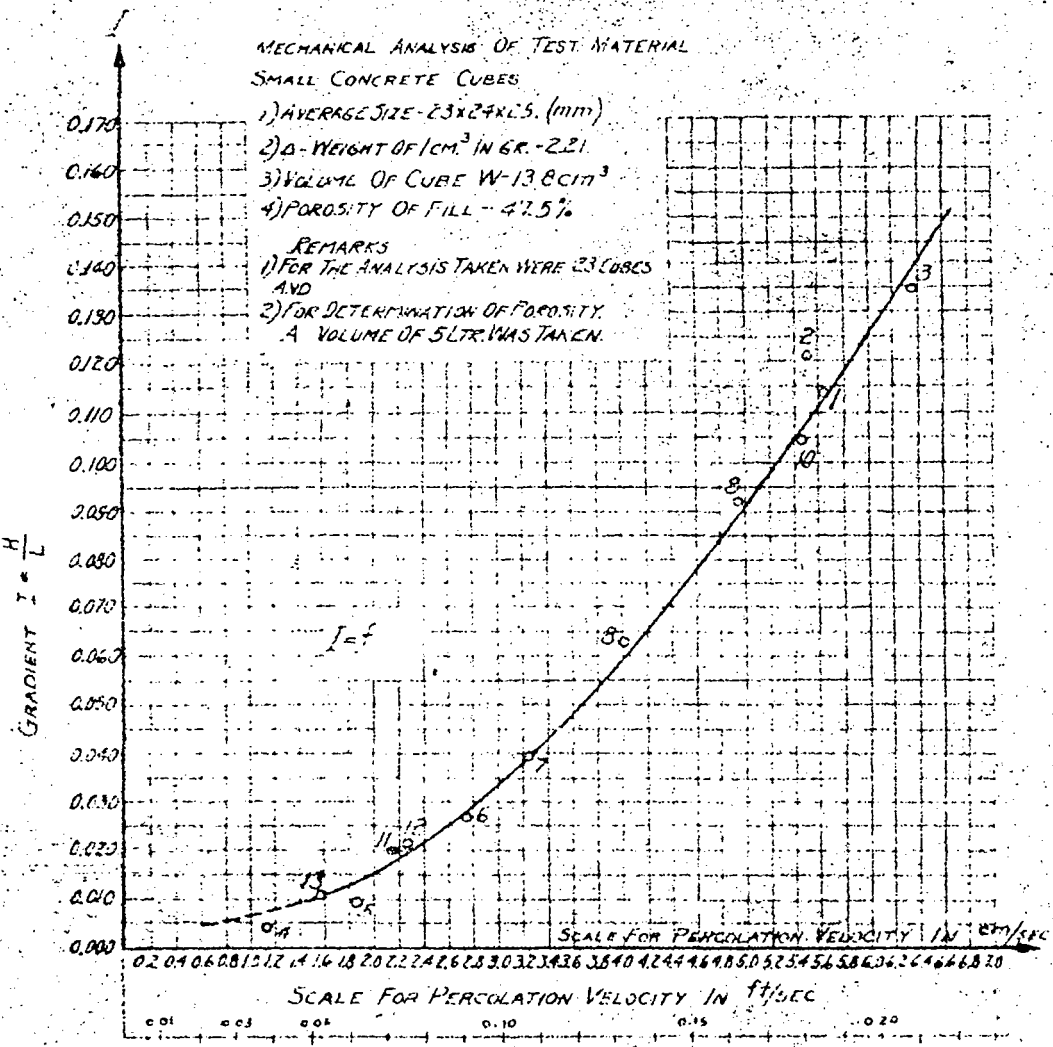

FIG 36 - DATA FROM EXPERMENTS FOR DETERMINATION OF THE COEFFICIENT OF PERCOLATION K AND THE EXPONENT m OF THE PERCOLATION VELOCITY IN THE FORMULA $V^m = K \cdot I$

DARCY TYPE TEST CONCRETE CUBES 23×24×25 (mm)

POROSITY OF FILL 47.5%, SPECIFIC WEIGHT OF CUBES 2.21

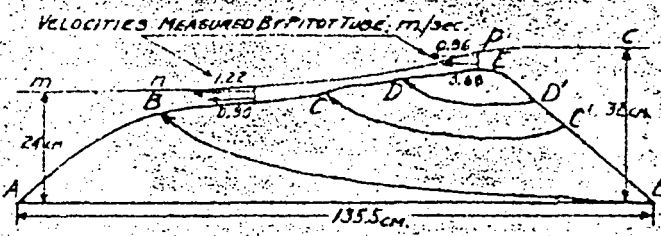

FIG. 37. ROCK FILL AT THE STAGE OF FREE OVERFLOW

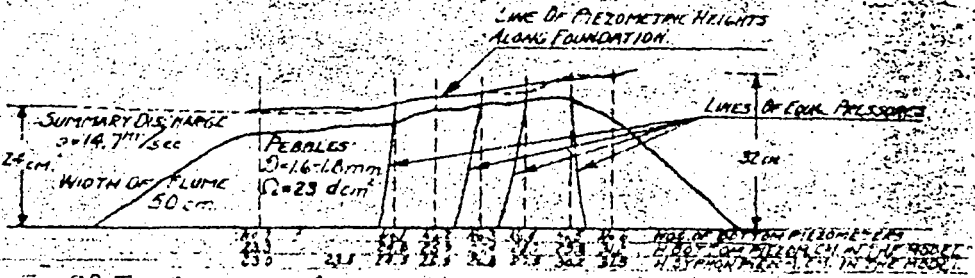

FIG. 38. THE CHARACTER OF PERCOLATION FLOW IN THE BODY OF A ROCK FILL DAM MADE OF ROUNDED STONES.

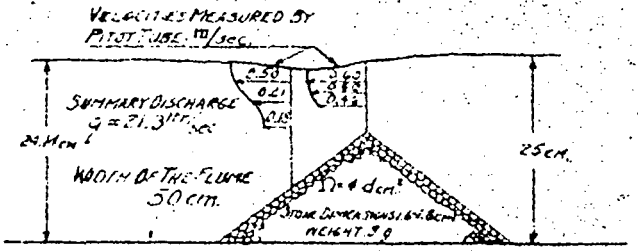

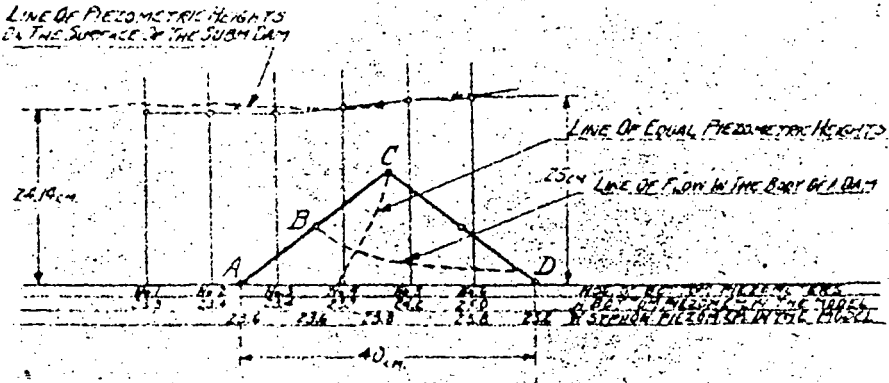

FIG. 39. ROCK FILL AT THE STAGE OF SUBMERGED OVERFLOW

NOTE: MODEL DIMENSIONS IN METRIC SYSTEM.
FOR CONVERSION OF MODEL DATA
TO FULL SCALE AND ENGLISH SYSTEM
SEE SUPPLEMENTARY SHEETS 1 TO 3 INCL.

FIG. 40a (SUBMERGED OVERFLOW)

FIG. 40b (FREE OVERFLOW)

CHARACTER OF FILTRATION FLOW FROM EXPERIMENTS ON ROCK-FILL DAM MADE OF SMALL CUBES

NOTE. FOR CONVERSION OF MODEL DATA TO FULL SCALE AND ENGLISH SYSTEM SEE SUPPLEMENTARY SHEETS 1 TO 3 INCL.

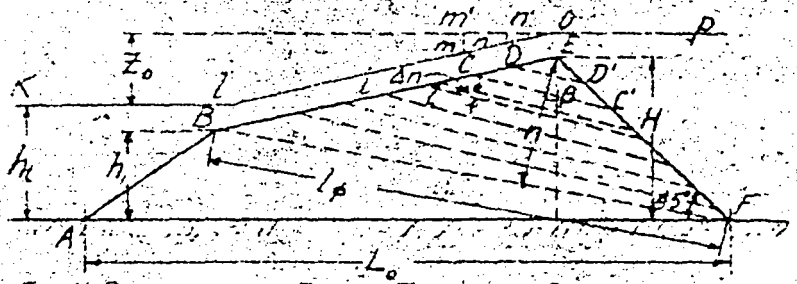

FIG 41 PERCOLATION FLOW THROUGH A SUBMERGED DAM AT THE STAGE OF FREE OVERFLOW

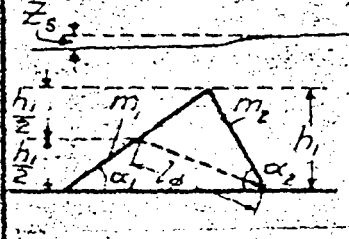

FIG. 42. PERCOLATION FLOW THROUGH A SUBMERGED DAM AT THE STAGE OF SUBMERGED OVERFLOW.

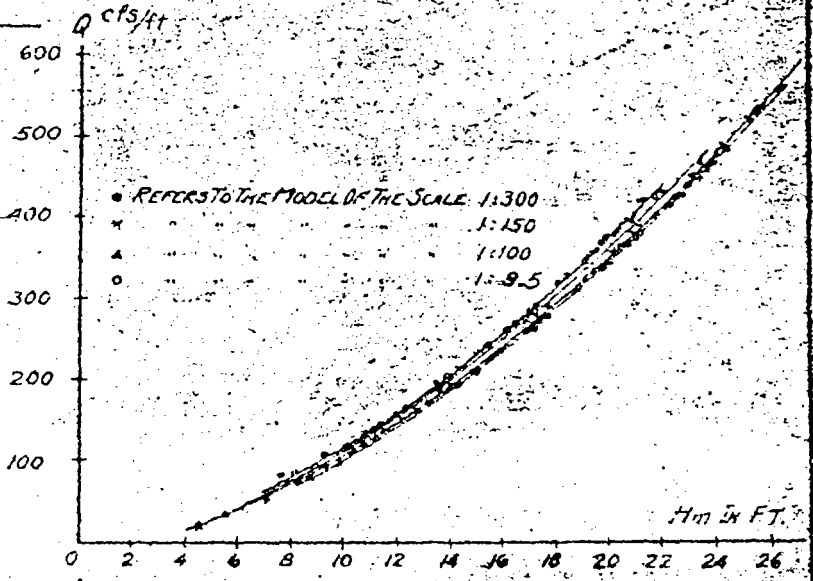

FIG. 43 INVESTIGATION OF THE EFFECT OF MODEL SCALE UPON OVERFLOW.

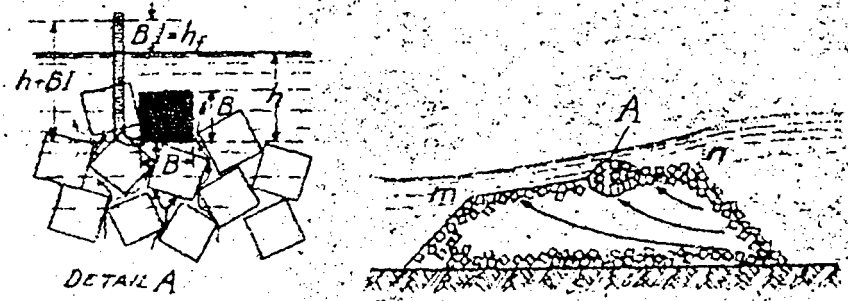

FIG. 44 MODEL FOR STUDYING THE UPLIFT PRESSURE OF PERCOLATION FLOW THROUGH A ROCKFILL.

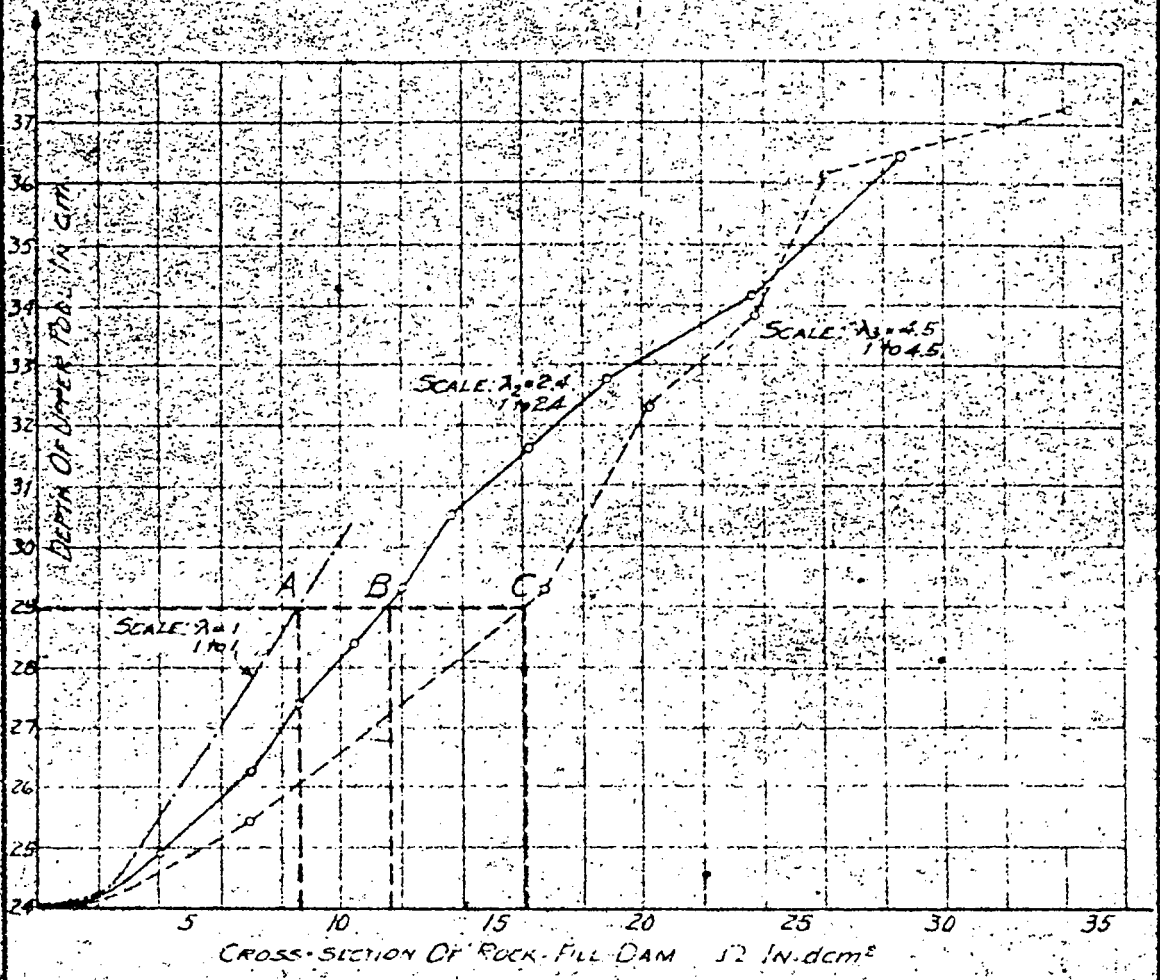

FIG. 45 EFFECT OF MODEL SCALE ON RESULTS OF EXPERIMENTS WITH ROCK-FILL DAMS - BUILT IN FLOWING WATER

THREE SIMILAR EXPERIMENTS:

SIZES OF CONCRETE CUBES: $d_1 = 1.0$ cm, $d_2 = 2.4$ cm, $d_3 = 4.5$ cm.

MODEL SCALES IN THE RATIO OF STONE SIZES:

$\lambda_1 : \lambda_2 : \lambda_3 = 1 : 2.4 : 4.5$

RESULTS EXPRESSED IN DIMENSIONS OF MODEL IN SCALE 1:25

SEE SUPPLEMENTARY SHEETS 1 TO 3 INCL.

ABSCISSA: CROSS SECTION OF ROCK-FILL DAM Ω in dcm²

ORDINATES: DEPTH OF UPPER POOL IN cm.

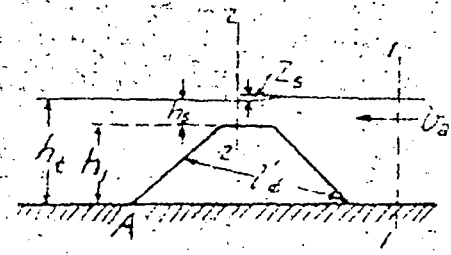

FIG. 46. NOTATION FOR THE STAGE OF SUBMERGED OVERFLOW

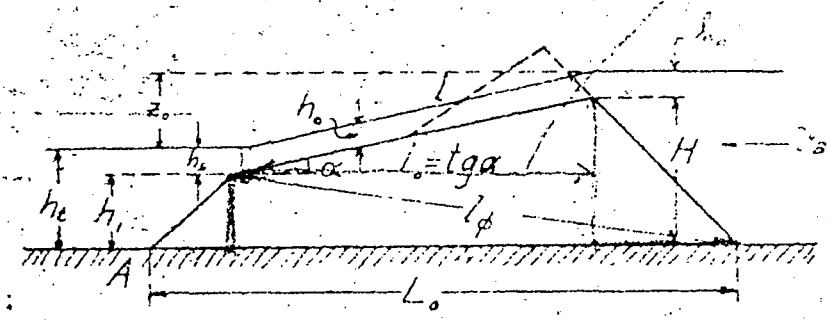

FIG 47. NOTATION FOR THE STAGE OF FREE OVERFLOW

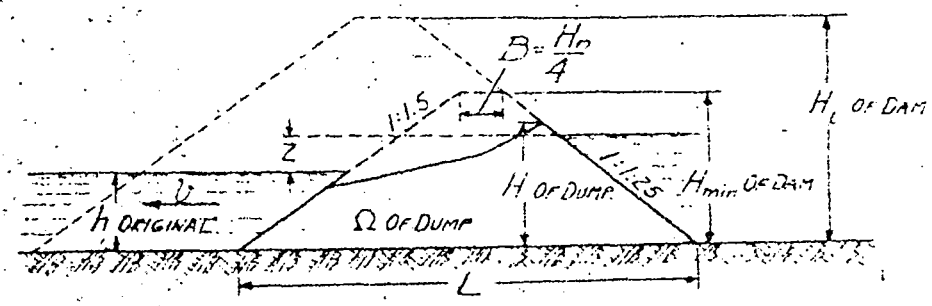

FIG. 56. LIMITS OF APPLICATION OF THE METHOD OF DAM CONSTRUCTION BY DUMPING STONE INTO FLOWING WATER.

FIGURE 52 - CHART I.

Critical transporting velocities and weights for stone of various sizes and unit weights.

$V_c = Y_1 \psi \sqrt{d}$ $V_c = Y_2 \psi \sqrt{d}$ $\psi = \sqrt{2g\left(\frac{\Delta_s}{\Delta_w} - 1\right)}$

$Y_1 = 0.86$ $Y_2 = 1.20$

Stone Weights
$\Delta = 175$ lb/cu ft
$\Delta = 165$ "
$\Delta = 155$ "

$V_c = 1.20 \psi \sqrt{d}$
Condition of free overflow

$V_c = 0.86 \psi \sqrt{d}$
Condition of submerged flow

Δ = 175
Δ = 165
Δ = 155

Δ = 155
Δ = 165
Δ = 175

Velocity in Feet per Second

Equivalent Spherical Diameter of Stone d - Feet

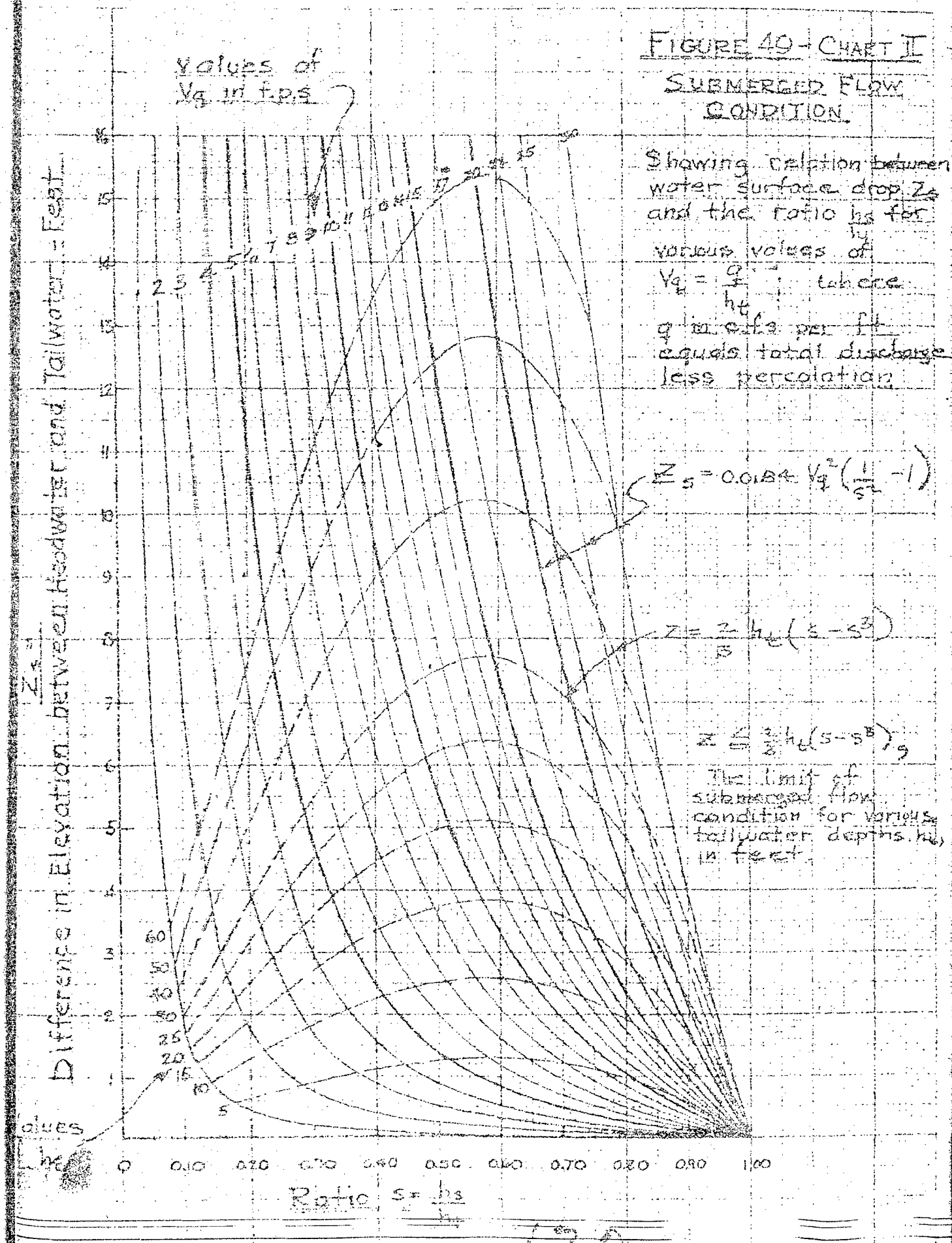

FIGURE 49 - CHART II

SUBMERGED FLOW CONDITION

Showing relation between water surface drop Z_s and the ratio $\frac{h_3}{h_2}$ for various values of $V_q = \frac{q}{h_t}$; where q = cfs per ft equals total discharge less percolation

$$Z_s = 0.018 V_q^2 \left(\frac{1}{s^2} - 1\right)$$

The limit of submerged flow condition for various tailwater depths h_2, in feet

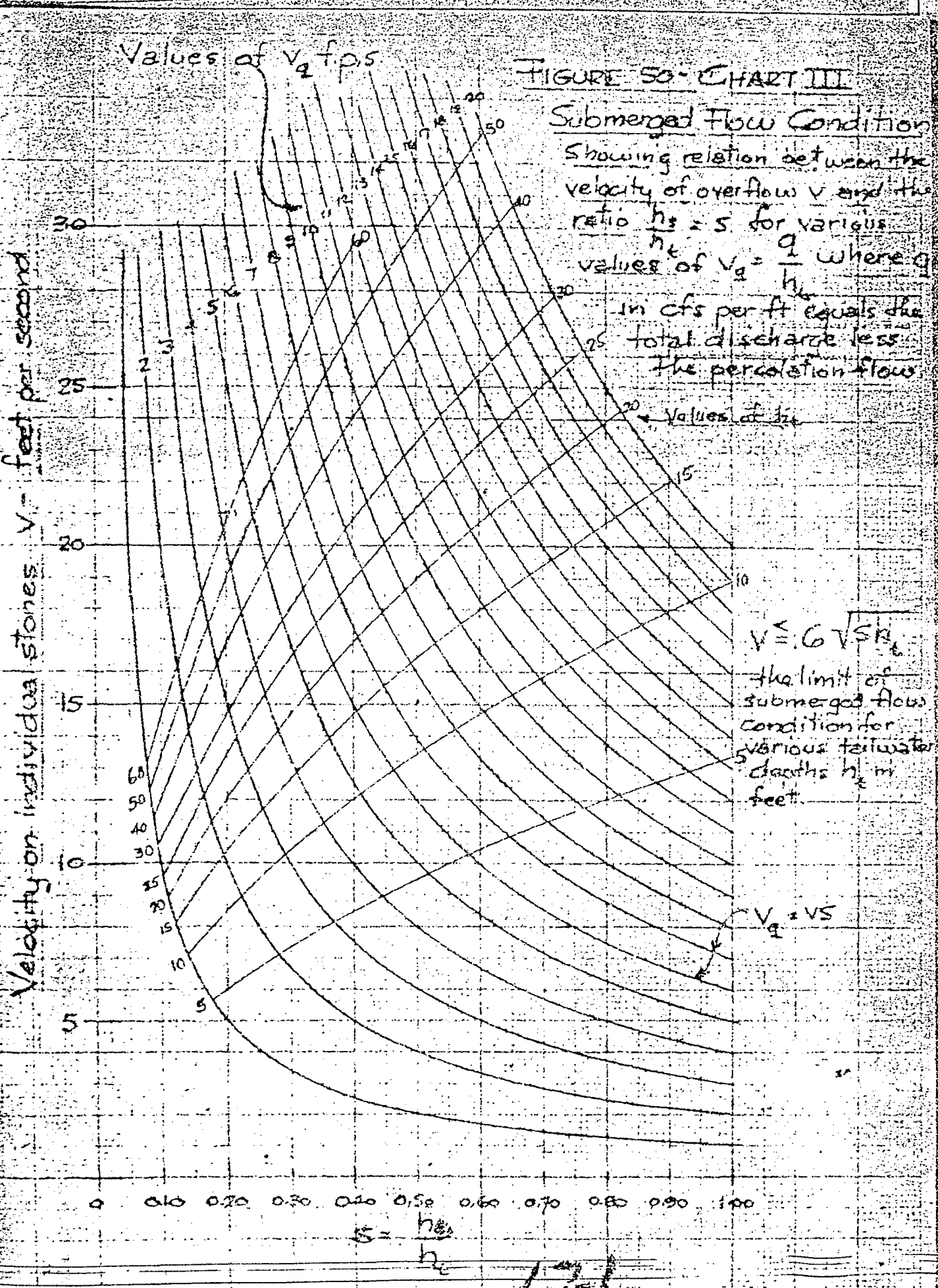

FIGURE 50 - CHART III

Submerged Flow Condition

Showing relation between the velocity of overflow V and the ratio $\frac{h_s}{h_t} = S$ for various values of $V_q = \frac{q}{h_t}$ where q in cfs per ft equals the total discharge less the percolation flow

FIGURE 6 - CHART IV

Percolation velocity V_p in feet per second, as a function of the diameter of stone d in feet.

Assumed void percentage $p = 0.35$

$V_p = C_o p \sqrt{d}$ $\quad C_o = 3.623 - \frac{0.063}{d}$

Percolation velocity V_p in feet per second

Diameter of stone d, in feet

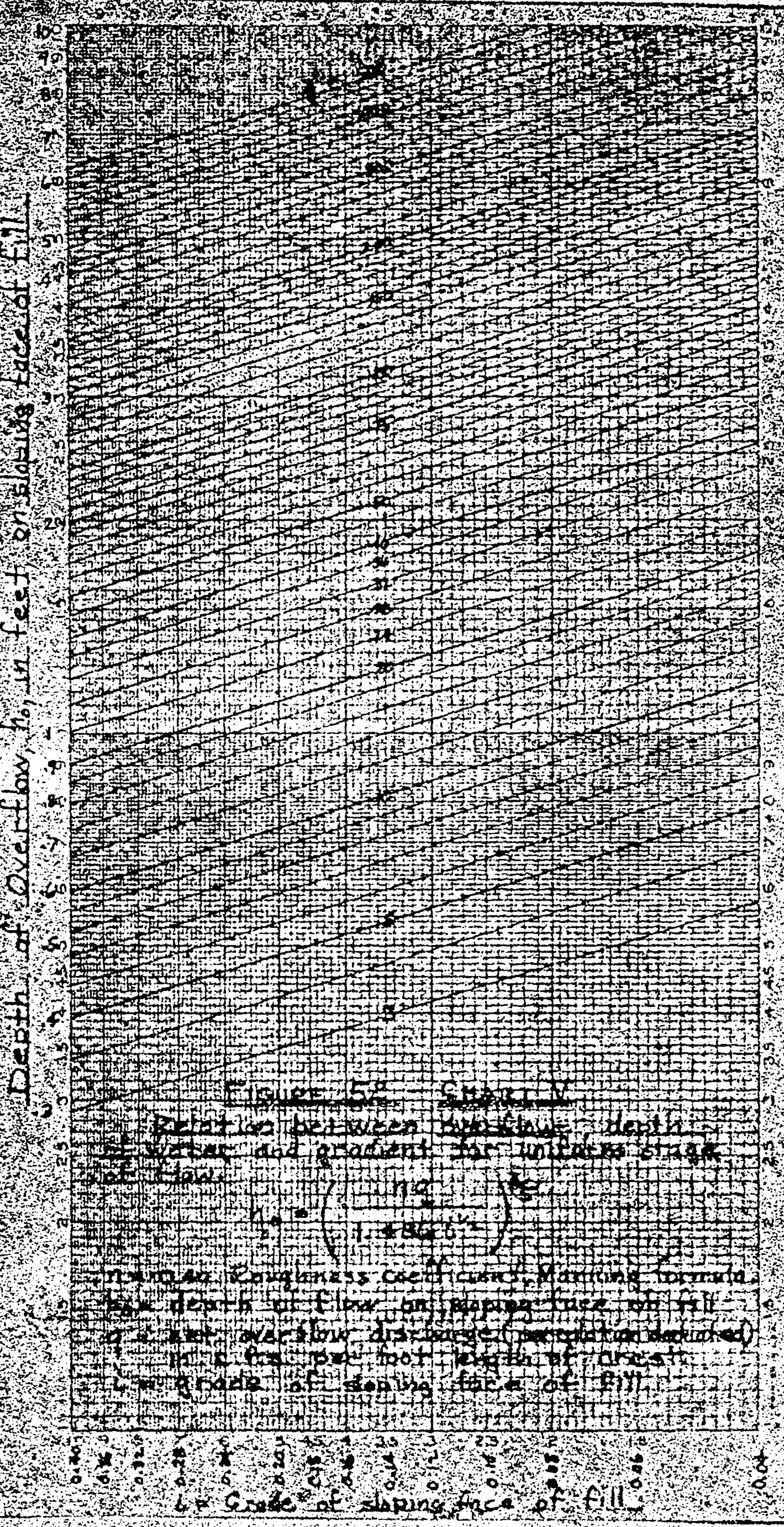

Figure 5? — Sheet V

Relation between overflow depth of water and gradient for uniform stage of flow.

$$h_o = \left(\frac{qn}{1.486\, b^{1/2}}\right)^{3/5}$$

n = Manning roughness coefficient, Manning formula.
h_o = depth of flow on sloping face of fill
q = net overflow discharge (percolation deducted) in c.f.s. per foot length of crest.
b = grade of sloping face of fill.

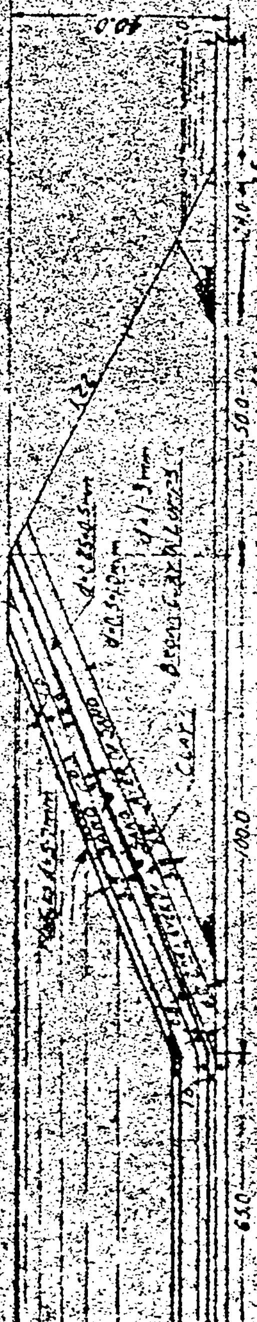

Fig. 53 Sketch of the Model
Model Scale 1:100
Model Dimensions in cm.
Material Sizes in mm.

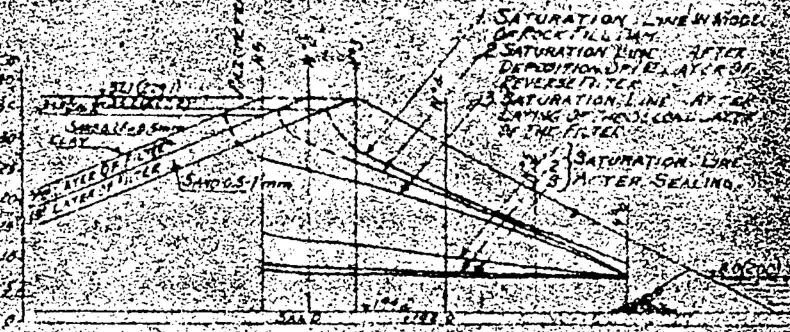

Fig. 54. Saturation Lines in Model for Various Steps In Construction of Up-Stream Blanket. Model Scale 1:100 Model Dimensions in cm.

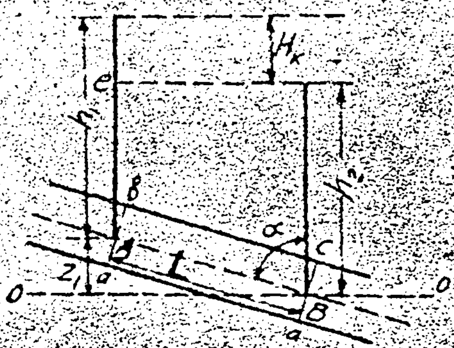

Fig. 55
Notation for Sealing Blanket Studies